Spray drying of protein precipitates

and

Evaluation of the Nano Spray Dryer B-90

Katja Christine Schmid

aus München

2011

Erklärung

Diese Dissertation wurde im Sinne von § 13 Abs. 3 bzw. 4 der Promotionsordnung vom 29. Januar 1998 (in der Fassung der vierten Änderungssatzung vom 26. November 2004) von Herrn Prof. Dr. Wolfgang Frieß betreut.

Ehrenwörtliche Versicherung

Diese Dissertation wurde selbstständig, ohne unerlaubte Hilfe erarbeitet.

München, am 03. Januar 2011

K. Schmid
_____
Katja Schmid

Dissertation eingereicht am 03. Januar 2011

1. Gutachter: Prof. Dr. Wolfgang Frieß

2. Gutachter: Prof. Dr. Gerhard Winter

Mündliche Prüfung am 03. Februar 2011

Acknowledgements

For my parents

Table of Contents

Chapter 1

Evaluating the concept of precipitation by volatile salts for protein stabilization during spray drying

Chapter 2

Evaluation of the Nano Spray Dryer B-90 for pharmaceutical applications

Chapter 3

Spray drying a BCS class II drug with the Nano Spray Dryer B-90

Chapter 4

Protein spray drying with the Nano Spray Dryer B-90 – evaluation of the stress factors and the methods of stabilization

Chapter 5

Appendix

Chapter 1

Evaluating the concept of precipitation by volatile salts for protein stabilization during spray drying

Abstract

The aim of this study was to evaluate an alternative approach to stabilize proteins against adsorption to and unfolding at the air–liquid interface in spray drying. Instead of adding surfactants to the spray solution, the concept of protein precipitation by volatile salts before the spray drying process was realized. The volatility of the precipitating excipients was considered to be of high importance, because spray drying was also utilized to simultaneously remove the precipitant from the resulting protein powder. Specifically, ammonium carbamate showed appropriate qualities as precipitating agent: by applying elevated spray drying temperatures, ammonium carbamate could be removed completely from the spray-dried powders. Furthermore, ammonium carbamate had excellent precipitation efficiency for a monoclonal IgG_1 antibody and recombinant human interleukin-11 (rhIL-11). The protein precipitates were spray dried with a Mini Spray Dryer B-290 and protein stability assessed by HP-SEC, light obscuration, SDS-Page, and FTIR analysis. Regarding the IgG_1, a beneficial effect on protein stability by the ammonium carbamate precipitation was not achieved as this protein has a low surface affinity and can be spray dried as surfactant-free formulation. However, the stability of spray-dried rhIL-11 was substantially improved by ammonium carbamate precipitation in comparison to a surfactant-free formulation. Therefore, for highly surface-active proteins like rhIL-11 the concept of precipitation by volatile salts before spray drying poses a valuable alternative to the addition of surfactant.

1 Introdyction

1.1 Surfactants in protein spray drying

Implementation of spray drying for protein formulation purposes requires detailed knowledge of the stress factors associated with atomization and drying, as both processes may compromise protein stability to a considerable extend. Besides the negative influences of drying due to temperature increase and loss of the protective hydration shell, proteins may also suffer from the tremendous increase of the air–liquid interface due to atomization into fine aerosols [1]. Many proteins exhibit a significant surface activity due to their amphiphilic structure and thus, are prone to adsorption to the air–liquid interface, where the unusual surface energy might cause protein unfolding and consequently aggregate formation [2]. These protein aggregates often show reduced or no biological activity, potential for immunogenicity or other side effects, and their formation during processing and upon storage must be avoided [3]. In order to prevent protein unfolding at air–liquid interfaces and subsequent aggregation, protein formulations are commonly fortified with surfactants as stabilizing excipients [4]. Numerous examples for the protective action of surfactants exist in protein literature. For example, Mumenthaler et al. could effectively reduce surface-induced protein aggregation for recombinant human growth hormone by adding the surfactant polysorbate 20 to the spray solution [5]. In a consecutive study, the direct correlation between the degree of aggregate formation, the surface area of the spray droplets, and the addition of surfactant could be established [6]. Another study correlated the residual enzymatic activity of trypsin after spray drying to the amount of surfactant present in the spray solution [7]. More recent research elucidated the mechanism of aggregation prevention by surfactants using electron spectroscopy for chemical analysis and atomic force microscopy: due to their innate surface activity, surfactants preferentially adsorb to the air–liquid interface, thus competing with protein molecules for the interfacial area and expelling them to the protected droplet core [8, 9].

Their effectiveness at low concentrations and their relative low toxicities made polysorbates to widely utilized excipients in order to prevent protein surface adsorption and aggregation under various processing conditions, such as refolding, shaking or stirring [10], freeze thawing [11], freeze drying [12], spray drying, and reconstitution [13]. Unfortunately, their use in protein preparations is also associated with potential adverse effects on protein stability, as surfactants with alkyl polyoxyethylene chains such as polysorbates are notorious for undergoing autoxidation with subsequent, chain-shortening degradation and formation of

residual peroxides [14]. Such peroxides in turn have been demonstrated to cause oxidation of proteins, both in solution [15] and in solid state [16]. The extent of oxidation of recombinant human granulocyte colony stimulating factor (rhGCSF) could be correlated to the amount of peroxides in the investigated formulations [17]. Indeed, polysorbates increase the short-term process stability of most proteins against surface-induced damage, but sometimes compromise protein stability during long-term storage as reported for interleukin-2 [18], pegylated GCSF [19] or rhIL-11 [20]. In addition, polysorbates could also affect the thermodynamic conformational stability of proteins due to a preferential binding to the unfolded state [13]. Finally, polysorbates in protein formulations might modulate the immune response. A famous example represents a recombinant human erythropoietin formulation, where polysorbate 80 was reported to extract phenolic stopper leachables, which could function as immunogenic adjuvant [21] and furthermore, the formation of mixed micelles of polysorbate and protein was postulated, which might trigger immune reactions due to their virus-like structure [22].

In view of the abovementioned downsides, the need for alternatives to surfactants, specifically polysorbates becomes clear. Human serum albumin (HSA) was initially used to stabilize proteins against surface induced aggregation. However, safety concerns about infectious agents in blood products (e.g. viruses, prions) made its application obsolete. Recombinant HSA could circumvent safety issues, but formation of unwanted degradation products due to the reaction of HSA cysteine residues with reactive protein sites still raises concerns [23]. Serno et al. tested the use of hydroxypropyl-β-cyclodextrin (HPβCD) as alternative to nonionic surfactants to inhibit agitation-induced aggregation of therapeutic antibodies and postulated the surface competition between HPβCD and antibody molecules at the air–liquid interface as the dominating aggregation preventive effect rather than incorporation of hydrophobic protein residues [24].

At this point, we suggest amorphous protein precipitation as alternative formulation strategy in order to stabilize therapeutic proteins against surface-induced stress during spray drying. The phenomenon of protein unfolding due to adsorption to the air–liquid interface preferably occurs when the protein molecules possess sufficient molecular mobility, as it is the case for protein molecules in solution. In contrast, protein molecules in a precipitated state exhibit a lower molecular mobility, as precipitation can be virtually regarded as controlled protein aggregation. In contrast to protein aggregates in the sense of irreversible assemblies of unfolded proteins [25], amorphous precipitates are known to contain mostly still native-like, active protein species [26]. Therefore, amorphous protein precipitation could be utilized to restrict protein mobility, and thereby reduce the likeliness of protein unfolding and

aggregate formation at air–liquid interfaces. Consequently, the addition of surfactants to the protein formulation for stabilization against surface-related aggregate formation may become dispensable and the risk of disadvantageous instability effects or potentially effects on immune responses may be avoided [27].

1.2   Introduction to amorphous protein precipitation

Protein precipitation established as indispensable technique in the life science field, for example as the most commonly applied purification step during downstream processing in monoclonal antibody production [28]. In the broadest sense, precipitation describes the reduction of protein solubility by alteration of solution conditions and the subsequent separation of the precipitated protein in a condensed, solid form via centrifugation or filtration [2]. In protein solutions, precipitation conditions may be achieved by the addition of neutral salts, organic solvents, nonionic hydrophilic polymers, polyvalent metal ions or acids and bases to induce isoelectric point precipitation [29]. The solubility of proteins is determined by protein structure, size, and charge, and by the various interactions (protein-protein, protein-water, protein-ion, and ion-water) resulting from the equilibrium between ionizable and hydrophobic groups on the protein surface [30]. Furthermore, solution composition, temperature, ionic strength, and pH are crucial solvent factors influencing protein solubility. In general, the term solubility refers to the protein concentration at the equilibrium of a saturated solution. In a saturated protein solution, protein molecules in the solid phase coexist with protein molecules in solution, and a net increase of the solid phase is prevented by the counterbalancing dissolution. For protein precipitation to occur, the protein solution must be transformed to the supersaturated state exceeding the solubility limit of the protein. By exclusion of protein molecules from the solute, precipitation poses the thermodynamic driving force for the system to return to the equilibrium state [31]. The reader is referred to literature for a more comprehensive essay on the thermodynamics of precipitation processes [32].

Literature describes various techniques for inducing protein precipitation [33]. One classical approach is the gradually increase of the saturation level of a salt, resulting in the 'salting-out' of the protein. Since Hofmeister established a series for salt ions with regard to their precipitation effectiveness [34], the interactions between proteins and salt ions have been extensively investigated to acquire a more comprehensive understanding of the mechanisms behind salt-induced precipitation. Timasheff et al. explained the 'salting-out' of proteins by the preferential exclusion model [35]. For salts with high charge density, so-called kosmotropes (e.g. ammonium sulfate) a 'negative' binding to the protein was measured, reflecting a higher

affinity of the protein for solvent than for salt molecules and leading to the exclusion of salt ions from the immediate vicinity of the protein. As preferential exclusion increases the surface free energy of the protein-solvent system and thereby constitutes a thermodynamically unfavorable process, the system is forced to reduce the area of protein-solvent interactions and is pushed towards protein self-association and finally protein precipitation [36]. Besides the use of salts as precipitating agents, nonionic, hydrophilic polymers like polyethylene glycol are also applied for protein precipitation. The precipitating effect of polymers is based on the preferential exclusion due to steric hindrance between the differently sized solvent and polymer molecules. Around the protein molecules, a hydration shell is formed at the radius of closet approach between protein and polymer. This shell is impenetrable to the polymer, but penetrable to water molecules, leading to a preferential hydration of the protein molecules. If the polymer concentration increases, the protein is concentrated in the extrapolymeric space, protein-protein interactions increase and finally protein precipitation occurs [35]. Isoelectric point (IEP) precipitation is based on the reduced solubility of proteins at IEP conditions (zero protein net charge), as the hydrophobic attractive forces dominate electrostatic repulsion, and lead to enhanced protein-protein interactions, causing protein agglomeration and precipitation. However, applicability and efficiency of this precipitation technique suffers from the limited pH range in which proteins are sufficiently stable, and the sometimes significant solubility of proteins even at their IEP [2]. Protein precipitation by a water miscible organic solvent (e.g. ethanol, acetone, methanol) occurs due to two effects reducing protein solubility. On the one hand, the low dielectric constant of the solvent compared to water enhances electrostatic attractions and van der Waals forces between protein molecules. On the other hand, the organic solvent competes with the protein for the hydrating water molecules, leaving less for protein hydration and thus promoting precipitation [33]. Particularly, precipitation by organic solvents and isoelectric point precipitation are often detrimental for protein stability because of irreversible protein denaturation or bioactivity reduction of the precipitated protein. However, precipitation as formulation technique must guarantee the stability of the precipitated protein as well as the biocompatibility of the precipitating agent or, in case of critical issues, the possibility must be given to replace the precipitant by another biocompatible nonsolvent [37].

1.3   Protein precipitation as formulation tool

Precipitation usually leads to the formation of amorphous protein suspensions, which can be separated from the solvent by decanting, filtration, or sedimentation, and washed, dried, or resuspended in another nonsolvent. Apart from that, in situ protein precipitation was implemented in the development of various dosage forms (e.g. microparticles, implants). Thus, precipitation reveals new options for liquid and solid protein formulations. The straightforward approach of protein precipitation with subsequent redissolution of the separated precipitate in less volume buffer was evaluated for the development of stable, ready-to-use cetuximab formulations of > 100 mg/mL [32]. Provided a subcutaneous administration of the protein, the precipitates themselves could serve as attractive alternative to highly concentrated liquid protein preparations as protein suspensions usually possess a lower viscosity. In addition, protein precipitates generally exhibit a slower protein dissolution, which can be utilized for a controlled release effect upon administration. Among the numerous literature examples related to this topic, the most prominent one is the alteration of insulin release after precipitation with zinc. By varying the proportions of amorphous and crystalline zinc-insulin, a sustained release profile could be achieved [38]. Precipitation of recombinant human bone morphogenetic protein by potassium phosphate led to an aqueous suspension of protein microparticles intended for sustained delivery [39]. Protein precipitation was also utilized to alter lysozyme release from in situ forming PLGA implants and microparticles, where lysozyme precipitation during manufacturing led to a reduction of the typical accelerated initial burst release [40]. Release rates of recombinant human interferon α-2a from lipidic implants were observed to be constant for a prolonged time period due to the in situ protein precipitation by polyethylene glycol [41].

1.4   The concept of precipitation by volatile excipients

Except in the rare case of an approved, fully biocompatible precipitating excipient, post-precipitation treatment will be necessary to remove excess precipitant from the protein formulation, however, without dissolving the protein precipitate at the same time, which more or less resembles the squaring of a circle. Here, we postulate the use of volatile precipitating agents as an elegant solution to this problem. The volatility of precipitating agents would enable the post-precipitation removal of excess precipitant without the risk of redissolving the protein precipitate. A conversion of precipitants into a volatile gaseous form could be achieved for example by an adequate temperature increase (e.g. by spray drying) or

pressure decrease (e.g. by vacuum drying). In literature, carbon dioxide and various ammonium salts have been investigated as volatile precipitants. In food industry, pressurized carbon dioxide was used for the isoelectric point precipitation of casein [42] and soybean protein [43]. Qi et al. analyzed the isoelectric point precipitation of bovine serum albumin by a carbon dioxide-water-ethanol system [44]. Watanabe et al. applied ammonium carbonate and other combinations of ammonia and carbon dioxide for the precipitation of trypsin [45]. After the subsequent vacuum- or freeze-drying step of the precipitates, the total activity recovery of trypsin was maximum 80%.

The scope of this work was to evaluate protein precipitation by volatile excipients as adequate measure to stabilize proteins during the spray drying process against adsorption to and unfolding at the air–liquid interface. Simultaneously we utilize the spray drying process for the removal of excess precipitant. Therefore, numerous excipients were screened in a small-scale batch method for the following crucial qualities:

- Quantitative protein precipitation
- Volatility upon drying
- Preservation of protein integrity

A preferred excipient should enable quantitative protein precipitation. Otherwise, the fraction of protein molecules remaining in solution could still be subject to adsorption to the air–liquid interface and thereby compromise the aim of improving protein stability by precipitation. Furthermore, the precipitant should be volatile upon application of rather moderate temperature levels to prevent a loss of protein stability due to heat denaturation. Finally, protein stability must not be jeopardized by the chemical reactivity of the decomposing precipitant itself. The most promising candidates were evaluated for spray drying various protein precipitates as surfactant-free formulations. The gained spray-dried powders were investigated for protein stability. The absence of surfactants, particularly polysorbates, in spray-dried protein powders could be of interest in a broader perspective. For example, by avoiding the issue of detrimental protein oxidation due to presence of peroxides, pure protein powders with increased long-term storage stability could be produced. Furthermore, surfactant-free protein powders could also be beneficial as basis for the production of highly concentrated protein formulations.

2 Materials and Methods

2.1 Materials

Glycine (> 99%) and L-histidine (> 99%) were purchased from Sigma (Munich, Germany), polysorbate 80 and L-methionine (> 99%) from Merck (Darmstadt, Germany), and trehalose from Ferro Pfanstiehl (Cleveland, USA). Precipitant stock solutions (Table 1) were prepared by dissolving ammonium salts in MilliQ water to the following concentrations:

Table 1 Precipitant stock solutions

Salt	M_r [g/mol]	Purity	Supplier	Conc. [%(w/w)]
Ammonium carbamate	78.07	puriss.	Sigma	39.4
Ammonium carbonate	157.13	puriss.	Sigma	23.0
Ammonium hydrogen carbonate	79.06	puriss.	Sigma	16.7
Ammonium acetate	77.08	puriss.	Merck	59.2
Ammonium formate	63.06	p.a.	Merck	5.0
Ammonium sulfate	132.14	p.a.	Merck	28.4

Bovine serum albumin (BSA), prepared by a modified Cohn cold ethanol fractionation method of bovine serum (Cohn fraction V) with a purity of minimum 96% was purchased as lyophilized powder from Sigma (Munich, Germany) and dissolved to 100 mg/mL in MilliQ water. A humanized monoclonal antibody of the IgG_1 class was provided at approx. 50 mg/mL in an aqueous buffer containing glycine and L-histidine. Recombinant human interleukin-11 was purchased from Wyeth (Andover, USA) as aqueous bulk solution containing 6 mM dibasic sodium phosphate, 4 mM monobasic sodium phosphate and 300 mM glycine at pH 7.0 . All protein solutions were filtered through a 0.2 μm polyethersulfone sterile syringe filter (VWR, Darmstadt, Germany) before use.

2.2 Methods

2.2.1 Protein precipitation

For precipitant screening studies, a 1.0 mL batch scale method was applied using 1.5 mL Eppendorf tubes as reaction vials (Safe-Lock Tubes, Eppendorf AG, Hamburg, Germany). Protein and precipitant were mixed by first presenting a specific amount of water in the reaction vial, then adding protein stock solution and finally pipetting precipitant stock solution to the protein solution. In the respective blank samples, either precipitant stock solution (= protein blank) or protein stock solution (= UV blank) was replaced by an equal amount of water. The protein / precipitant mixtures were homogenized by gentle manual agitation before incubation at 2 – 8 °C for 1, 3, 8 or 24 hours, respectively. After incubation, precipitation samples were centrifuged for 5 min at 6000*g. Blank samples were treated likewise. Precipitate and supernatant were separated by carefully removing the supernatant with a pipette. The protein concentration in the supernatant phase was determined photometrically at 280 nm using an Agilent 8453 UV-Vis spectrophotometer (Agilent, Waldbronn, Germany) and the precipitation efficiency (in %) calculated according to

$$Eff\left[\%\right] = \frac{UV_{280}^{supernatant} - UV_{280}^{protein\ blank}}{UV_{280}^{protein\ blank}} * 100$$

For preparation of protein precipitates suitable for spray drying, protein precipitation was conducted in 50 mL Falcon tubes (Cellstar Tubes, Greiner Bio-One, Essen, Germany). The protein solutions were presented, the precipitant stock solutions added to the desired concentration, and the protein / precipitant mixtures carefully homogenized, incubated for 1 hour at 2 – 8 °C and then spray dried without further processing.

2.2.2 Redissolution and ultrafiltration of precipitates

For further analysis of the precipitated protein, the precipitates were redissolved in 1000 µL of the corresponding formulation buffer. Vivaspin 500 centrifugal concentrator units (Vivascience Ltd., Stonehouse, UK) with a 30 kDa MWCO polyethersulfone membrane and a maximum volume of 500 µL were used for ultrafiltration. The membrane was preconditioned by filtrating 0.1 N NaOH and two times MilliQ water before adding the redissolved protein. The protein solution was washed six times by addition of fresh formulation buffer and

subsequent centrifugation for 10 min at 5000*g. Finally, the concentrated protein solution (approx. 75 µL) was dissolved in 1000 µL formulation buffer for FTIR analysis.

2.2.3 Transmission Fourier transform infrared spectroscopy (FTIR)

FTIR spectroscopy was used to monitor the conformational stability of the precipitated proteins. Infrared spectra of the protein solutions were recorded by a Tensor 27 spectrometer (Bruker Optics, Ettlingen, Germany). The solutions were analyzed in transmission by application of the Confocheck AquaSpec cell. The temperature was kept constant at 20 °C. For each spectrum 120 scan interferograms from 4000 - 850 cm^{-1} were collected at single beam mode with 4 cm^{-1} resolution. Blank spectra were recorded with reference buffer in the cell under identical conditions. Collected interferograms were Fourier transformed and the corresponding blank spectrum was subtracted by the Protein Dynamics software Opus 6.5 (Bruker Optics, Ettlingen, Germany). The amide I region of the spectra (1700 - 1600 cm^{-1}) was vector normalized, processed via a 25-point Savitzky-Golay smoothing algorithm [46] and displayed as second derivative amide I spectrum.

2.2.4 High performance size exclusion chromatography (HP-SEC)

Protein samples were analyzed for soluble aggregates by HP-SEC using a HP 1100 instrument (Agilent, Waldbronn, Germany) equipped with TSKgel® SW_{XL} columns (300-7.8 mm) and guard column (Tosoh Bioscience, Tokyo, Japan). Samples were centrifuged prior to analysis in order to remove insoluble aggregates. Protein aggregates, monomer and fragments were detected photometrically at 280 nm (IgG_1) or 225 nm (rhIL-11), respectively. Typical HP-SEC chromatograms are shown in Figure 1. The chromatograms were integrated manually using the HP ChemStation software 9.0 (Agilent, Waldbronn, Germany). Percentage of aggregates was calculated by comparing the area under the curve (AUC) of the aggregate peak to the total AUC. Of each sample, three chromatographic samples were prepared and analyzed.

▪ HP-SEC of IgG_1
   A TSKgel® G3000 SW_{XL} column was applied for analysis of IgG_1 aggregates. The running buffer was composed of 0.1 M disodium hydrogen phosphate dihydrate and 0.1 M sodium sulfate and was adjusted with ortho-phosphoric acid 85% to pH 6.8 . The flow rate was set to 0.5 mL/min and the injection volume to 25 µL.

- HP-SEC of rhIL-11

A TSKgel® G2000 SW$_{XL}$ column was applied for analysis of rhIL-11 aggregates. The running buffer was composed of 0.1 mM glycine, 500 mM sodium chloride and 50 mM morpholinoethane sulfonic acid (MES) at pH 6.0 . The flow rate was set to 0.75 mL/min and the injection volume to 50 µL. The column was immersed in cold water to run the analysis at a constant temperature of 4 +/-1 °C.
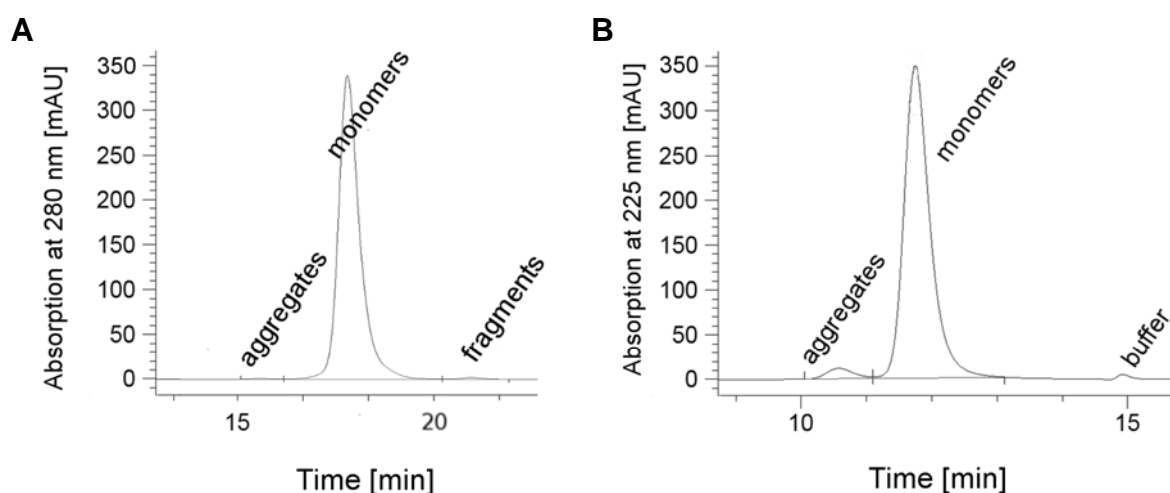
Figure 1 Exemplary HP-SEC chromatograms of IgG$_1$ **(A)** and rhIL-11 **(B)**

2.2.5 *Sodium dodecyl sulfate polyacrylamide gel electrophoresis (SDS-Page)*

Formation of aggregates was analyzed by SDS-Page under non-reducing conditions. Gel electrophoresis was carried out in a X-Cell II Mini electrophoresis chamber (Noves, San Diego, USA) with a Power Pac 200 power supply (BioRad, Munich, Germany) using NuPage® 7% Tris-Acetate gels (1.0 mm, 10 wells) and NuPage® Tris-Acetate SDS Running Buffer (all Invitrogen, Karlsruhe, Germany). The samples contained 0.1 mg/mL protein and 50% Tris-Acetate SDS Sample Buffer. After heating to 95 °C for 20 min, 10 µL of each sample containing 1 µg protein were loaded per lane and focused. Separation was conducted at constant voltage for antibody formulations (150 V for approx. 45 min) or constant current for rhIL-11 formulations (80 mA for approx. 1.5 hours). A standard Coomassie staining protocol including a washing, fixing, staining, destaining and drying step was applied for the detection of the resulting protein bands. In order to analyze the molecular weight of the detected zones a Mark12™ Unstained Standard was used.

2.2.6 Spray drying with the Mini Spray Dryer B-290

Spray drying was performed with a B-290 Mini Spray Dryer (Büchi Labortechnik AG, Flawil, Switzerland) consisting of heating system, nozzle, drying chamber, sensors for measuring inlet temperature (T_{in}) and outlet temperature (T_{out}), cyclone, collecting vessel, filter and aspirator. The aspirator was located behind the fine particle filter and aspirated the drying air by means of vacuum at an aspirator rate of 90% or 35 m^3/h. For product separation a high performance cyclone was used in order to increase especially the yield of smaller particles. An electrically conductive layer of zirconium oxide on the inner wall of the cyclone prevented the product form electrostatic binding to the cyclone wall and minimized the product loss. A LT Mini dehumidifier (Deltatherm, Much, Germany) controlled the residual moisture of the system (approx. 25% r.h.).

Spray solutions were atomized by a two fluid nozzle (tip Ø 0.7 mm, cap Ø 1.5 mm) or a three fluid nozzle (inner tip Ø 0.7 mm, outer tip Ø 2.0 mm, cap Ø 2.8 mm) using the in-house compressed air supply of 8 bars. The atomizing air volumetric flow rate was set to 670 L/min for the two fluid nozzle or 1334 L/min for the three fluid nozzle. Flow rates were adopted to ensure comparable atomizing conditions for both nozzle types, resulting in comparable droplet and particle sizes. Cooling of the spray nozzles was ensured by circulation of cool water through the nozzle jacket. Spray solutions were pumped using the inbuilt peristaltic pump of the spray dryer or an external IPS 12 peristaltic pump (Sotax AG, Basel, Switzerland) at varying flow rates suitable to reach the desired outlet temperatures. Pump settings and the corresponding flow rates are shown in Figure 2. Product recovery from the collecting vessel was performed in controlled atmosphere (< 15% r.h., 20 °C) and samples were stored in glass vials in a dessicator (< 20% r.h., 20 °C).
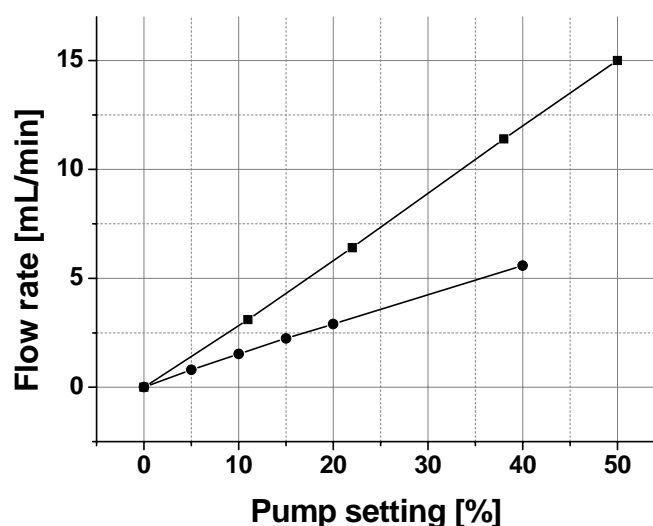
Figure 2 Flow rate of the inbuilt spray dryer pump (-- ■ --) and the external pump (-- ● --)

2.2.7 Elementary analysis (CHN analysis)

The amount of residual volatile precipitant in spray-dried powders was determined by elementary analysis. A vario EL instrument (Elementar, Hanau, Germany) equipped with a high temperature combustion unit and a dynamic gas component separation and detection was used to pyrolize 5.000 mg of spray-dried powder with oxygen at approximately 1200 °C in a helium atmosphere. Samples decomposed to carbon dioxide, nitrogen and water, which were separated by condensation and quantified by thermal conductivity to report the content of carbon, hydrogen, and nitrogen (CHN) in the sample (in %).

2.2.8 Karl-Fischer analysis

Residual moisture of the spray-dried powders was determined by Karl-Fischer titration with a titrator Aqua 40.00 (Analytik Jena AG, Jena, Germany) using a head space module oven to heat up approx. 10 mg powder to 80 °C.

2.2.9 X-ray powder diffraction (XRD)

The morphology of the spray-dried products was analyzed by X-ray powder diffraction on the X-ray diffractometer XRD 3000 TT (Seifert, Ahrensburg, Germany) using Cu-Kα-radiation (λ = 0.15418 nm, U = 40 kV, I = 30 mA). The samples were scanned from 5 to 40 °2-Theta, with steps of 0.05 °2-Theta and duration of 2 s per step.

2.2.10 Scanning electron microscopy (SEM)

The particle morphology of the spray-dried powders was determined with a JSM-6500F JEOL scanning electron microscope (JEOL, Eching, Germany). For analysis, the samples were fixed on self-adhesive tapes on an aluminum stub and sputtered with carbon.

2.2.11 Nephelometry and optical density

Turbidity of reconstituted, spray-dried powders was determined by nephelometry and optical density measurements. For nephelometry, the NEPHLA nephelometer (Hach Lange, Düsseldorf, Germany) was used as described in the European Pharmacopoeia method <2.2.1>. Briefly, the samples were measured by 90° light scattering at 860 nm and turbidity was reported as formazine nephelometric units (FNU). Optical density measurements were performed at 350 nm with an Agilent 8453 UV-Vis spectrophotometer (Agilent, Waldbronn, Germany).

2.2.12 Subvisible particle analysis by light obscuration

Concentration and size distribution of particles in reconstituted, spray-dried powders were determined by light obscuration using a SVSS C32 apparatus (PAMAS, Rutesheim, Germany). The system was flushed with particle free water until there were less than 100 particles larger than 1 µm per 1 mL. Test measurements with particle free water were performed at the beginning and at the end of analysis. The average value of three measurements was calculated and correlated to a sample volume of 1 mL. After each measurement, the system was flushed with 5 mL of particle free water to exclude cross contamination. After this cleaning procedure, less than 100 particles larger than 1 µm per 1 mL were detected.

2.2.13 Statistical analysis

An unpaired one-tailed t-test was performed to test the significance of difference. A P-value of 0.05 was defined as statistically significant.

3 Feasibility of protein precipitation by volatile ammonium salts

3.1 Volatile ammonium salts

By screening chemical databases, the following ammonium salts were identified as possible candidates for protein precipitation with subsequent precipitant removal by spray drying (Table 2). The requirements for suitable excipients comprise, besides the ability of quantitative protein precipitation, a comparatively low decomposition temperature, a low toxicity of the bulk material and the decomposition products, and a complete decomposition upon the temperature increase during spray drying.

The overview lists ammonium salts according to their decomposition temperature. Ammonium carbamate has with 35 °C the lowest decomposition temperature followed by ammonium carbonate and ammonium hydrogen carbonate. Ammonium acetate decomposition requires a minimum of 90 °C, thereby reaching the limits of spray drying with the Mini Spray Dryer B-290. Based on experience, an inlet temperature of 190 °C would be necessary to gain an outlet temperature of 90 °C, which is yet insufficient to generate equivalent temperature conditions inside the aerosol droplets. For the same reason, ammonium formate seemed inappropriate for an elimination of precipitant by spray drying. Di-Ammonium oxalate and Tri-Ammonium citrate were both excluded from investigations as they show critical qualities: Di-Ammonium oxalate possesses with 9 mL/kg a rather low LD_{50} value and its decomposition leads to the formation of carbon monoxide, whereas Tri-Ammonium citrate forms a critical anhydride component.

Table 2 Overview of ammonium salts with their corresponding physicochemical qualities according to the respective material safety datasheets

Ammonium Salt	Molecular Formula	Decomp. Products	Decomp. Temp. [°C]	LD$_{50}$ rat [mg/kg] oral	Melting point [°C]	pH [100 g/L]	Water solubility [g/L] 20°C	Vapor pressure [hPa] 20°C
Ammonium carbamate	$H_2NCOONH_4$	2 NH_3, CO_2	35	681-1470	152	10	790	82
Ammonium carbonate	NH_4HCO_3 + $H_2NCOONH_4$ (1:1)	H_2O, 3 NH_3, 2 CO_2	58	1975	-	9.4	320	69
Ammonium hydrogen carbonate	NH_4HCO_3	H_2O, NH_3, CO_2	60	1576	106	8 (for 50 g/L)	220	67
Ammonium acetate	CH_3COONH_4	NH_3, CH_3COOH	90	632 (intraperitoneal)	114	6.7-7.3	1489	n.a.
Ammonium formate	$HCOONH_4$	H_2O, NH_3, CO	180	2250 (mouse)	116	5.5-7.5	n.a.	n.a.
Di-Ammonium oxalate	$(NH_4)_2C_2O_4$	NH_3, CO_2, CO	> 70	9 mL/kg	70	6.4	45	n.a.
Tri-Ammonium citrate	$(NH_4)_3C_6H_5O_7$	H_2O, NH_3, CO_2, methyl maleic anhydride	185 (melting point)	1090 (methyl maleic anhydride)	n.a.	n.a.	n.a.	n.a.

3.2　Precipitation efficiency

In the precipitation screening study, the following salts were evaluated for their efficiency to precipitate proteins: ammonium carbamate, ammonium hydrogen carbonate, ammonium carbonate, ammonium acetate, and ammonium formate. Ammonium sulfate was used for rhIL-11 as a default non-volatile precipitating agent.

3.2.1　Precipitation of BSA

BSA / precipitant mixtures were prepared containing either 2.5 mg/mL or 10.0 mg/mL BSA. While adding the precipitant stock solution to the protein solution, no instantaneous effect, like coagulation or turbidity increase, occurred. The reaction vials were then incubated for 24 hours at $2 - 8\,°C$. However, despite the prolonged reaction time, neither of the investigated volatile ammonium salts was found capable of precipitating BSA quantitatively. Figure 3 exemplifies BSA precipitation efficiency for ammonium carbamate. If BSA is present in the lower concentration of 2.5 mg/mL, ammonium carbamate is able to precipitate 10% of the initial protein at most. For the higher protein content of 10 mg/mL, the precipitation efficiency of ammonium carbamate is negligible, which can be explained by the relatively lower precipitating agent content compared to the amount of protein. All other investigated ammonium salts showed similar or less precipitation power (data not shown). Thus, it appears difficult to precipitate BSA under the conditions applied. Consequently, the precipitant screening studies were continued with IgG_1.
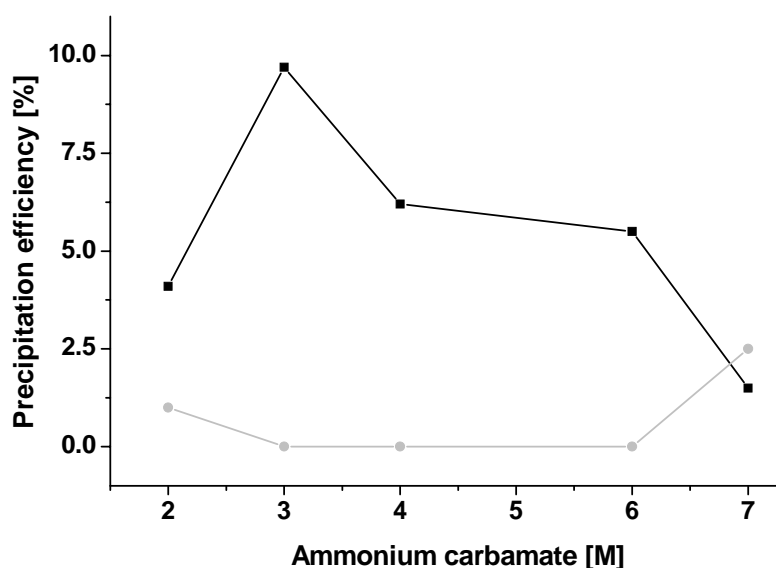
Figure 3 Precipitation efficiency [%] of ammonium carbamate for BSA at 2.5 mg/mL (-- ■ --) and 10.0 mg/mL (-- ● --)

3.2.2 Precipitation of IgG$_1$

In analogy to BSA / precipitant mixtures, IgG$_1$ was utilized in two concentrations for screening possible protein precipitants: 2.5 mg/mL and 10.0 mg/mL. Only ammonium carbamate induced an immediate protein precipitation, visible by the formation of an opaque precipitate in the reaction vial. Although ammonium acetate, ammonium hydrogen carbonate, ammonium carbonate, and ammonium formate were added at the highest possible concentration using stock solutions containing the salts at the respective maximum solubility, precipitation could not be observed. After incubation for 24 hours at 2 – 8 °C and subsequent centrifugation, only in case of the ammonium carbamate system a sediment could be separated. The visual impression was confirmed by spectroscopic determination of the protein content in the assumed supernatant (data not shown). Complete protein recovery in the supernatant of the ammonium acetate, ammonium hydrogen carbonate, ammonium carbonate, and ammonium formate system indicated full protein solubility.

The successful IgG$_1$ precipitation by ammonium carbamate was further investigated. In order to reduce absolute process times, the incubation of IgG$_1$ / precipitant mixtures was reduced from 24 hours to 8, 3 and 1 hour, respectively and in addition, trehalose as a potential stabilizer was tested for the precipitated protein at 2.5 mg/mL. Figure 4A shows the precipitation efficiency of ammonium carbamate for a 2.5 mg/mL IgG$_1$ solution at different incubation times. Increasing ammonium carbamate concentrations led to a more efficient protein precipitation. A reduction of the incubation time resulted in a reduced protein precipitation efficiency. In fact, precipitant concentration and incubation time were identified as the most important factors to achieve quantitative precipitation. A precipitation efficiency of more than 97% was defined as quantitative. Ammonium carbamate could be applied either at 26% for 24 hours or at 28% for 1 hour to achieve 97% efficiency. Figure 4B presents the precipitation study with IgG$_1$ / trehalose / ammonium carbamate mixtures. The addition of trehalose to the protein solution before precipitation had no significant influence on protein precipitation efficiency. Therefore, addition of sugars to the protein formulation seemed uncritical with regard to complete protein precipitation. In Figure 4C, the precipitation efficiency of ammonium carbamate was analyzed for a 10 mg/mL IgG$_1$ solution without addition of trehalose. Also at the higher protein content, the same ammonium carbamate concentrations were sufficient to precipitate IgG$_1$ quantitatively, keeping protein solubility at the same low level.

Figure 4 Precipitation efficiency [%] of ammonium carbamate for
(A) 2.5 mg/mL IgG$_1$
(B) 2.5 mg/mL IgG$_1$ / trehalose
(C) 10.0 mg/mL IgG$_1$
after different incubation times:
— ■ — 1 hour
— ● — 3 hours
— ▲ — 8 hours
— ▼ — 24 hours
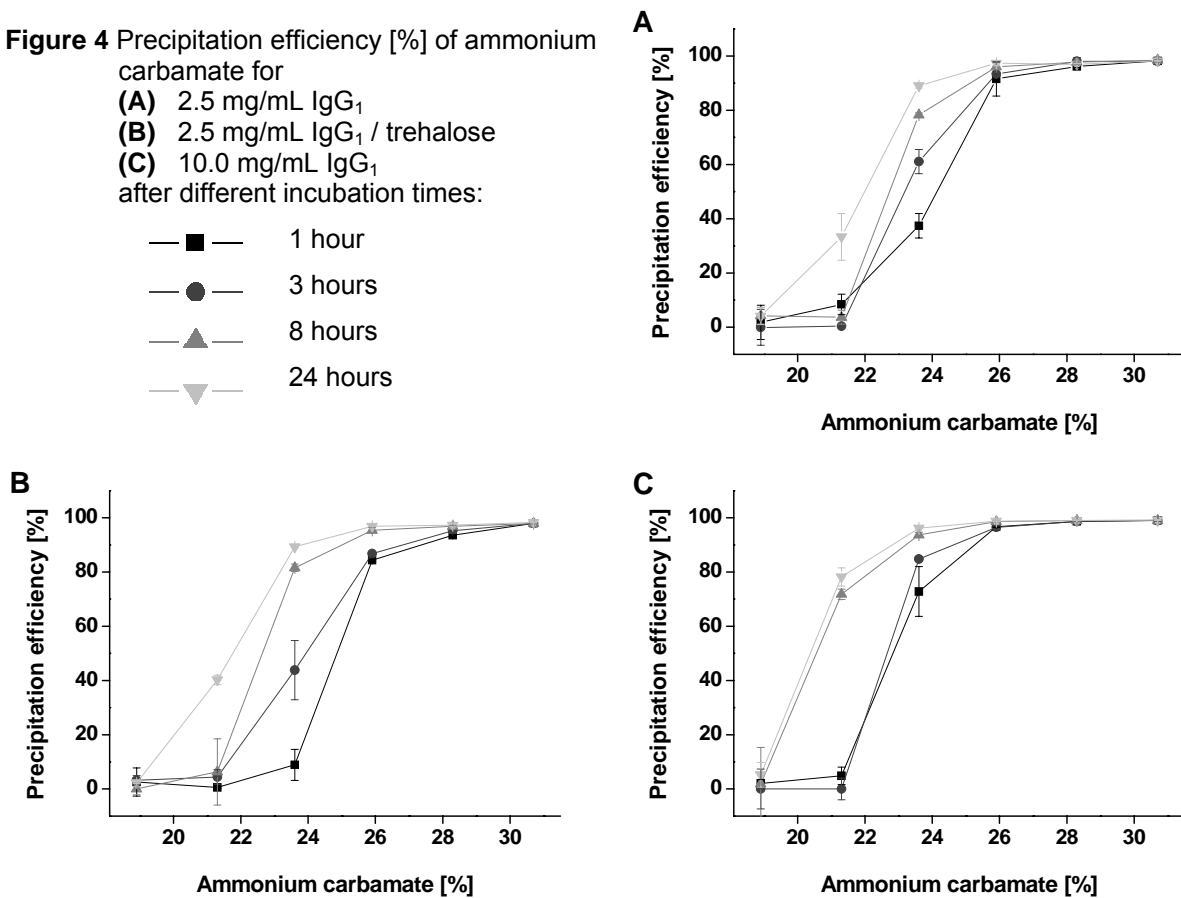
Protein precipitation is known to occur more readily at pH conditions near the isoelectric point (IEP) of the protein, because of the lower electrostatic repulsion and consequently lower protein solubility once the protein does not carry any net charge. Typically, IgG$_1$ molecules have an IEP of approx. 8.3 to 9.5 [47]. Therefore, the conditions of the ammonium carbamate system with its pH of 9.3 to 9.4 (measured at ammonium carbamate concentrations of 18.9 to 30.7%) assisted the quantitative IgG$_1$ precipitation. All other applied ammonium salt solutions exhibited lower pH values (Table 2), and the salting-out effect on proteins remained insignificant. The example of the ammonium carbonate system, which also provides a pH in the IEP region of the antibody without causing protein precipitation, clarifies that the high efficiency of ammonium carbamate must be ascribed to a considerable extent to the presence of the carbamate anion.

3.2.3 Precipitation of rhIL-11

In a next step, the approach of protein precipitation by ammonium carbamate was tested for rhIL-11, which in comparison to the IgG_1 antibody can be viewed as a representative for lower molecular weight proteins. Due to its limited availability, rhIL-11 was not tested with other volatile precipitation agents. Instead, ammonium sulfate precipitation was conducted to compare the influence of volatile and non-volatile precipitants on protein stability. A 5.0 mg/mL rhIL-11 solution was precipitated quantitatively by 20% ammonium carbamate (Figure 5), which indicates a higher sensitivity of rhIL-11 towards salting-out compared to IgG_1, where at least 26% ammonium carbamate were necessary for its quantitative precipitation. This higher susceptibility of rhIL-11 can be partly ascribed to its hydrophobic nature caused by the unusual amino acid composition of 23% leucine reducing protein solubility [48]. Furthermore, its basic IEP in the range of 11.8 favors protein precipitation by ammonium carbamate. In addition, rhIL-11 was precipitated quantitatively by a 26.3% ammonium sulfate solution indicating a strong effect of the precipitants on the rhIL-11 solubility. In comparison, quantitative precipitation of trypsin [45] and a monoclonal IgG_1 antibody [32] was only achieved in the presence of 50% ammonium sulfate.
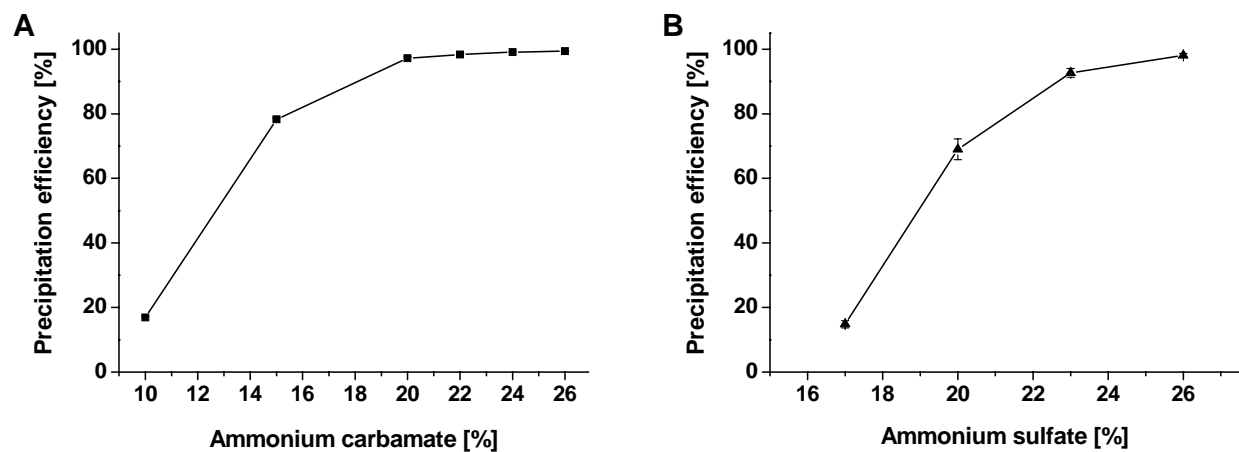
Figure 5 Precipitation of rhIL-11 by ammonium carbamate **(A)** and ammonium sulfate **(B)**

3.3 Effect of precipitation with ammonium carbamate on protein stability

Precipitation as alternative for protein stabilization during spray drying can only be successful if perturbations of protein stability can be ruled out. In order to exclude protein destabilization by ammonium carbamate precipitation, protein aggregation was analyzed by HP-SEC analysis and structural protein changes were investigated by FTIR analysis.

3.3.1 Stability of IgG₁ upon precipitation with ammonium carbamate

IgG$_1$ was precipitated with 28% ammonium carbamate, incubated and redissolved before HP-SEC analysis was conducted to evaluate the formation of soluble aggregates. As shown in Figure 6, a minor increase of aggregated protein species was observed. After one hour of precipitate incubation, the amount of aggregates was nearly doubled (0.35% instead of 0.19%). The slightly negative effect of precipitation conditions became more relevant with prolonged incubation of the IgG$_1$ / ammonium carbamate mixture and after 24 hours, an amount of 0.63% aggregates could be observed. Overall, the formation of aggregates due to ammonium carbamate incubation was very moderate.
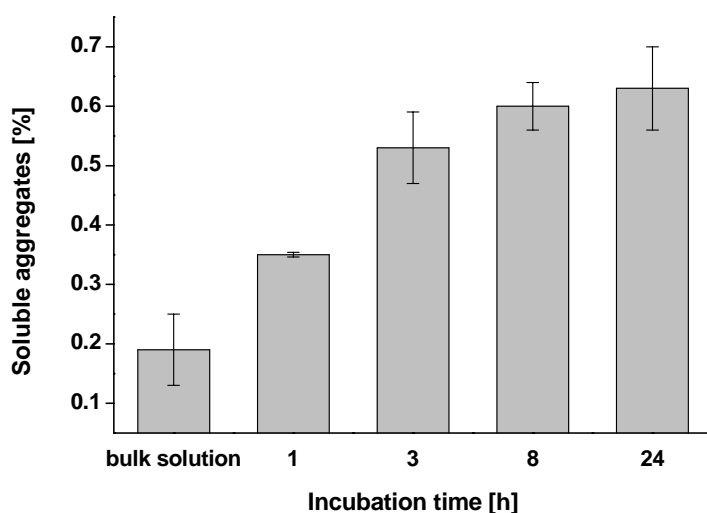
Figure 6 Amount of soluble aggregates induced by ammonium carbamate precipitation

FTIR spectra of redissolved, diafiltrated IgG$_1$ precipitates were obtained to investigate the influence of ammonium carbamate on the protein secondary structure. The secondary structure of IgGs is dominated by β-sheet elements at the wavenumbers of 1614, 1639 and 1690 cm^{-1} [49]. Structural changes of the protein conformation usually coincide with band shifts towards higher wavenumbers, band broadening and loss of intensity [50]. In order to eliminate

the interfering signals of residual ammonium in the redissolved IgG_1 precipitates, samples were diafiltrated against formulation buffer prior to FTIR analysis. The obtained IgG_1 spectrum after precipitation, redissolution and ultrafiltration aligned well with the spectrum of IgG_1 bulk solution (Figure 7A), suggesting that precipitation with ammonium carbamate did not cause alterations in protein secondary structure. The results depicted in Figure 7B support this finding, as increasing incubation times of the IgG_1 precipitates did not influence the conformational stability of the protein.
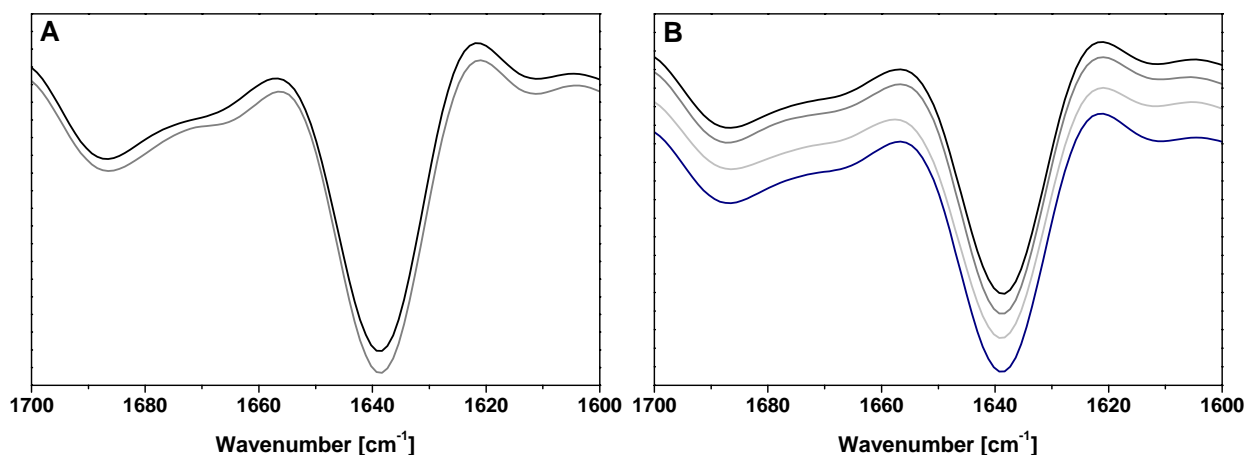
Figure 7 (A) FTIR spectra of IgG_1 standard solution (black) and redissolved, diafiltrated precipitate (gray)
(B) FTIR spectra of redissolved, diafiltrated precipitates after 1, 3, 8 and 24 hours incubation time (top down)

3.3.2 Stability of rhIL-11 upon precipitation with ammonium carbamate and sulfate

The effect of precipitation by ammonium carbamate and ammonium sulfate on rhIL-11 stability was evaluated by HP-SEC analysis for soluble aggregates, by SDS-Page analysis for soluble, covalently linked aggregates and turbidity measurements of insoluble aggregates. SDS-Page was also performed to investigate the formation of rhIL-11 fragments, which is described to occur upon stress [51]. The rhIL-11 precipitates were incubated for 24 hours at $2-8\,°C$ and redissolved before analysis. RhIL-11 bulk solution was incubated under the same conditions and analyzed as reference.

The initial amount of soluble aggregates in the rhIL-11 bulk material was determined with 3.1% (Figure 8A). The incubation of the rhIL-11 bulk solution led to a slight, but insignificant (P > 0.05) reduction of soluble aggregates to 2.6%. Turbidity measurements indicated no formation of insoluble aggregates due to incubating the bulk solution for 24 hours at $2-8\,°C$ (Figure 8B). The precipitation of rhIL-11 with ammonium carbamate

increased the amount of soluble aggregates to 4.6%, whereas the precipitation with ammonium sulfate raised the soluble aggregate level to 3.6%. The turbidity increase in the ammonium sulfate sample was accompanied by a high standard deviation and therefore was determined as insignificant (P > 0.05).
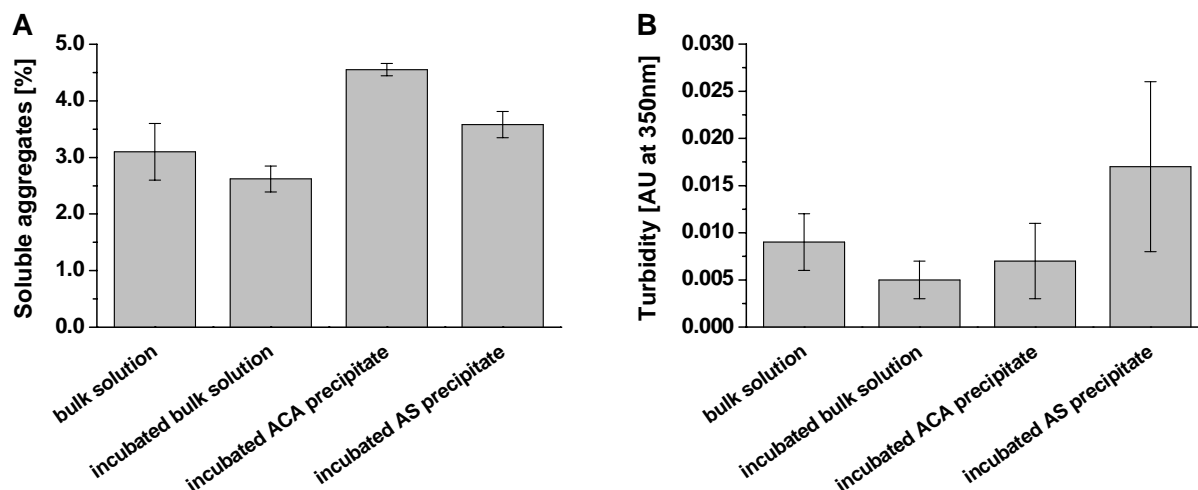
Figure 8 Soluble aggregates **(A)** and insoluble aggregates **(B)** of rhIL-11 bulk solution and precipitates with ammonium carbamate (ACA) and ammonium sulfate (AS)

SDS-Page analysis also revealed that covalently linked or insoluble aggregates did not form (Figure 9). The apparent resistance of rhIL-11 against aggregation under precipitation conditions was regarded as advantageous for further processing of protein precipitates. However, the precipitation with ammonium salts induced the formation of rhIL-11 fragments as in both precipitate samples additional bands appeared at lower molecular weight. These bands can be ascribed to protein fragments of 13.8 kDa and 5.2 kDa, which are main degradation products of rhIL-11 due to deamidation related peptide bond cleavage under stress conditions [51].

Conclusively, quantitative rhIL-11 precipitation was achieved using ammonium carbamate and ammonium sulfate. Precipitation conditions did not lead to formation of protein aggregates. However, traces of protein fragments were detected indicating that the precipitation itself might be stressful for rhIL-11.
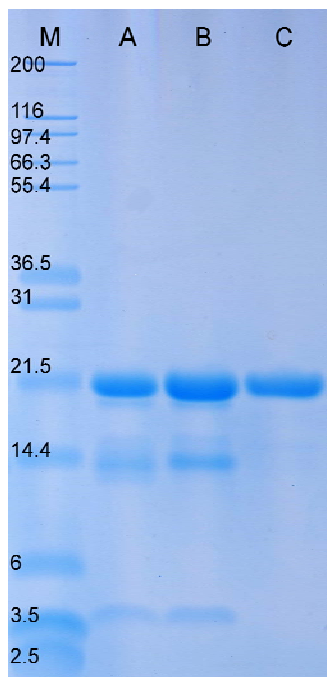
Figure 9 SDS-Page gel of different rhIL-11 formulations:
- **(M)** Standard protein marker
- **(A)** Incubated ammonium sulfate precipitate
- **(B)** Incubated ammonium carbamate precipitate
- **(C)** Incubated bulk solution

4 Evaluation of volatility upon spray drying

The results of the previous section revealed that quantitative precipitation with the potentially volatile precipitating agent ammonium carbamate could be achieved for IgG_1 and rhIL-11. Both proteins were sufficiently stable during the precipitation process. The next step was to demonstrate the quantitative removal of the precipitating agent based on its volatility in the spray drying process. Therefore, a placebo solution containing 10% (w/v) ammonium carbamate and 10% (w/v) mannitol was spray dried at different temperatures and different feed flow rates. The applied inlet temperature T_{in} ranged from 110 to 210 °C, corresponding to outlet temperatures T_{out} of 60 to 110 °C. The feed flow rate was set to 1.5 mL/min or 3.0 mL/min, respectively. In order to evaluate the conditions at which ammonium carbamate would be completely removed by decomposition, CHN analysis of the spray-dried powders was conducted to detect residual ammonium.

As shown in Figure 10, ammonium carbamate was readily decomposed by exposure to the hot drying air in the spray chamber and the initial amount of 50% ammonium carbamate was drastically diminished in the spray-dried powders. However, by applying rather mild drying conditions of 110 / 60 °C, approximately 2.8% ammonium carbamate could still be detected in the spray-dried powder. An increase of the spray drying inlet temperature

was necessary to reduce the residual precipitant content further, and by spray drying at 210 / 110 °C, ammonium carbamate was completely evaporated. Given that these high temperatures might be critical with regard to protein stability, a reduction of the feed flow rate was additionally investigated for its effect on precipitant decomposition. The feed flow rate was reduced from 3.0 mL/min to 1.5 mL/min. A temperature setting of 150 / 75 °C was not sufficient for a complete evaporation of ammonium carbamate. However, if the spray drying temperature was adjusted to 170 / 90 °C, CHN analysis revealed that ammonium carbamate was completely removed.
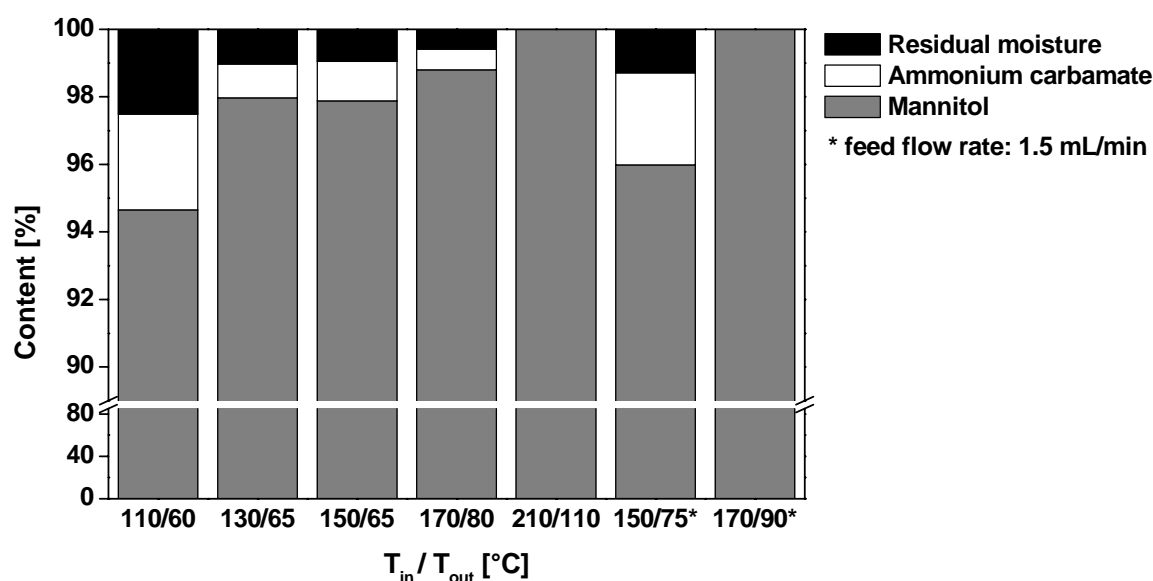
Figure 10 Composition of spray-dried 10% mannitol / 10% ammonium carbamate powder determined by CHN analysis and Karl-Fischer measurements

The potential of eliminating the precipitant by means of spray drying was further challenged by increasing the initial ammonium carbamate content. A placebo solution containing 50% (w/v) ammonium carbamate and 10% (w/v) mannitol was spray dried at different temperatures and different feed flow rates (Figure 11). After spray drying, the collected powders were exposed to an additional vacuum drying step by incubation of the unclosed product vials at 0.05 hPa for 24 hours. CHN analysis of the spray-dried powders was performed immediately after spray drying and after the vacuum drying step.
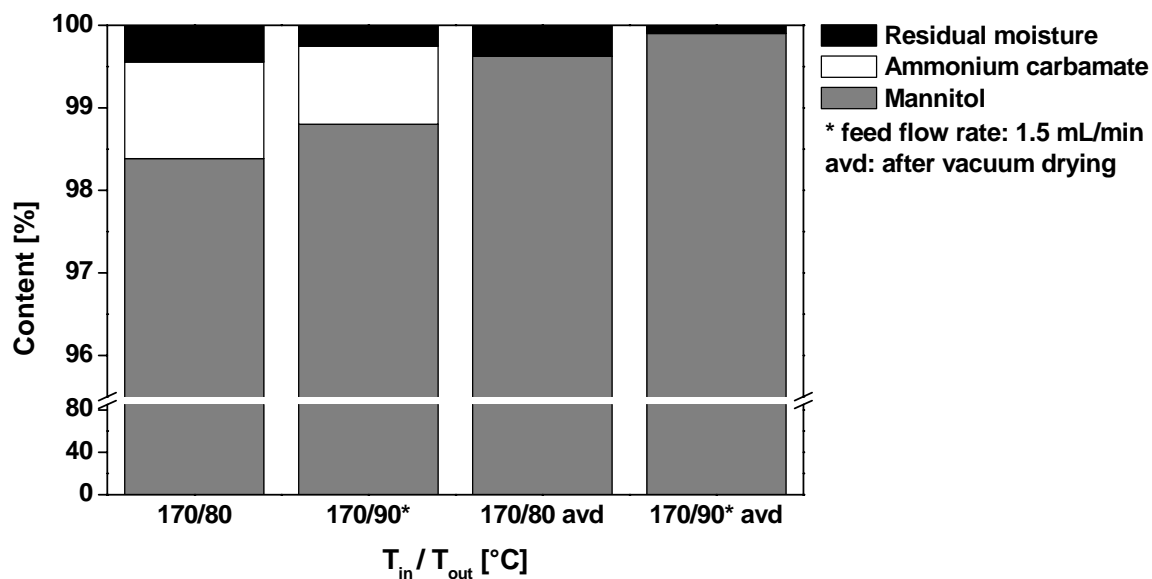
Figure 11 Composition of spray-dried 10% mannitol / 50% ammonium carbamate powder
determined by CHN analysis and Karl-Fischer measurements

Using the 50% ammonium carbamate containing solution, higher residual precipitant concentrations in the spray-dried powders were found compared to the 10% ammonium carbamate solution. Immediately after spray drying, 1.2% ammonium carbamate (instead of 0.6%) were detected for spray drying temperatures of 170 / 80 °C, and 1.0% (instead of 0.0%) for 170 / 90 °C. Obviously, the applied spray drying conditions were not adequate to decompose ammonium carbamate completely in the high concentration solution. Therefore, vacuum drying of the spray-dried powders was performed as an additional treatment step post spray drying. Thereby, the content of ammonium carbamate was reduced below the detection limit of CHN analysis. This additional process step ensures the complete removal of the volatile precipitant.

In conclusion, the volatility of ammonium carbamate was distinct enough to remove the precipitating agent from placebo powders by spray drying. Therefore, further investigations covered the spray drying of ammonium carbamate protein precipitates.

5 Spray drying of protein precipitates

After evaluation of the efficiency of ammonium carbamate to precipitate IgG_1 and rhIL-11 and the successful application of spray drying for the removal of ammonium carbamate from placebo powders, the spray drying of protein precipitates was performed and the influence on protein stability was investigated.

5.1 Spray drying of IgG_1 precipitates

Table 3 summarizes the IgG_1 formulations prepared for evaluating the protein precipitate spray drying process. All samples contained 2.5 mg/mL IgG_1 and 1.1 mg/mL trehalose in MilliQ water resulting in a protein / sugar ratio of 70:30. This very ratio had been identified as optimal to preserve antibody stability during spray drying [52]. Spray drying conditions were comparable for all formulations:

- T_{in} 170 - 172 °C
- T_{out} 76 - 79 °C
- Feed flow   1.5 mL / min

After spray drying, the collected powders were exposed to a vacuum drying step by incubation of the unclosed product vials at 0.05 hPa for 24 hours.

Table 3 IgG_1 formulations for evaluating the spray drying of protein precipitates

#	Formulation	Precipitant	Additional parameters
Mab_1a	Solution	-	-
Mab_1b	Solution at pH 9.3	-	Adjusted to pH 9.3 with 1N NaOH
Mab_2	Precipitate	Ammonium carbamate	-
Mab_3	Solution	Ammonium carbamate	Below precipitation concentration
Mab_4	Precipitate	Ammonium sulfate	-

Mab_1a constitutes a reference formulation, as the IgG_1 / trehalose standard was spray dried as solution without any precipitant. With Mab_1a, influences of the spray drying process on the protein stability were investigated. For Mab_1b, the pH of the IgG_1 / trehalose standard solution was adjusted with 1N NaOH to pH 9.3 . The pH shift reflected the pH conditions in the ammonium carbamate precipitate formulation to evaluate negative influences of a slightly alkaline environment on protein stability. Ammonium carbamate was used at a concentration of 28% (w/w) to precipitate IgG_1 / trehalose and the precipitate was

spray dried as Mab_2. In addition, ammonium carbamate was applied at a far lower concentration (19%), which was not adequate to cause protein precipitation. Thereby, the effect of the presence of the precipitant was evaluated (Mab_3). Finally, ammonium sulfate as alternative, non-volatile protein precipitant was utilized to induce IgG_1 precipitation (Mab_4). The investigation of ammonium sulfate as alternative precipitating agent served as proof of concept. In contrary to ammonium carbamate, ammonium sulfate is a default, widely applied protein precipitant and remains in the spray-dried product due to its non-volatility. By comparing both ammonium salts, a clearer statement should be possible whether the concept of precipitation before spray drying is beneficial with regard to protein stability.

Spray-dried powders were analyzed for soluble aggregates by HP-SEC and insoluble aggregates by turbidity measurements (Table 4). IgG_1 showed an excellent stability in the spray-dried product, if the protein solution was spray dried as standard formulation. If the pH of the solution was increased to 9.3, the amount of soluble aggregates increased slightly from 0.5% to 0.9% and the turbidity increased from 0.016 to 0.044 AU. This result indicated robustness of the antibody in an alkaline milieu. However, when spray drying Mab_2 (IgG_1 / ammonium carbamate precipitate), soluble aggregates and turbidity increased drastically to 10.0% and 0.276 AU, respectively. If the concentration of ammonium carbamate was kept below the precipitation limit (Mab_3), the negative effect was less pronounced, however with 3.1% soluble aggregates and 0.197 AU the formulation was worse than the standard IgG_1 formulation. The reference formulation containing ammonium sulfate (Mab_4) was slightly less detrimental for the protein with regard to protein stability (2.4%, 0.090 AU), but the concept of stabilizing IgG_1 by precipitation before spray drying failed.

Table 4 Aggregate status of different IgG_1 formulations as determined by HP-SEC and turbidity measurements

#	Formulation	HP-SEC aggregates [%]	Turbidity / OD_{350nm} [AU]
Mab_1a	Solution	0.5 ± 0.1	0.016
Mab_1b	Solution at pH 9.3	0.9 ± 0.1	0.044
Mab_2	Precipitate	10.0 ± 0.2	0.276
Mab_3	Solution	3.1 ± 0.5	0.197
Mab_4	Precipitate	2.4 ± 0.2	0.090

Conclusively, IgG$_1$ revealed severe instabilities in the formulations containing an ammonium salt, independently of the kind of salt (carbamate or sulfate) or the state of the protein (solution or precipitate). As IgG$_1$ showed good protein stability when spray dried at pH 9.3, the alkaline milieu in the ammonium carbamate precipitate cannot be hold responsible for protein aggregation. Furthermore, the chemistry of the decomposing ammonium carbamate was considered as possible source for protein aggregation. The decomposition of the ammonium carbamate could have detrimental effects on protein stability due to formation of aggressive decomposition species (e.g. carbon dioxide, ammonia). In addition, dissolution of the protein precipitate might occur in the atomized spray solution, as ammonium carbamate is thermally decomposed at temperatures above its decomposition temperature (35 °C) and the precipitant concentration might fall below the concentration necessary for quantitative protein precipitation. Even if the precipitate was just partially dissolved, the stabilization of the protein cannot be guaranteed. By using ammonium sulfate, both issues, the possible effects of chemically reactive decomposition products and the dissolution of precipitate, were eliminated. However, the ammonium sulfate precipitate also showed decreased protein stability.

Therefore, two possible conclusions could be drawn:
- Either the concept of protein precipitation lacks the ability to stabilize the protein during the spray drying process.
- Alternatively, IgG$_1$ was an inappropriate model protein to determine the effect of precipitation on protein stability during spray drying, as the antibody is quite resistant towards surface induced aggregation. Its persistency is proven by the fact, that it was possible to formulate IgG$_1$ as stable, surfactant-free powder using spray drying.

5.2 Spray drying of rhIL-11 precipitates

RhIL-11 was used as a second protein to evaluate the possibility to stabilize proteins during spray drying by precipitation with volatile salts. The rationale for the use of rhIL-11 was the distinct surface binding activity of this protein, which makes rhIL-11 exceptionally prone to surface adsorption and consequently protein unfolding and aggregation [48]. The higher sensitivity of rhIL-11 compared to IgG$_1$ towards surface induced aggregation obligated the use of a surfactant in the spray drying formulation, entailing negative consequences like reduced long-term protein stability [16]. The use of rhIL-11 should reveal if precipitation would be an effective method to prevent protein adsorption at the air–liquid interface and thereby protein aggregation during spray drying.

The following rhIL-11 formulations were prepared (Table 5). The standard formulation was adopted from Fitzner [20], who proved the possibility to prevent surface adsorption and consequently denaturation and aggregation of rhIL-11 by addition of 0.02% polysorbate 80 to the spray solution. The standard formulation without surfactant served as negative reference as protein aggregation at the air–liquid interface was caused deliberately. Ammonium carbamate was investigated as volatile precipitant and ammonium sulfate as reference precipitating agent. In all formulations, methionine acted as antioxidant, and glycine and trehalose as water-replacing stabilizers.

Table 5 RhIL-11 formulations in 10mM phosphate buffer for evaluating the spray drying of protein precipitates

Excipient Formulation	Standard formulation	Standard formulation without surfactant	Ammonium carbamate precipitate	Ammonium sulfate precipitate
rhIL-11 [mg/mL]	5	5	5	5
Methionine [mM]	10	10	10	10
Trehalose / Glycine	15 / 85	15 / 85	15 / 85	15 / 85
- Trehalose [mM]	40.84	40.84	40.84	40.84
- Glycine [M]	1.057	1.057	1.057	1.057
Polysorbate 80 [%]	0.02	-	-	-
Ammonium carbamate [%]	-	-	26.3	-
Ammonium sulfate [%]	-	-	-	26.3

Table 6 summarizes the analysis for protein aggregates in the reconstituted spray-dried powders. Spray drying the rhIL-11 standard formulation resulted in the formation of 5.4% soluble aggregates (initial rhIL-11 bulk solution: 3.1%) and a turbidity of 0.029 AU or 5.8 FNU, respectively. However, if the standard formulation was spray dried without the addition of surfactant, a massive increase of soluble aggregates to 10.4% and higher turbidity were observed. This higher aggregate status of the surfactant-free formulation showed the innate surface activity of rhIL-11, which led to protein adsorption at the air–liquid interface and protein unfolding and aggregation. The results for the ammonium carbamate precipitate pointed in a different direction: 5.2% soluble aggregates and a turbidity of 0.032 AU / 4.9 FNU were measured. Obviously, although the spray drying solution contained no surfactant, the aggregate status was comparable to the standard formulation. Thereby, protein precipitation was capable to prevent the adsorption of rhIL-11 at the surface of aerosol droplets and to reduce protein aggregation. The reference formulation with

ammonium sulfate as precipitating agent contained even less soluble aggregates, however, a drastic increase of insoluble aggregates (0.287 AU, 127.4 FNU) was observed.

Table 6 Analysis of spray-dried rhIL-11 powders after reconstitution

Analysis method \ Formulation	Standard formulation	Standard formulation without surfactant	Ammonium carbamate precipitate	Ammonium sulfate precipitate
HP-SEC aggregates [%]	5.4 ± 0.5	10.4 ± 0.1	5.2 ± 0.1	3.2 ± 0.2
OD_{350nm} [AU]	0.029 ± 0.003	0.052 ± 0.002	0.032 ± 0.004	0.287 ± 0.009
Turbidity [FNU]	5.8 ± 0.5	37.7 ± 3.7	4.9 ± 1.1	127.4 ± 17.1

The formation of larger rhIL-11 aggregates by ammonium sulfate was confirmed by particle analysis using light blockage. Figure 12 shows that the standard formulation and the ammonium carbamate precipitate contained similar numbers of particles. However, the standard formulation without surfactant showed an increased amount of smaller particles, whereas the ammonium sulfate precipitate formed higher numbers of particles in the 2 to 50 µm range. The crystallization of ammonium sulfate during spray drying might account for the formation of protein aggregates.
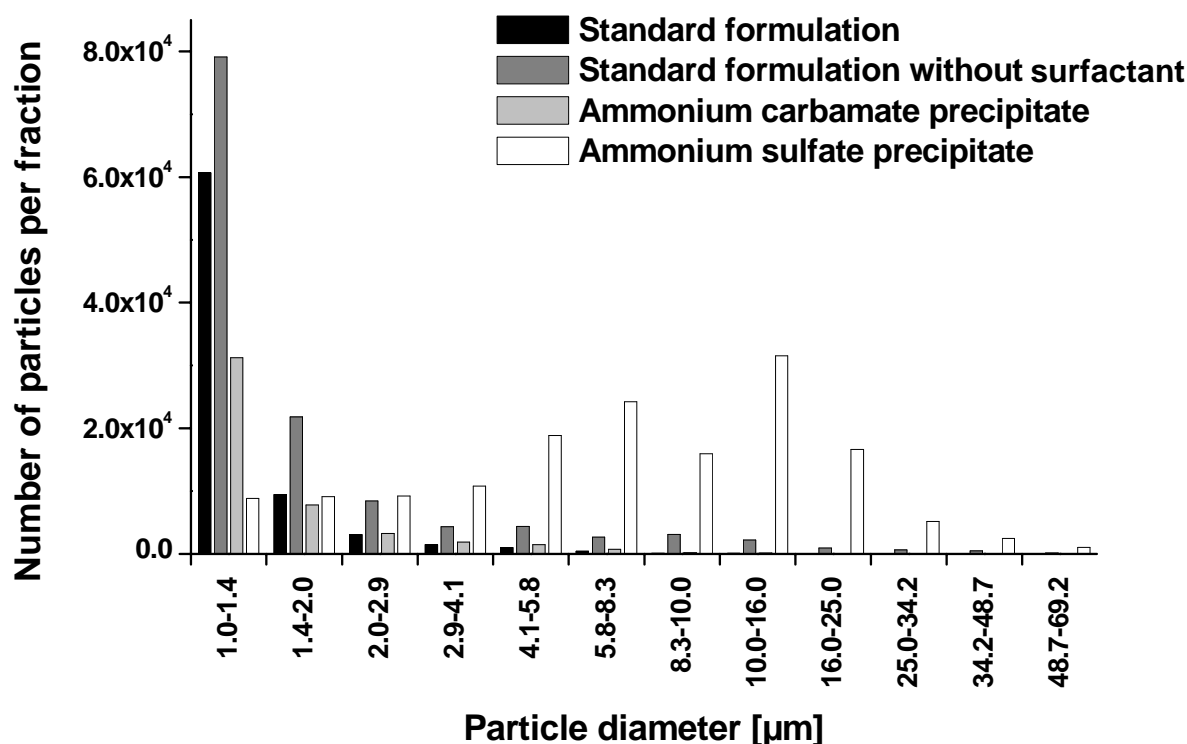
Figure 12 Subvisible particles of reconstituted rhIL-11 powders

Figure 13 also supports this distinct aggregate formation in the ammonium sulfate precipitate, as the reconstituted solution appeared explicitly opalescent compared to all other samples.
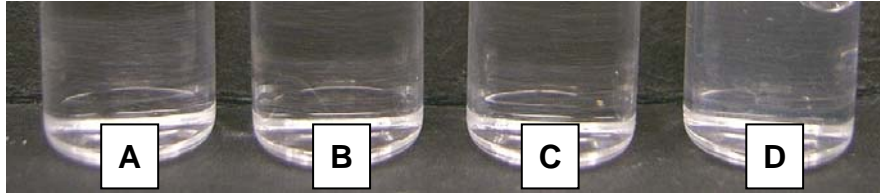
Figure 13 Reconstituted spray-dried rhIL-11:
        (A) Standard formulation
        (B) Standard formulation without surfactant
        (C) Ammonium carbamate precipitate
        (D) Ammonium sulfate precipitate

Gel electrophoresis (Figure 14) revealed that all formulations, including the unprocessed bulk solution, contained small amounts of fragments. However, the spray-dried ammonium sulfate precipitate contained significantly more fragments, indicating the reduced protein stability due to peptide cleavage in this formulation. None of the analyzed samples contained covalent aggregates indicating that the subvisible particles formed originated from aggregated unfolded protein.
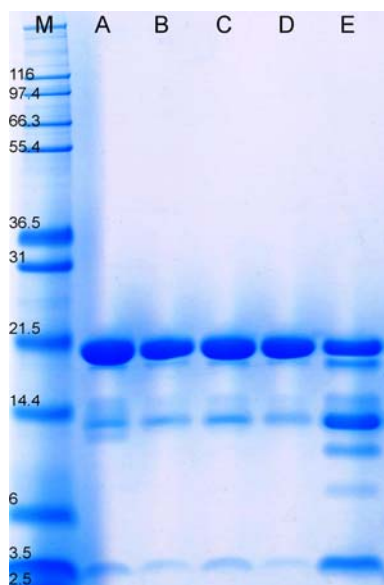
Figure 14 SDS-Page gel of different rhIL-11 formulations after
        reconstitution:
        (M) Standard protein marker
        (A) Unprocessed bulk solution
        (B) Standard formulation
        (C) Standard formulation without surfactant
        (D) Ammonium carbamate precipitate
        (E) Ammonium sulfate precipitate

Figure 15 shows SEM pictures of the spray-dried rhIL-11 powders. The powder of rhIL-11 standard formulation consisted of spherical particles with a smooth surface and a broad particle size distribution. If the standard formulation was spray dried without surfactant, the powder particles appeared wrinkled with a rugged surface, which has previously been observed by Fitzner [20]. Both precipitants caused the formation of coarse particles.
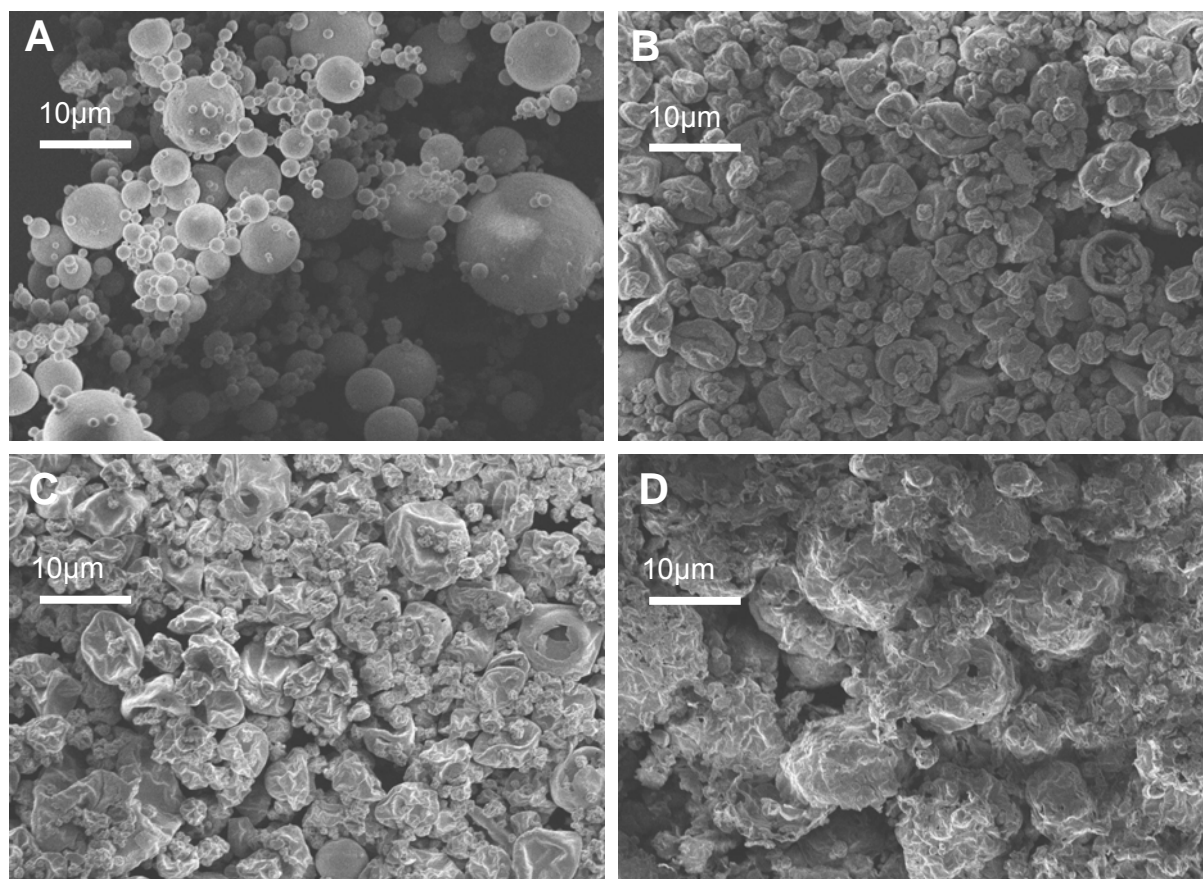
Figure 15 SEM of spray-dried particles
  (A) Standard formulation
  (B) Standard formulation without surfactant
  (C) Ammonium carbamate precipitate
  (D) Ammonium sulfate precipitate

Powder diffraction analysis of the spray-dried powders revealed distinct differences between the formulations containing non-precipitated rhIL-11 and the formulations containing protein precipitate (Figure 16). Both diffractograms of the standard formulation with (A) and without (B) surfactant indicated a partial crystalline state of the powder with the characteristic pattern of glycine in its β-modification, which is the least stable glycine modification according to literature [47]. The pattern of the ammonium carbamate precipitate diffractogram (C) was assigned to γ-glycine according to literature references [48][49] as pattern agreement was found for 21.8, 25.3, 29.2, 29.7, 30.1, 35.9, 38.9 and 39.0 °2-Theta. The assignment of the peaks in

the ammonium carbamate precipitate to glycine was proved by spray drying and analysis of a reference formulation containing ammonium carbamate precipitate, but no glycine. The resulting powder (D) was completely amorphous and showed no indication of residual ammonium carbamate, as the respective ammonium carbamate peaks (E) did not appear. In the spray-dried ammonium sulfate precipitate (F), the peaks of ammonium sulfate (G) dominated the diffractogram and the powder showed complete crystallinity. This pronounced crystallinity might explain the higher aggregate status of rhIL-11, if spray dried as ammonium sulfate precipitate. Even if trehalose remained amorphous during spray drying, the crystallization of ammonium sulfate by itself could be detrimental for rhIL-11 stability. Furthermore, phase separation during drying might amplify the negative impact on protein stability.
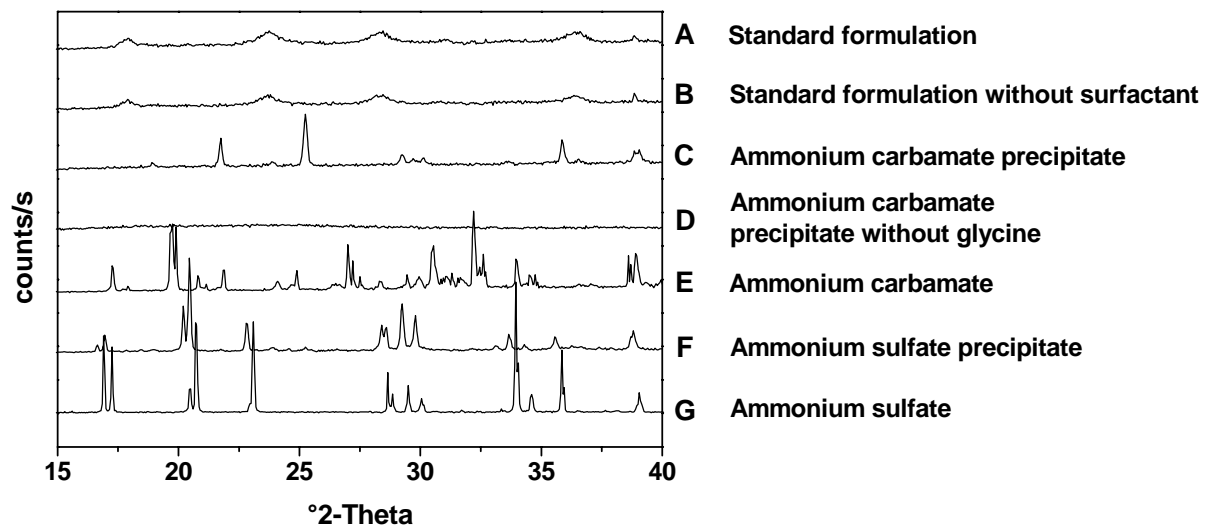
Figure 16 XRD diffractograms of spray-dried powders and references (ammonium carbamate, ammonium sulfate)

6   Summary and Conclusions

The hypothesis of stabilizing proteins by precipitation before spray drying and the thereby possible omission of surfactants was evaluated for an IgG_1 and rhIL-11. Ammonium carbamate was chosen as preferred precipitating excipient, as it showed high precipitation efficiency for both proteins and was eliminable by spray drying and an additional vacuum drying step, rendering a precipitant removal step unnecessary. For IgG_1, no beneficial effect of ammonium carbamate precipitation could be observed, as the minor surface affinity of this protein enables spray drying of a surfactant-free formulation. However, the stability of spray-dried rhIL-11 was immensely improved by ammonium carbamate precipitation in comparison to a surfactant-free formulation. Therefore, for highly surface-active proteins like rhIL-11 the concept of precipitation by a volatile salt before spray drying poses a valuable alternative to the addition of surfactant.

7 References

1 Sollohub K, Cal K. Spray drying technique: II. Current applications in pharmaceutical technology. *J Pharm Sci* 2009; 99: 1-11.

2 Maa YF, Prestrelski SJ. Biopharmaceutical powders: particle formation and formulation considerations. *Curr Pharm Biotechnol* 2000; 1: 283-302.

3 Wang W, Nema S, Teagarden D. Protein aggregation - Pathways and influencing factors. *Int J Pharmacol* 2010; 390: 89-99.

4 Chang BH, Kendrick BS, Carpenter JF. Surface-induced denaturation of protein drugs during freezing and its inhibition by surfactants. *J Pharm Sci* 1996; 85: 1554-1559.

5 Mumenthaler M, Hsu CC, Pearlman R. Feasibility study on spray-drying protein pharmaceuticals: recombinant human growth hormone and tissue-type plasminogen activator. *Pharm Res* 1994; 11: 12-20.

6 Maa YF, Nguyen PA, Hsu SW. Spray-drying of air-liquid interface-sensitive recombinant human growth hormone. *J Pharm Sci* 1998; 87: 152-159.

7 Millqvist-Fureby A, Malmsten M, Bergenstahl B. Spray-drying of trypsin - surface characterisation and activity preservation. *Int J Pharm* 1999; 188: 243-253.

8 Adler M, Unger M, Lee G. Surface composition of spray-dried particles of bovine serum albumin/trehalose/surfactant. *Pharm Res* 2000; 17: 863-870.

9 Gunning PA, Wilde PJ, Morris VJ. Effect of surfactant type on surfactant-protein interactions at the air-water interface. *Biomacromolecules* 2004; 5: 984-991.

10 Kiese S, Papppenberger A, Friess W, Mahler HC. Shaken, not stirred: mechanical stress testing of an IgG1 antibody. *J Pharm Sci* 2008; 97: 4347-4366.

11 Lang R, Winter G, Vogt L, Zurcher A, Dorigo B, Schimmele B. Rational design of a stable, freeze-dried virus-like particle-based vaccine formulation. *Drug Dev Ind Pharm* 2009; 35: 83-97.

12 Hawe A, Friess W. Development of HSA-free formulation for a hydrophobic cytokine with improved stability. *Eur J Pharm Biopharm* 2008; 68: 316-325.

13 Randolph TW, Jones LS. Surfactant-protein interactions. *Pharm Biotechnol* 2002; 13: 159-175.

14 Kerwin BA. Polysorbates 20 and 80 used in the formulation of protein biotherapeutics: structure and degradation pathways. *J Pharm Sci* 2008; 97: 2924-2935.

15 Knepp VM, Whatley JL, Muchnik A, Calderwood TS. Identification of antioxidants for prevention of peroxide-mediated oxidation of recombinant human ciliary neurotrophic factor and recombinant human nerve growth factor. *J Pharm Sci Technol* 1996; 50: 163-171.

16 Ha E, Wang W, Wang YJ. Peroxide formation in polysorbate 80 and protein stability. *J Pharm Sci* 2002; 91: 2252-2264.

17   Herman AC, Boone TC, Lu HS. Characterization, formulation, and stability of Neupogen (Filgrastim), a recombinant human granulocyte colony stimulating factor. *Pharm Biotechnol* 1996; 9: 303-328.

18   Wang W, Wang YJ, Wang DQ. Dual effects of Tween 80 on protein stability. *Int J Pharm* 2008; 347: 31-38.

19   Treuheit MJ, Kosky AA, Brems DN. Inverse relationship of protein concentration and aggregation. *Pharm Res* 2002; 19: 511-516.

20   Fitzner M. Chemical and physicochemical stability of spray-dried rhIL-11 formulations (*Thesis*) 2003.

21   Schellekens H. Factors influencing the immunogenicity of therapeutic proteins. *Neph Dial Trans* 2005; 20: vi3-vi9.

22   Mahler HC, Mekking A. Formulation Development of Therapeutic Proteins. In: Mahler HC, Borchard G and Luessen HL eds. *Protein Pharmaceuticals - Formulation, Analytics and Delivery*. Pharma Reflexions 2010: 144-161.

23   Arakawa T, Ejima D, Li T, Philo JS. The critical role of mobile phase composition in size exclusion chromatography of protein pharmaceuticals. *J Pharm Sci* 2010; 99: 1674-1692.

24   Serno T, Carpenter JF, Randolph TW, Winter G. Inhibition of agitation-induced aggregation of an IgG antibody by hydroxypropyl-beta-cyclodextrin. *J Pharm Sci* 2010; 99: 1193-1206.

25   Chi EY, Krishnan S, Randolph TW, Carpenter JF. Physical Stability of Proteins in Aqueous Solution: Mechanism and Driving Forces in Nonnative Protein Aggregation. *Pharmaceutical Research* 2003; 20: 1325-1336.

26   Krishnamurthy R, Manning MC. The stability factor: importance in formulation development. *Curr Pharm Biotechnol* 2002; 3: 361-371.

27   Schjerning H. Further contributions to the chemistry of protein precipitation. *Z anal Ch* 1898; 37: 73-87.

28   Burgess RR. Protein precipitation techniques. *Methods Enzymol* 2009; 463: 331-342.

29   Harrison RG. Bioseparations science and engineering. 2002: 432.

30   Trevino SR, Scholtz JM, Pace CN. Measuring and increasing protein solubility. *J Pharm Sci* 2008; 97: 4155-4166.

31   McPherson A. Current approaches to macromolecular crystallization. *Eur J Biochem* 1990; 189: 1-23.

32   Matheus S. Development of High Concentration Cetuximab Formulations using Ultrafiltration and Precipitation Techniques (*Thesis*) 2006.

33   Englard S, Seifter S. Precipitation techniques. *Methods Enzymol* 1990; 182: 285-300.

34   Hofmeister F. Zur Lehre von der Wirkung der Salze. Zweite Mittheilung. *Arch Exp Pathol Pharmakol* 1888; 24: 247-260.

35   Timasheff SN, Arakawa T. Mechanism of Protein Precipitation and Stabilization by Co-Solvents. *J Crystal Growth* 1988; 90: 39-46.

36   Arakawa T, Timasheff SN. Preferential interactions of proteins with salts in concentrated solutions. *Biochemistry* 1982; 21: 6545-6552.

37   Bechtold-Peters K. Protein immobilization by crystallization and precipitation: an alternative to lyophilization. *Biotechnol: PharmAspects*; 11: 149-175.

38   Tzannis S, Dasovich N, Kumar S, Sadrzadeh N. Improved sustained release compositions for delivery of pharmaceutical proteins. 2005 (Patent: 2005067898).

39   Schwartz D. Development of an Aqueous Suspension of Recombinant Human Bone Morphogenetic Protein-2 (rhBMP-2) (*Thesis*) 2005.

40   Koerber M, Bodmeier R. Development of an in situ forming PLGA drug delivery system. *EurJPharmSci* 2008; 35: 283-292.

41   Herrmann S, Mohl S, Siepmann F, Siepmann J, Winter G. New insight into the role of polyethylene glycol acting as protein release modifier in lipidic implants. *Pharm Res* 2007; 24: 1527-1537.

42   Tomasula PM, Craig JC, Jr., Boswell RT, Cook RD, Kurantz MJ, Maxwell M. Preparation of casein using carbon dioxide. *J Dairy Sci* 1995; 78: 506-514.

43   Hofland GW, de Rijke A, Thiering R, van der Wielen LAM, Witkamp GJ. Isoelectric precipitation of soybean protein using carbon dioxide as a volatile acid. *J Chromat B: Biomedical Sciences and Applications* 2000; 743: 357-368.

44   Qi X, Yao S, Guan Y, Zhu Z. A novel system for protein precipitation - carbon dioxide-water-ethanol system. *Huagong Xuebao (ChinEd)* 2005; 56: 135-141.

45   Watanabe EO, Pessoa PD, Miranda EA, Mohamed RS. Evaluation of the use of volatile electrolyte system produced by ammonia and carbon dioxide in water for the salting-out of proteins: precipitation of porcine trypsin. *Biochem Eng J* 2006; 30: 124-129.

46   Savitzky A, Golay MJE. Smoothing and differentiation of data by simplified least squares procedures. *Anal Chem* 1964; 36: 1627-1639.

47   Schur PH. IgG subclasses - a review. *Ann Allergy* 1987; 58: 89-99.

48   Page C, Dawson P, Woollacott D, Thorpe R, Mire-Sluis A. Development of a lyophilization formulation that preserves the biological activity of the platelet-inducing cytokine interleukin-11 at low concentrations. *J Pharm Pharmacol* 2000; 52: 19-26.

49   Byler DM, Susi H. Examination of the secondary structure of proteins by deconvolved FTIR spectra. *Biopolymers* 1986; 25: 469-487.

50   Bandekar J. Amide modes and protein conformation. *BiochimBiophysActa, Protein StructMolEnzymol* 1992; 1120: 123-143.

51   Zhang W, Czupryn MJ, Boyle PT, Amari J. Characterization of Asparagine Deamidation and Aspartate Isomerization in Recombinant Human Interleukin-11. *Pharm Res* 2002; 19: 1223-1231.

52   Schuele S, Schulz-Fademrecht T, Garidel P, Bechtold-Peters K, Friess W. Stabilization of IgG$_1$ in spray-dried powders for inhalation. *Eur J Pharm Biopharm* 2008; 69: 793-807.

Chapter 2

Evaluation of the Nano Spray Dryer B-90 for pharmaceutical applications

Abstract

The vibrating mesh spray technology implemented in the Nano Spray Dryer B-90 was evaluated for pharmaceutical applications by spray drying common pharmaceutical excipients (trehalose, mannitol) and model drugs (e.g. griseofulvin). Aerosol droplet size measurements investigated the influence of spray solution factors like viscosity, conductivity, and surface tension and the influence of the vibrating mesh aperture size on particle characteristics. Particle deposition on the spray nozzle was addressed by analyzing the influence of spray solute concentration and solvent on the process outcome. Submicron particles with 0.5 µm and 0.8 µm mean particle size were obtained at high yields for 50 mg powder amounts.

1 Introduction

Sophisticated drug delivery approaches frequently demand the development and production of innovative micro- and nanoparticles [1]. For example, controlled release via pulmonary drug delivery was attempted with microparticles containing therapeutic proteins [2] and the nasal administration route was assessed by spray-dried IgG antibody microparticles [3]. To keep pace with the fast growing requirements to particle characteristics and abilities, scientists constantly seek for new options to produce micro- and nanoparticles with specific features. Among the various techniques evaluated for particle engineering, spray drying is well-established and widely used in research, development and production. In general, spray drying offers one main advantage over other particle engineering techniques: particle size and density, both crucial features with regard to drug delivery, can be controlled in one single step [4]. However, during the early stages of product development, only minute amounts (milligrams scale) of new active pharmaceutical ingredients are typically available for formulation design. Traditional spray dryers require at least 30 mL of liquid sample to start with. To overcome this challenge, the novel Nano Spray Dryer B-90 (Büchi Labortechnik AG, Flawil, Switzerland) was developed [5]. The aim of this study was to evaluate it for its benefits as lab scale spray dryer in pharmaceutical formulation applications as it allows spray drying sample volumes as small as 1 mL.

1.1 Characteristics of the Nano Spray Dryer B-90

The Nano Spray Dryer B-90 (Figure 1) comprises three technological novelties concerning the spray drying process: a vibrating mesh spray technology was implemented to generate fine aerosol droplets, a laminar drying air flow in the spray chamber to provide instant drying of the aerosol at mild conditions, and an electrostatic particle collector to effectively separate finest particles from the drying air. The combination of the innovative atomization principle and the efficient product separation provides the opportunity to utilize spray drying for a whole variety of new applications.

Figure 1 Nano Spray Dryer B-90 (left) and atomization by spray nozzle (right)

In a traditional spray dryer the dispersion of the spray solution is achieved either by pressure (two fluid nozzle), centrifugal forces (rotary disk atomizer) or ultrasound agitation (ultrasonic nozzle) [6]. The Nano Spray Dryer B-90 uses the vibrating mesh spray technology to generate the aerosol (Figure 1). A piezoelectric actuator causes the vibration of a thin, perforated stainless steel membrane with ultrasonic frequencies. The vibration of the membrane (spray mesh) causes a 'micro pumping action' [7] and the formation of droplets with very narrow size distribution. Spray meshes are available with 4.0 µm, 5.5 µm and 7.0 µm apertures. Instead of using a cyclone to collect the dry particles, the Nano Spray Dryer is equipped with an electrostatic particle collector consisting of a stainless steel cylinder (anode = particle collecting electrode) and a star-shaped counter electrode (cathode) inside the cylinder. During the spray process, high voltage is applied between the electrodes and spray-dried particles get electrically charged and deposited on the inner wall of the cylinder electrode. After completion of the spray drying process, the fine powder is conveniently collected using a particle scraper. This particle separation principle enables the collection of powder particles in the micron to submicron size range at high yields even for small sample quantities in the milligrams range [8].

1.2   Evaluation procedure

First of all, the ability of the new atomization technique to generate a fine aerosol was assessed by laser diffraction droplet size measurements. Spray drying experiments were conducted using the common formulation excipients mannitol and trehalose, together with the surfactant polysorbate 20 and buffer components like phosphate salts. Particle size and shape were analyzed to adequately control and fine tune the whole spray drying process. The influences of the spray rate, mesh size, drying air temperature and spray fluid characteristics were investigated. In addition, the minimal required drying temperature to gain a dry powder was determined to evaluate the technology for the future spray drying of heat sensitive compounds e.g. therapeutic proteins. This evaluation procedure should reveal the pros and cons of using the Nano Spray Dryer B-90 as lab scale formulation tool in comparison to already existing spray drying technologies and evaluate the suitability of the new spray drying device to produce submicron particles at high yields.

2 Materials and Methods

2.1 Materials

Griseofulvin (Welding, Frankfurt, Germany), benzocaine (Fagron, Barsbüttel, Germany), trehalose (Ferro Pfanstiehl, Cleveland, USA), disodium phosphate (VWR, Leuven, Belgium), polysorbate 20 and salicylic acid (both Merck, Darmstadt, Germany) were used to evaluate the Nano Spray Dryer B-90. Methanol, acetone and ethyl acetate were obtained from Sigma (Munich, Germany) in analytical grade. All sprayed solutions mentioned in the individual sections were prepared as % (w/w) solutions using either MilliQ water or the respective organic solvent. At least 10 mL of each solution was spray dried.

2.2 Methods

2.2.1 Spray drying with the Nano Spray Dryer B-90

The Nano Spray Dryer B-90 was operated in open loop for aqueous solutions with in-house pressurized air at a flow rate of 120 L/min. For organic solvent solutions the spray dryer was connected to the Inert Loop B-295 (Büchi Labortechnik AG, Flawil, Switzerland). Nitrogen gas was used at a flow rate of 120 L/min. The residual oxygen level in the system was controlled below 4%. Unless otherwise mentioned, the spray drying experiments were typically run at an inlet temperature T_{in} of 70 °C using a spray mesh with 4.0 µm aperture size. The yield was calculated from the actually obtained powder amount in relation to the solid content of the used spray solution.

2.2.2 Droplet size analysis

Droplet sizes of aerosols generated by the various spray meshes were determined by laser diffraction using a Mastersizer X (Malvern, Herrenberg, Germany). The nozzle of the Nano Spray Dryer B-90 was operated outside the spray dryer and was installed 8 cm (y) vertically above the He-Ne laser beam and in 6 cm (x) distance to the lens (Figure 2). A plastic shield with a hole in the center for the laser beam protected the lens of the Mastersizer X from droplet deposition. Droplet size distribution was determined in triplicate and reported using d_{10}, d_{50}, d_{90} and span values [$(d_{90} - d_{10}) / d_{50}$].
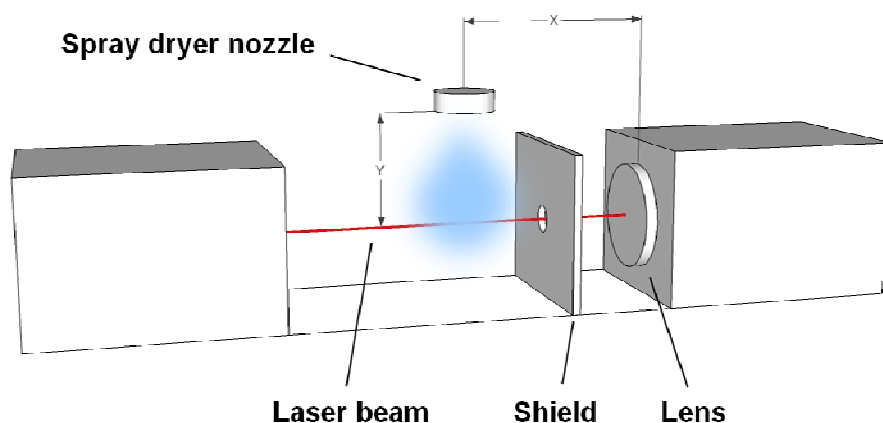
Figure 2 Experimental setup for droplet size analysis with the Mastersizer X

2.2.3 Conductivity measurements

The conductivity of spray solutions was measured with an Orion Star™ Series Meter and a 2-Cell conductivity electrode 013016MD with a cell constant of 0.1 cm^{-1} and a recommended application range of 0.01-300 µS/cm. Calibration of the conductivity electrode was achieved using Orion Conductivity / TDS Standard solutions (all Thermo Electron Cooperation, Beverly, USA).

2.2.4 Viscosity measurements

The viscosity of spray solutions was determined in triplicate at 25 °C using an AMVn Automated Micro Viscosimeter (Anton Paar, Osfilden, Germany).

2.2.5 Surface tension measurements

The surface tension of spray solutions was determined at 25 °C using a K100 tensiometer (Krüss, Hamburg, Germany) equipped with either the Krüss standard plate or the Krüss curved standard plate. The reported surface tensions are the average values of at least three measurements in the equilibrated state.

2.2.6 Particle size analysis

Spray-dried powders consisting of sugar or salt were analyzed by laser diffraction using a Partica LA-950 laser diffraction particle size analyzer (Horiba Ltd., Kyoto, Japan). Approximately 5 mg of the spray-dried powder was dispersed in Miglyol 812 using a UP50H Ultrasound Processor (Hielscher, Teltow, Germany) and analyzed in triplicate. Spray-dried drug powders were analyzed using a Helos H 2178 laser diffraction instrument in combination with a Rodos dry dispersing unit and a Vibri vibratory feeding unit (both Sympatec, Clausthal, Germany). The powder was fed with 60% intensity and dispersed at 4.0 bars. The used R2 lens covered a sample size range from 0.45 - 87.5 µm. All samples were measured in triplicate.

2.2.7 Karl-Fischer analysis

Residual moisture of the spray-dried powders was determined by Karl-Fischer titration with a titrator Aqua 40.00 (Analytik Jena AG, Jena, Germany) using a head space module oven to heat up approx. 10 mg powder to 80 °C.

2.2.8 Scanning electron microscopy (SEM)

The particle morphology of the spray-dried powders was determined by a JEOL scanning electron microscope JSM-6500F (Jeol, Eching, Germany). The samples were fixed on self-adhesive tapes on an aluminum stub and sputtered with carbon.

3   Results and Discussion

3.1   Droplet size analysis

Traditional pneumatic air spray nozzles offer various possibilities to influence droplet sizes. Apart from the nozzle design, a reduction in droplet size is achieved by increasing the gas–liquid mass ratio (relative velocity) and by decreasing the viscosity of the spray solution [6]. The spray formation in the Nano Spray Dryer B-90 is based on the vibrating mesh spray technology and operates without the use of pressurized air. The aperture size of the spray mesh is supposed to be one of the strongest factors influencing the droplet size, in addition to solution based parameters such as viscosity and surface tension. As the atomization principle of the vibrating mesh spray technology is not yet comprehensively investigated, the list of possible influences on droplet size might be amended by e.g. spray solution conductivity and other experimental parameters.

In a first study, spray meshes with 4.0, 5.5 and 7.0 μm aperture sizes were tested by spraying MilliQ water directly into the beam of the laser diffraction instrument. The resulting aerosols contained droplets of 3.3 μm (d_{10}) to 14.7 μm (d_{90}) size depending on the apertures of the mesh (Figure 3). The mean droplet size (d_{50}) ranged from 4.8 μm for the 4.0 μm mesh to 7.2 μm for the 7.0 μm mesh. A good correlation between the applied mesh size and the resulting droplet size was found.
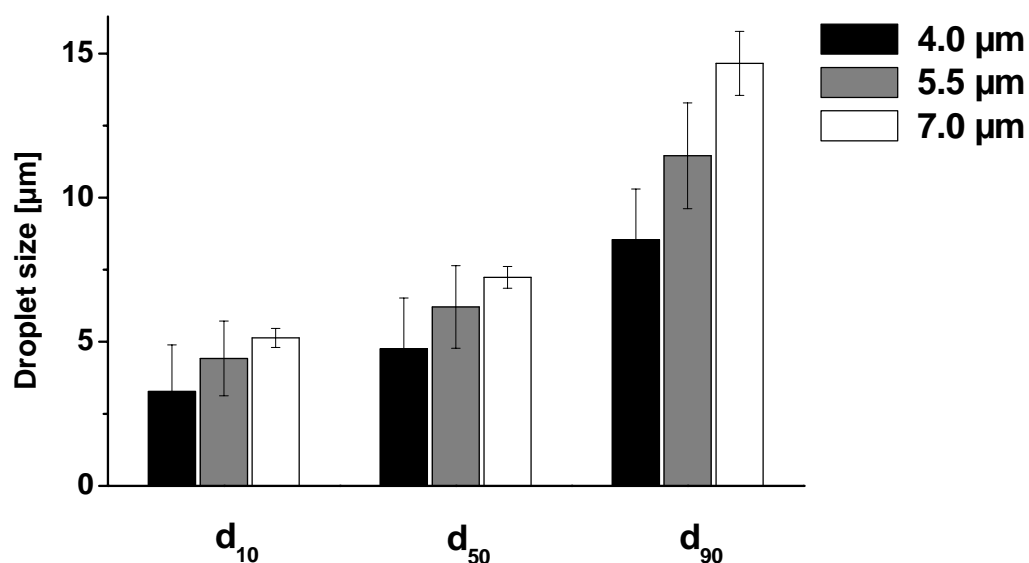
Figure 3 Droplet sizes of MilliQ water sprayed with different spray mesh aperture sizes

These droplet sizes were compared with the traditional lab scale Mini Spray Dryer B-290 (Büchi Labortechnik AG, Flawil, Switzerland), which atomizes liquids by means of a two-fluid nozzle and pressurized gas. As already mentioned, the amount and relative velocity of the atomizing gas has a direct impact on the resulting droplet size. For example, Maltesen et al. used a nozzle gas flow rate of 670 L/h as centre level for their quality by design study on spray drying insulin with the Mini Spray Dryer B-290 and found an average droplet diameter of 15.9 µm [9]. With applying the same gas flow rate to the Mini Spray Dryer B-290 nozzle in our laboratory, water droplet sizes of approx. 5.0 µm (d_{10}), 13.9 µm (d_{50}) and 29.5 µm (d_{90}) were measured. In general, the Nano Spray Dryer B-90 produced smaller droplets compared to the Mini Spray Dryer B-290. The maximal droplet size of approx. 15 µm when using the Nano Spray Dryer B-90 might limit certain applications. On the other side, the aerosols from the Nano Spray Dryer B-90 showed a narrower size distribution (span values approx. 1.2) compared to the Mini Spray Dryer B-290 aerosols (span values approx. 1.8). Atomization by the vibrating mesh spray technology is well-known to produce droplets with small size variations, which is especially utilized in pulmonary drug delivery, where vibrating mesh nebulizers produce larger fractions of inhalable droplets compared to conventional jet or ultrasonic nebulizers [7].

Pharmaceutical applications, such as inhalative drug delivery naturally ask for reproducible aerosol formation. A spray dryer has to fulfill the same requirements in order to establish a robust formulation process leading to particles of a defined size, if specific process parameters are applied. As the aperture size of the vibrating mesh mainly determines the droplet size, the consequences of a mesh replacement due to an excess of its wear lifespan were investigated. Three different spray meshes with the same aperture size (7.0 µm) were analyzed by droplet size measurements. The data show a good reproducibility of the droplet size within +/- 0.5 µm (Figure 4).
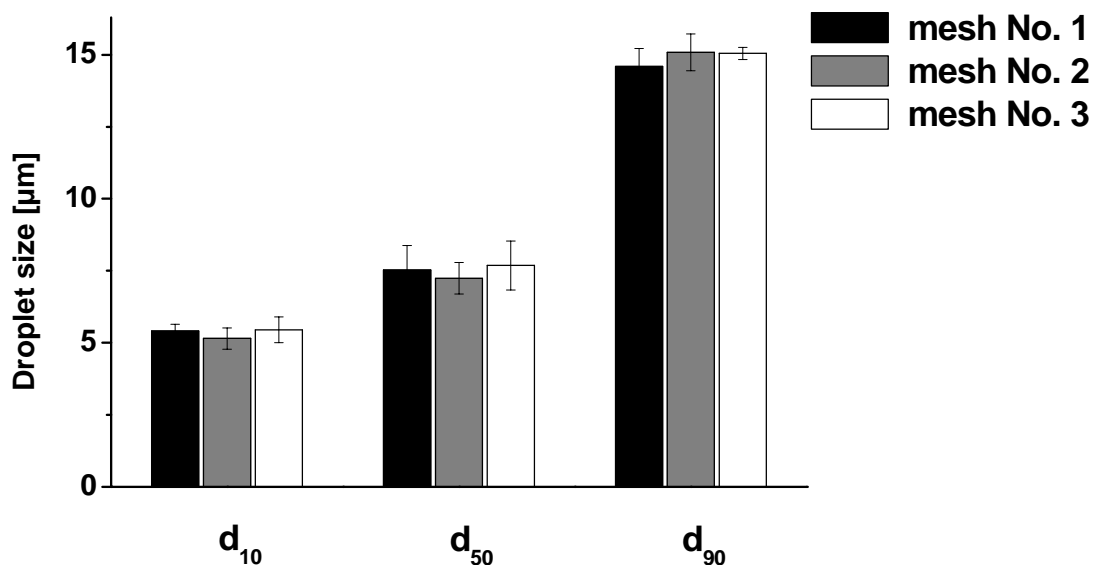
Figure 4 Droplet sizes of MilliQ water sprayed with three different meshes of the same aperture size

In addition, the viscosity and surface tension (Table 1) and droplet size (for a 4.0 µm spray mesh) of three different trehalose solutions (0.1, 1 and 10% concentrations) with and without the addition of polysorbate 20 (ratio sugar / surfactant 200:1) were analyzed. Polysorbate 20 is widely used as surfactant in spray drying [10]. Mean droplet sizes of approx. 5 µm were achieved independently of the sugar concentration or the addition of surfactant (Figure 5). Only the d_{90} values showed a slight increase in droplet size from 7.8 µm (without surfactant) to about 9.0 µm (with surfactant). This indicates that neither the total solid content, nor the viscosity or the surface tension of the spray solution greatly influence the droplet size formation with the vibrating mesh spray technology.

Table 1 Viscosity and surface tension of trehalose and trehalose / polysorbate 20 spray solutions

Spray solution	Viscosity [mPa*s]	Surface tension [mN/m]
0.1% Trehalose	1.01 ± 0.01	71.66 ± 0.05
1% Trehalose	1.02 ± 0.01	72.12 ± 0.04
10% Trehalose	1.33 ± 0.02	69.42 ± 0.03
0.1% Trehalose / PS20	1.01 ± 0.01	38.44 ± 0.06
1% Trehalose / PS20	1.02 ± 0.01	38.51 ± 0.03
10% Trehalose / PS20	1.33 ± 0.02	38.84 ± 0.06
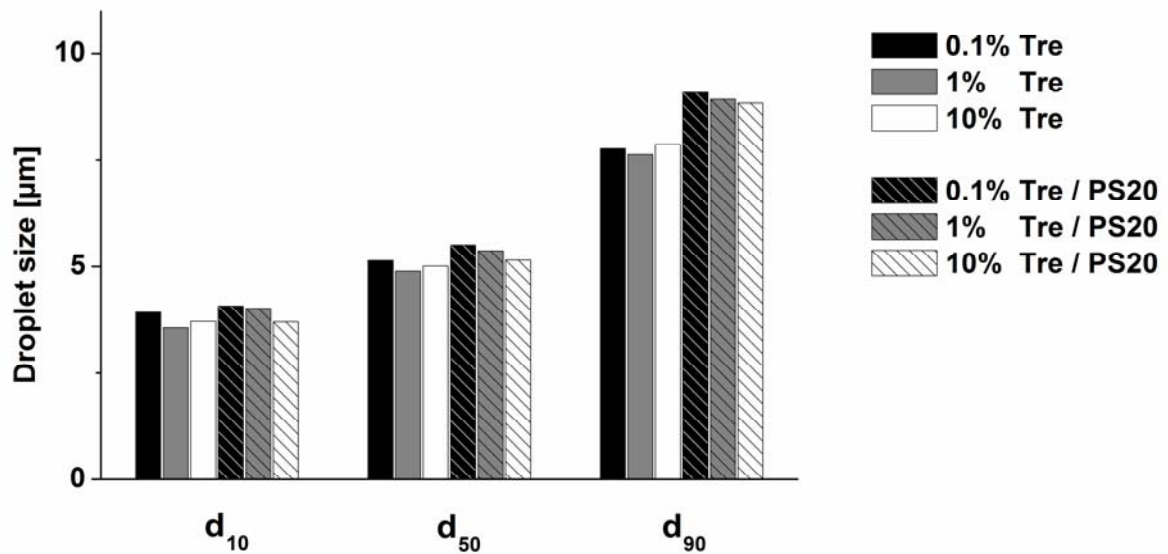
Figure 5 Droplet sizes of trehalose spray solutions with / without polysorbate 20

Ghazanfari et al. analyzed the influence of viscosity and surface tension on the aerosol properties with an Omron® MicroAir vibrating mesh nebulizer (Omron Healthcare, Kyoto, Japan) [11], which uses the same spray technology as the Nano Spray Dryer B-90. In their study, no clear influence was observed regarding the surface tension. However, an increased fluid viscosity decreased aerosol droplet size. These findings were based on more viscous solutions compared to the rather diluted trehalose spray solutions (Table 1) in our study and a comparable viscosity increase did not significantly change the droplet sizes. The spray generated by sugar / surfactant solutions appeared optically denser and stronger compared to pure sugar solutions. Moreover, the surfactant addition increased the throughput of spray solution through the apertures of the vibrating mesh (Figure 6).
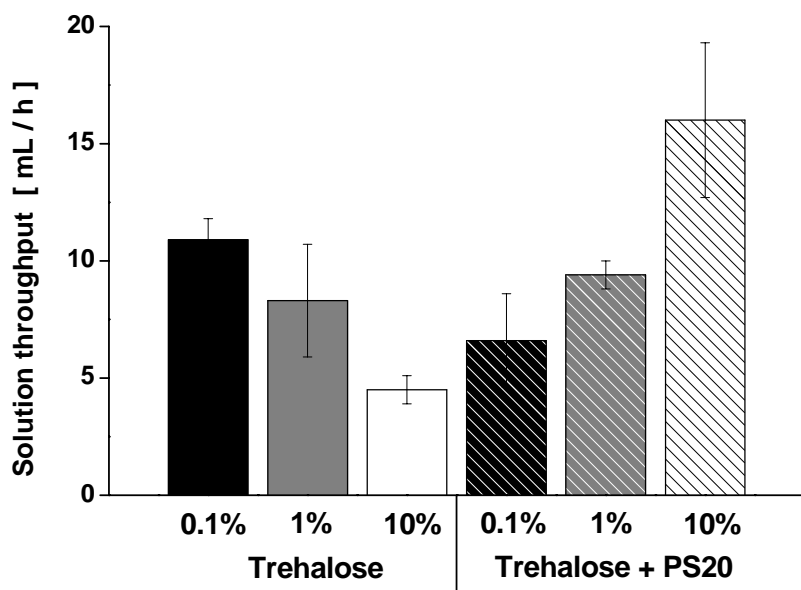
Figure 6 Throughput of trehalose spray solutions with / without polysorbate 20

3.2   Evaluation of minimal spray drying temperature

Spray drying is often the drying method of choice to prepare powders with specific features (e.g. size, morphology, density) in the chemical, pharmaceutical or food industry. On the other side there are various stresses acting on the product during spray drying, such as shear forces in the pump and the nozzle, adsorption at the enlarged air–liquid interface and heat impact. The influence of the drying temperature is considered to be a minor stress factor due to the temporary impact of heat on the droplets and particles. In fact, the droplets dry in a few milliseconds, and the overall residence time in the hot drying air is roughly in the range of a few seconds [6]. Moreover, evaporation of moisture keeps the surface of the drying droplets cool and prevents the rise of product temperature above the level of the outlet gas temperature of the spray dryer [12]. In order to reduce temperature induced stress on spray-dried products, lower inlet temperatures are preferred as long as the corresponding outlet temperatures are still high enough to obtain a powder with adequate moisture content, yield, flowability, particle size distribution, fine particle fraction, and other qualities [13].

Table 2 Yield and residual moisture (rM) of mannitol / polysorbate 20 and trehalose / polysorbate 20 spray dried with the 4.0 μm mesh at different inlet / outlet temperature conditions

Inlet Temp. [°C]	Outlet Temp. [°C]	Mannitol / PS20		Trehalose / PS20	
		Yield [%]	rM [%]	Yield [%]	rM [%]
120	55 - 59	78	0.12	75	4.2
100	50 - 54	75	0.37	59	2.6
80	40 - 45	71	0.11	66	3.2
70	37 - 41	70	0.28	64	2.0
60	33 - 36	65	0.19	63	3.2
50	28 - 32	67	0.29	50	5.0

Table 2 summarizes the spray drying conditions of 1% mannitol and trehalose solutions with 0.05% polysorbate 20 to evaluate the minimal drying temperatures in the Nano Spray Dryer B-90. In general, both mannitol and trehalose were effectively spray dried at low outlet temperatures in a range of 28 - 59 °C. The residual moisture of mannitol powders was below 0.5%, independently of the inlet temperature, which corresponds well to literature [14]. Trehalose powders with 2.0 to 5.0% residual moisture indicate an amorphous product. However, as demonstrated in literature [14] no clear dependency on the inlet temperature was found. The overall yields were slightly higher for mannitol (65 - 78%) compared to trehalose (50 - 75%). For comparison, Adler et al. found a massive yield reduction for trehalose to less than 30% with a traditional spray dryer at inlet / outlet temperatures below 140 / 85 °C. In contrary, the Nano Spray Dryer B-90 was capable of spray drying both excipients at much lower temperatures without relevant yield reductions. Thus, the Nano Spray Dryer B-90 becomes a valuable device to formulate temperature sensitive excipients and drugs.

3.3 Evaluation of product deposition at the spray nozzle

Some spray drying experiments resulted in reduced product yields due to product depositions on the spray nozzle (Figure 7). The deposits occurred either extensively on the whole spray nozzle or were limited to the surroundings of the spray mesh. In both cases, the deposited powder was lost and the overall yield diminished. In addition, in some instances, the deposited powder became a heavy crust and burst off as product lumps contaminating the fine powder in the electrostatic particle collector.
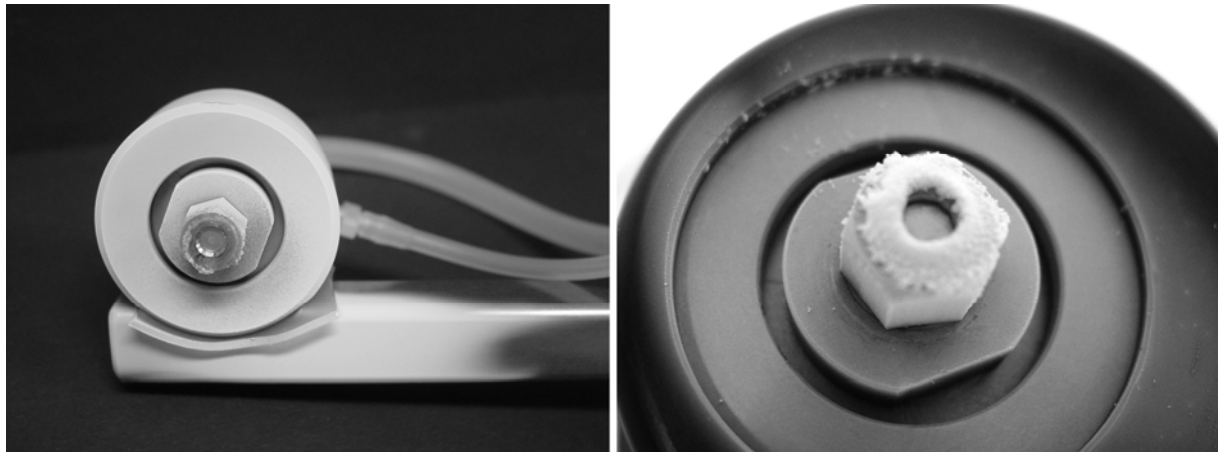
Figure 7 Crust formations on the nozzle of the Nano Spray Dryer B-90

Factors influencing the crust formation could be especially the used solvent, the spray-dried substance and the applied process parameters (Table 3). Among the factors related to the vibrating mesh spray technology, the drying air flow profile inside the spray dryer might be of significance. Although the drying air is laminar through the drying chamber, the spray nozzle works like a barrier in the gas flow and leads to the formation of local gas currents, which tend to entrain the spray [15]. As a consequence, generated droplets flow back and deposit on the nozzle surface. Another reason for product deposits might be the electrostatic attraction of aerosol droplets towards the metallic surfaces of the spray nozzle. This effect might be further aggravated by temperature differences between the aerosol and the metallic nozzle surfaces. As user a certain influence on the outcome of a specific spray drying experiment can be exerted by changing process conditions, as well as substance and solvent related factors.

Table 3 Possible influences on crust formation tendency during spray drying processes

Technology related	Process related	Substance related	Solvent related
▪ Flow profile / entrainment	▪ Inlet temperature	▪ Solubility	▪ Surface tension
▪ Electrostatic effects	▪ Mesh size	▪ Hygroscopicity	▪ Viscosity
▪ Temperature differences	▪ Air flow rate	▪ Stickiness	▪ Conductivity
▪ Spray pulse			▪ Permittivity
			▪ Boiling point

When working with traditional spray dryers, yield and success of a spray drying experiment are influenced by optimizing drying air inlet temperature, nozzle gas flow rate, liquid feed flow rate, and aspirator capacity. Traditional spray dryers offer a larger setting of the drying air inlet temperature (typically up to 220 °C). The nozzle gas flow rate exerts a direct influence on the particle size due to an increase in kinetic energy for the liquid atomization [9]. The drying air inlet temperature in the Nano Spray Dryer B-90 can be adjusted between 60 - 120 °C. The high thermal efficiency of the process allows drying without damage of the product. Moreover, the smaller droplets evaporate quickly and require a lower drying temperature. The aperture size of the applied vibrating mesh is the critical parameter for particle size adjustment, which is equivalent to the spray gas flow in traditional pressurized air nozzles. The spray solution throughput in the Nano Spray Dryer B-90 is mainly determined by the aperture size of the applied mesh. In contrast, the liquid feed rate in traditional spray dryers is adjusted by the pump speed to obtain a certain outlet temperature and particle size [16, 17]. The outlet gas temperature in the Nano Spray Dryer B-90 is controlled by the drying air flow rate (80 - 120 L/min) and the spray intensity (0 - 100%). The electrostatic particle collector works at fixed conditions and can not be influenced by the spray dryer operator directly. The system controls optimal particle separation conditions.

It is clearly recognized that the nozzle deposition is affected by the physicochemical nature of the spray-dried substance. Its maximal possible solute concentration limits the maximal achievable particle size and throughput. The substance hygroscopicity is inter alia responsible for the residual moisture content of the spray-dried powder. Some substances, like trehalose, have a highly sticky nature compared to noncohesive substances like salts [17]. This might also lead to an increased sticking behavior of droplets to the nozzle. In addition, solvent physicochemical parameters, like surface tension, viscosity and conductivity, are considered to impact the crust formation. Some investigations regarding the influence of surface tension and viscosity on aerosol properties have been conducted [11]. However, the processes during spray drying are more complex than during spraying into room air and the possibility remains that the additional drying factors provoke crustification of spray solutions.

Various spray drying experiments were conducted in order to analyze the effects of surface tension, viscosity and conductivity of spray solutions on nozzle deposition and yield reduction. Table 4 compares the experimental results in sets of two. Each set of experiments was performed under identical spray drying conditions (mesh size, inlet temperature, drying air flow rate). For example, set 1 comprises two experiments of griseofulvin with identical spray drying parameters (70 °C T_{in} / 5.5 µm mesh size), but different organic solvents. Griseofulvin dissolved in methanol / acetone (ratio 80:20) led to satisfying spray drying

results with no crustification, whereas dissolution in pure acetone formed a heavy crust on the spray nozzle and the final powder product was contaminated by crusty lumps. For the sets 2 - 5, the choice of either solute concentration or solvent clearly led to differences in process quality and crust formation.

Table 4 Sets of spray drying experiments for evaluation of crust formation

Set	No crustification		Crustification	
1	0.44%	Griseofulvin in methanol / acetone	0.15%	Griseofulvin in acetone
2	5%	Salicylic acid in acetone	5%	Salicylic acid in ethyl acetate
3	1%	Benzocaine in ethanol	1%	Benzocaine in acetone
4	1%	Salicylic acid in ethyl acetate	5%	Salicylic acid in ethyl acetate
5	0.44%	Griseofulvin in methanol / acetone	0.5%	Griseofulvin in ethyl acetate

Figure 8 depicts the viscosity, surface tension and conductivity values of the respective spray solutions. No significant correlation between spray solution properties and crustification tendency could be established, neither for the experiments without crustification (circles), nor for the ones with crustification (squares). These findings indicate that virtually any substance can be spray dried successfully, as long as the right experimental setup (solvent, concentration, etc.) is used.
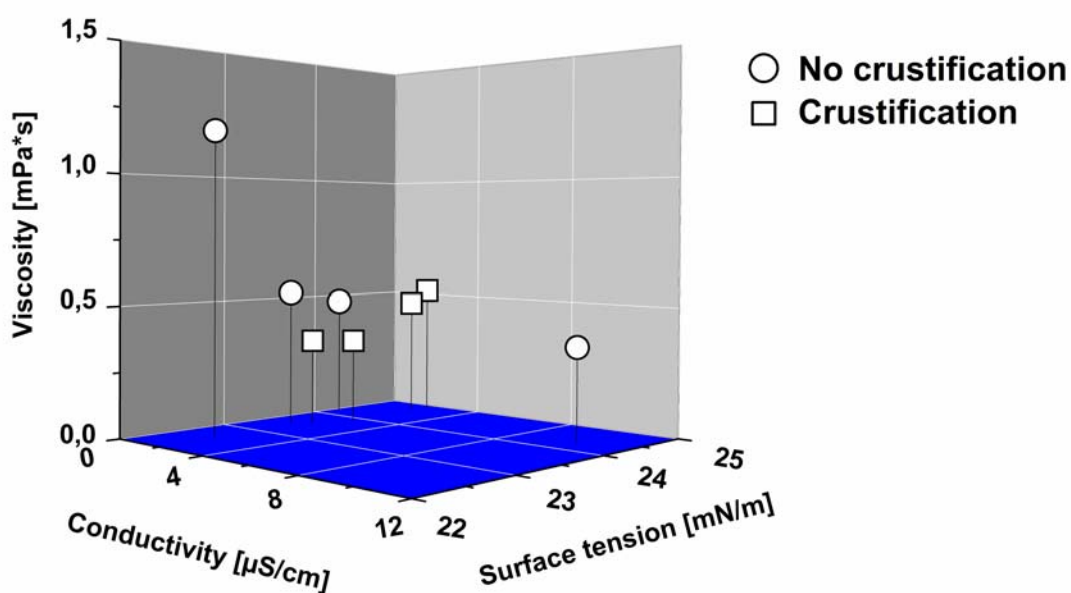
Figure 8 Plot of viscosity, conductivity and surface tension of spray solutions

3.4 Preparation of submicron particles

Finally, the possibility to use the Nano Spray Dryer B-90 for the preparation of particles in the submicron size range was investigated. Based on the droplet size analysis of the aerosol and the knowledge that the droplet size is dependent on the applied vibrating mesh, the smallest available mesh with an aperture size of 4.0 µm was applied. Mean droplet sizes of approx. 5 µm have been measured independently of the total solids concentration (Figure 5). However, due to mass balance a smaller solute concentration finally leads to smaller solid particles after drying. Therefore, solutions with 0.1% disodium phosphate or trehalose with addition of 0.005% polysorbate 20 were spray dried at 120 °C inlet temperature. Approx. 50 mL of each solution were spray dried to obtain a representative amount of powder for analysis (approx. 50 mg in this study).
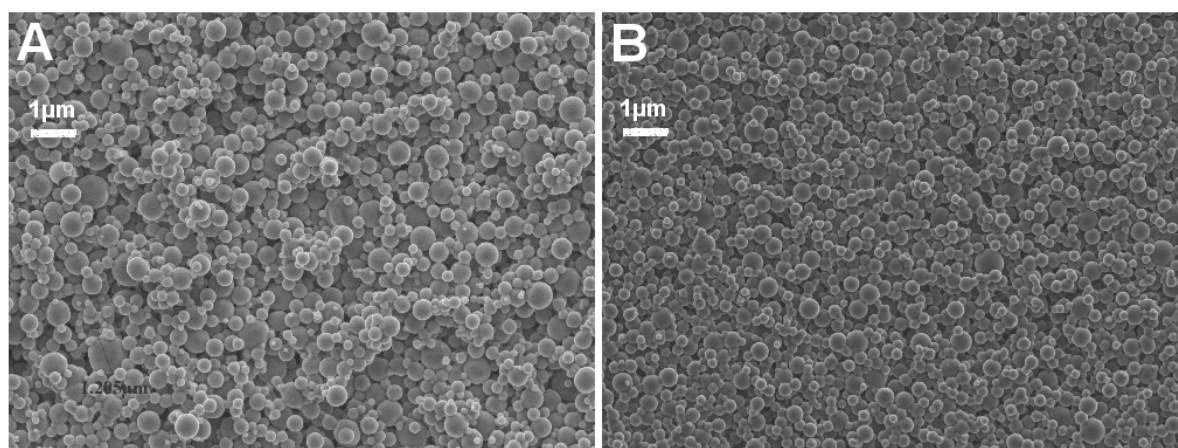
Figure 9 SEM of spray-dried phosphate salt **(A)** and trehalose **(B)** particles

Figure 9 shows SEM photographs of spray-dried disodium phosphate with a mean particle size of 0.5 µm and spray-dried trehalose particles with a mean particle size of 0.8 µm. It can be stated that the atomization device of the Nano Spray Dryer B-90 enables the production of particles with an average diameter below 1 µm. This ability raises expectations with regard to novel particle design possibilities in pharmaceutical applications using spray drying. A reduction in particle size offers various new options for the application of spray-dried particles. For example, achieving submicron particle sizes of poorly water-soluble drugs enhances their dissolution properties and therefore their bioavailability after oral administration [18]. Even more unique is the electrostatic particle collector as a highly efficient particle separator. The yield for disodium phosphate reached 75% for 50 mg of

powder. With 0.1% trehalose solution the yield was 49% due to stronger crust formation. The spray drying process became rather time-consuming due to the low solute concentration and the limited throughput through the spray mesh. The separation of particles in the submicron size range is known to be difficult with traditional spray dryer setups. Prinn et al. found for example that particles smaller 2 μm were unattainable using a standard cyclone [16]. Even with a 'high-performance' cyclone capable of separating particles smaller 2 μm from the drying air [19], the median particle size could not be reduced below 1.4 μm [9]. An electrostatic particle collector tremendously extends the size spectrum of separable particles [8].

4   Summary and Conclusions

The vibrating mesh spray technology implemented in the new Nano Spray Dryer B-90 produced aerosols with mean droplet sizes down to 4.8 µm (using the 4.0 µm mesh) with narrow size distribution (span values of approx. 1.2). Spray drying of highly diluted disodium phosphate and trehalose solutions (0.1%) containing surfactant enabled the production of submicron particles with 0.5 µm and 0.8 µm mean particle size, respectively, for 50 mg powder amounts. In order to ensure an effective separation and collection of those fine particles, the Nano Spray Dryer B-90 is equipped with an electrostatic particle collector and laminar drying gas regulation. The laminar drying gas allows gentle drying of heat sensitive products and prevents the deposition of the fine particles on the glass cylinder walls. Although, turbulent drying air is favorable with regard to mass and heat transfer in traditional spray dryers, a laminar flow is efficient enough in the new spray dryer to dry the fine aerosol immediately. The electrostatic particle collector eventually allows the collection of the particles in the submicron size range, which is commonly not achieved by traditional cyclone separators. However, formulation scientists have to be aware of the necessary process development time for optimal product formulation in order to avoid curst formation at the spray nozzle. Since the nozzle of the Nano Spray Dryer B-90 has not been designed to produce solid particles larger than 5 µm, it is suggested to design new vibrating meshes with > 7.0 µm aperture size to extent the application range for pharmaceuticals. The production of submicron particles was found feasible despite the elongated process time.

5   References

1   Vehring R. Pharmaceutical Particle Engineering via Spray Drying. *Pharm Res* 2008; 25: 999-1022.

2   Salama RO, Ammit AJ, Young PM. Preparation and evaluation of controlled release microparticles for respiratory protein therapy. *J Pharm Sci* 2009; 98: 2709-2717.

3   Kaye RS, Purewal TS, Alpar OH. Development and testing of particulate formulations for the nasal delivery of antibodies. *J Contr Rel* 2009; 135: 127-135.

4   Elversson J, Millqvist-Fureby A. Particle size and density in spray drying-effects of carbohydrate properties. *J Pharm Sci* 2005; 94: 2049-2060.

5   Buechi Labortechnik A. G. Flawil Switzerland. Brochure Nano Spray Dryer B-90. 2009

6   Masters K. Spray Drying1976: 684.

7   Dhand R. Nebulizers that use a Vibrating Mesh or Plate with Multiple Apertures to generate Aerosol. *Respiratory Care* 2002; 47: 1406.

8   Riehle C. Basic and theoretical operation of ESPs. *Appl Electrost Precip* 1997: 25-88.

9   Maltesen MJ, Havelund S, van de Weert M. Quality by design - Spray drying of insulin intended for inhalation. *Eur J Pharm Biopharm* 2008; 70: 828-838.

10   Wang W, Wang YJ, Wang DQ. Dual effects of Tween 80 on protein stability. *Int J Pharm* 2008; 347: 31-38.

11   Ghazanfari T, Elhissi AMA, Ding Z, Taylor KMG. The influence of fluid physicochemical properties on vibrating-mesh nebulization. *Int J Pharm* 2007; 339: 103-111.

12   Cal K, Sollohub K. Spray Drying Technique. I: Hardware and Process Parameters. *J Pharm Sci* 2010; 99: 575-586.

13   Tomoda K, Nakajima T, Makino K. Preparation and properties of inhalable nanocomposite particles: Effects of the temperature at a spray-dryer inlet upon the properties of particles. *Colloids and Surfaces B: Biointerfaces* 2008; 61: 138-144.

14   Adler M. Sprueheinbettungen von Proteinen in Geruestbildner: Stabilitaet und Oberflaechenanalyse (*Thesis*) 1999.

15   Spurk JH, Aksel N. Grundzuege turbulenter Stroemungen: 2006: 221-246.

16   Prinn KB, Costantino HR, Tracy M. Statistical modeling of protein spray drying at the lab scale. *AAPS Pharm SciTech* 2002; 3: E4.

17   Maury M, Shi L, Lee G. Effects of process variables on the powder yield of spray-dried trehalose on a laboratory spray-dryer. *Eur J Pharm Biopharm* 2005; 59: 565-573.

18   Oh DM, Curl RL, Yong CS, Amidon GL. Effect of micronization on the extent of drug absorption from suspensions in humans. *Arch Pharm Res* 1995; 18: 427-433.

19   Brandenberger H. Development of a novel high-performacne cyclone to increase the Yield in a Mini Spray Dryer. *Information Bulletin Buechi Labortechnik* 2003; 27.

Chapter 3

Spray drying a BCS class II drug with the Nano Spray Dryer B-90

Abstract

An increasing number of new chemical entities emerging from industry pipelines show low oral bioavailability. Development of micronized or solubilized formulations can improve the bioavailability by accelerating the drug dissolution rate. In this study, the Nano Spray Dryer B-90 was implemented for inert spray drying of organic solvent solutions of the model drug griseofulvin. Griseofulvin powders with medium particle sizes of 3.4 to 6.5 µm were produced and compared to the 'gold standard' micronized griseofulvin concerning particle properties with relevance for drug absorption. Particularly, drug dissolution and cell culture permeability of spray-dried griseofulvin were analyzed and correlated to drug particles size. Spray drying of griseofulvin yielded a comparably fast dissolving and permeable powder compared to micronized milled material. The addition of Lutrol F127 as solubilizing agent improved the wettability of griseofulvin to such an extent that the dissolution rate was even faster than for micronized material.

1   Introduction

An increasing number of new chemical entities emerging from industry pipelines show low oral bioavailability [1]. In fact, these drug candidates are highly permeable due to their innate lipophilicity, however, their aqueous dissolution is limited and determines the rate and degree of absorption after oral administration. Substances with poor water solubility and high permeability are categorized as class II drugs according to the biopharmaceutical classification system (BCS) [2]. Their low solubility in the gastrointestinal tract challenges the formulation scientist, as oral drug application remains the preferred route of administration due to low production costs, good patient compliance, and convenience of use. Manifold strategies emerged to increase solubility and absorption of class II drugs, starting with their chemical modification into more water-soluble species like prodrugs and salts. However, prodrugs must be activated e.g. by enzymes and require an intact metabolic activity, and salts can undergo pH-dependent precipitation during the gastrointestinal passage losing their bioavailability [3]. Another traditional approach to increase drug dissolution is the co-administration of lipophilic pharmaceuticals with a meal rich in fat. This significantly increased the oral bioavailability of several lipophilic drugs [4-7] and led to the development of more sophisticated formulation strategies, which are based on the following principles:

- Dispersion
- Micronization
- Solubilization

1.1   Dispersion

Dispersion aims at facilitating drug absorption by presenting the drug in its dissolved and readily absorbable form or in its amorphous state. Microemulsions, self-(micro-) emulsifying drug delivery systems (SEDDS/SMEDDS), and solid dispersions are utilized for this purpose. Microemulsions are thermodynamically stable, isotropic mixtures of lipid, water, and surfactant, frequently in combination with a co-surfactant, and served as model for the development of SEDDS and SMEDDS, which use the concept of in situ drug (micro-) emulsification upon contact of the preparation with the gastrointestinal fluids in vivo [1]. SEDDS and SMEDDS have contributed to the improvement of oral bioavailability of several poorly water-soluble drugs, like halofantrine [8], simvastatin [9], and itraconazol [10]. One of the best known examples for a successfully marketed SMEDDS is the Neoral® cyclosporine

formulation, which in contrast to the earlier Sandimmun® formulation improved drug dispersion and absorption, and reduced inter- and intrapatient variability of bioavailability [11]. The concept of solid dispersions was initially introduced by Sekiguchi et al. [12], who used crystalline carriers like urea and mannitol to form eutectic, readily soluble mixtures with poorly soluble drugs. In general, solid dispersions can be defined as homogenous mixtures of one or more active ingredients in a pharmacologically inert matrix carrier in the solid state [13], and can be classified according to their structural variety (Table 1).

Table 1 Classification of solid dispersions according to Forster [13] (A = amorphous, C = crystalline)

Category	Type	Number of phases	Physical state of phase(s)
1	Eutectic mixture	≥ 2	C/C
2	Solid solution	1	C
3	Complex	1	A or C
4	Glass solution	1	A
5	Amorphous suspension	2	A/A or A/C

To enhance oral drug bioavailability, solid dispersions with amorphous character were quickly considered more attractive, as they avoid the crystal lattice energy barrier to be overcome before dissolution [14]. However, the sole implementation of polymeric carriers (e.g. PVP, PVA, HPMC, HPC, ethyl cellulose, and PEG) often resulted in heterogeneous mixtures due to the only partial miscibility of amorphous drug dissolved in the polymer carrier and non-dissolved small microcrystalline drug particles. Thus, modern solid dispersions typically keep the drug in an amorphous state and prevent drug precipitation by implementing surface-active carriers like glyceryl behenate and polyoxylglycerides [15]. Classical techniques to prepare solid dispersions comprise solvent evaporation and melt extrusion. Solvent evaporation by vacuum-, freeze-, or spray drying is considered as method of choice for amorphous polymers that either do not melt or degrade before melting. However, the need for a suitable solvent in large quantities and its cost, toxicological and environmental impact restricts the applicability of this approach. Instead, melt extrusion offers the advantage of a solvent-free, continuous, and scalable process, whose application at early drug development stages is on the other hand limited by the need for large quantities of drug material [13]. Patterson et al. compared spray drying and melt extrusion for preparing glassy solutions of several poorly water-soluble drugs, and analyzed the influence of the preparation process on the product morphology and stability [16]. Their results indicated that melt extrudates are more homogeneous. However, the manufacturing technique had minimal influence on the physical stability of the products and recrystallization processes of the amorphous drugs were

successfully inhibited by all glass solutions. In general, solid dispersions are more amenable to be developed into the preferred solid dosage form compared to the above mentioned semi-solid drug delivery approaches. Examples of marketed solid dispersion products are Grispeg® (griseofulvin/PEG), Cesamet® (nabilone/PVP), and Certican® (everolimus/HPMC).

1.2 Micronization

Another technology to solve the problem of low oral bioavailability is the micronization of drugs. Micronized formulations improve the bioavailability by accelerating the drug dissolution rate, which depends on the particle size and is, according to the Noyes–Whitney equation, directly proportional to the specific surface area. In addition, micronization below 1 µm increases the saturation solubility of drugs, because their solubility increases exponentially as a function of particle size, as demonstrated by the Kelvin and the Ostwald–Freundlich equations [17]. Micronization technologies can be divided into downsizing (top-down) and up-building (bottom-up) approaches. The top-down approach, where the original drug crystals are disrupted by mechanical force, can be further divided into milling (e.g. jet milling, wet ball milling or cryogenic milling) and homogenization using high pressure [15]. The combination of both techniques is also common as, for example, jet milling is used to obtain a drug 'macro-'suspension, which is then further processed to a nanosuspension in a high pressure homogenizer. Such a homogenizer increases the dynamic fluid pressure and creates cavitation forces strong enough to break the drug microparticles into nanoparticles [17]. However, the high-energy input also disrupts the crystal lattice and induces partial or total amorphization or polymorph conversion of drug particles. These disordered regions are thermodynamically unstable, and physical instability and chemical degradation during storage are to be expected [3]. In order to avoid impairment of dissolution and bioavailability by recrystallization tendencies, transformation of suspensions into solid products is recommended using freeze- or spray drying [18]. Bottom-up micronization initially starts from a drug solution, which is precipitated e.g. through a nozzle into an anti-solvent to form a colloidal suspension. Challenges of this method are [19]

- the necessity of a solvent that quantitatively dissolves the investigated drug,
- the necessity of a drug anti-solvent that is miscible with the solvent and
- the inhibition of crystal growth during the precipitation procedure by surfactant addition.

Recently, the use of supercritical technology to improve solubility gained increased attention. Supercritical fluids (SCF), like carbon dioxide, are used as solvents for drug substances, as anti-solvents for precipitation and as media for other fluid techniques. Several SCF methods evolved: precipitation with compressed anti-solvent, solution enhanced dispersion by SCF, supercritical anti-solvent processes, and aerosol solvent extraction systems [19]. Advantages of the SCF technology lie in the omission of organic solvents and heating stress, however, the high machine expenditure must be named as possible drawback.

1.3   Solubilization

Solubilization constitutes a further attempt to increase saturation solubility and oral bioavailability of poorly soluble drugs. In principle, solubilization is defined as enhancement of solubility of a substance in a solvent by adding a third substance (solubilizer). Depending on the mechanism of solubilization, micellar solubilization, complexation, and co-solvency are distinguished [17]. Micellar solubilization is achieved by addition of surfactants to a concentration exceeding their critical micelle concentration (CMC) and entrapping drugs inside the micelles. Even at a concentration below CMC, surfactants can improve the dissolution of lipophilic drugs by lowering the surface tension and increasing wettability. Surfactants are also frequently used to stabilize microemulsions and - suspensions. The complexation of lipophilic drugs can be non-specific (e.g. by addition of PEG) or specific (by use of cyclodextrins). The specific interaction of drugs with the cyclodextrin cavity leads to drug / cyclodextrin complexes, commonly known as inclusion complexes. Advantages of these inclusion complexes are their simple production method, their rapid and quantitative dissociation and their often lower toxicity compared to surfactants and co-solvents. However, the solubility enhancement for drugs with extremely poor solubility is often low and regulatory and quality control issues regarding the use of cyclodextrins still need to be addressed. Co-solvency describes the increase of drug solubility by addition of a water miscible solvent in which the drug has good solubility. Frequently used co-solvents comprise PEG, PVA, and PVP for solid formulations and ethanol, propylene glycol, glycerol, and DMSO for liquid formulations [20].

1.4   The scope of this study

In this study, two formulation principles were investigated to improve dissolution properties of the model drug griseofulvin: (1) organic drug solutions were spray dried with the new Nano Spray Dryer B-90 to obtain micronized drug powder and (2) surfactant was added to the formulation to enhance particle wettability. Additional aims were the evaluation of the suitability of the Nano Spray Dryer B-90 for inert organic solvent spray drying processes and the development of a robust and efficient spray drying process for griseofulvin, exploiting the possibility to start from minute drug quantities. Micronized griseofulvin bulk material served as 'yardstick' throughout the in vitro dissolution and cell culture absorption experiments, and it was hypothesized that griseofulvin powder with equal qualities could be produced.

The oral bioavailability of griseofulvin, a BCS class II drug with poor water solubility (approx. 0.001% at 37°C), has been subject of investigations since its first use in 1958 [21]. Atkinson et al. established the correlation of oral bioavailability and particle surface area for micronized griseofulvin powder of 1.6 to 10 µm particle size [22]. Nuernberg et al. found increased drug dissolution rates and solubilities for spray-dried griseofulvin / methylcellulose formulations. However, high amount of excipient was necessary to obtain an amorphous, fast dissolving product [21]. The same was observed for griseofulvin / cyclodextrin inclusion complexes with drug / excipient ratios of 1:1 to 1:2, where drug solubility increased accord to the cyclodextrin amount added [23]. However, for the improved drug dissolution large quantities of solubilizing excipients were necessary.

2　Materials and Methods

2.1　Materials

Micronized griseofulvin EP5 bulk material was obtained from Welding (Frankfurt, Germany). Lutrol F127 (poloxamer 407) was supplied by BASF (Ludwigshafen, Germany). Dulbecco's modified eagle's medium (DMEM), fetal bovine serum (FBS), sodium pyruvate, 0.25% trypsin with EDTA, minimum essential medium (MEM) containing non-essential amino acids, Pen-Strep (10,000 units Penicillin G and 10,000 µg Streptomycin sulfate per mL 0.85% saline) and 100x vitamins for MEM were obtained from GIBCO Invitrogen (Carlsbad, California, USA). Lucifer yellow dilithium salt, HEPES, MES, lipoic acid, zinc sulfate, sodium bicarbonate, and Hank's balanced salt solution (HBSS) were purchased from Sigma (St. Louis, Missouri, USA). Potassium phosphate dibasic anhydrous, acetic acid, triethanolamine, methanol and acetonitrile were supplied by Caledon (Georgetown, Ontario, Canada).

2.2　Methods

2.2.1　Spray drying with the Nano Spray Dryer B-90

The Nano Spray Dryer B-90 was operated in short assembly as closed-cycle system in connection with an Inert Loop B-295 (Büchi Labortechnik, Flawil, Switzerland). Nitrogen gas as drying medium was used at a flow rate of 120 L/min. The residual oxygen level in the system was controlled below 4%. System-controlled carbon dioxide gas injections ensured efficiency of the electrostatic powder collection. The spray intensity was set to 100% and the inlet temperature T_{in} to 60 °C or 70 °C, depending on the solvent used. Different spray meshes were applied with aperture sizes of 4.0 µm, 5.5 µm or 7.0 µm, respectively. Griseofulvin was dissolved together with surfactant (optional) in acetone or methanol / acetone (ratio 80 : 20) and 25 - 70 g of various % (w/w) formulations were spray dried (overview of the formulations in Table 2). Process parameters, including inlet temperature and outlet temperature, spray head temperature, nitrogen / carbon dioxide flow rate, residual oxygen level, and spray intensity were recorded, and the spray-dried powder was manually collected after the process for yield determination and further analysis.

2.2.2 Spray drying with the Mini Spray Dryer B-290

Griseofulvin formulations (Table 2) were spray dried with the Mini Spray Dryer B-290 as closed-cycle system in connection with an Inert Loop B-295 (Büchi Labortechnik, Flawil, Switzerland) and a LT Mini dehumidifier (Deltatherm, Much, Germany). Approx. 70 g of various % (w/w) formulations were atomized by a two fluid nozzle (0.7 mm tip). A high performance cyclone was applied for powder collection. Nitrogen gas was used at a flow rate of 830 L/h. The aspirator rate was set to 35 m^3/h, the feed flow rate to 3.85 mL/min, and the inlet temperature T_{in} to 70 °C, resulting in an outlet temperature T_{out} of 50 °C.

Table 2 Overview of griseofulvin spray drying experiments (Met = methanol)

Griseofulvin [% (w/w)]	Lutrol F127 [% (w/w)]	Solvent	Spray dryer	Mesh [µm]	T_{in} / T_{out} [°C]	Yield [%]	Particle size [µm]
0.5	-	Met/Acetone	B-90	4.0	70/45	43.3	3.4
0.5	-	Met/Acetone	B-90	5.5	70/43	52.5	4.9
0.5	-	Met/Acetone	B-90	7.0	70/40	62.7	6.5
1.5	-	Acetone	B-90	5.5	60/40	74.5	4.9
0.44	-	Acetone	B-90	5.5	60/40	63.6	4.7
0.15	-	Acetone	B-90	5.5	60/40	34.1	4.2
0.5	-	Met/Acetone	B-90	4.0	70/45	40.0	3.6
0.5	-	Met/Acetone	B-290	-	70/50	31.0	3.8
0.5	0.05	Met/Acetone	B-90	4.0	70/45	34.0	3.8
0.5	0.05	Met/Acetone	B-290	-	70/50	40.2	3.8
0.5	0.0025	Met/Acetone	B-90	4.0	70/45	44.7	3.6
0.5	0.0025	Met/Acetone	B-290	-	70/50	48.1	4.1

2.2.3 Particle size analysis

Spray-dried drug powders were analyzed using a Helos H 2178 laser diffraction instrument in combination with a Rodos dry dispersing unit and a Vibri vibratory feeding unit (both Sympatec, Clausthal, Germany). The powder was fed with 60% intensity and dispersed at 4.0 bars. The used R2 lens covered a sample size range from 0.45 - 87.5 µm. All samples were measured in triplicate and the mean diameter reported.

2.2.4 X-ray powder diffraction (XRD)

The morphology of the spray-dried products was analyzed by X-ray powder diffraction (XRD) on the X-ray diffractometer XRD 3000 TT (Seifert, Ahrensburg, Germany) using Cu-Kα-radiation ($\lambda = 0.15418$ nm, $U = 40$ kV, $I = 30$ mA). Samples were scanned between 5 - 40 °2-Theta, with steps of 0.05 °2-Theta and duration of 2 s per step.

2.2.5 Scanning electron microscopy (SEM)

The particle morphology of the spray-dried powders was determined with a JSM-6500F JEOL scanning electron microscope (JEOL, Eching, Germany). For analysis, the samples were fixed on self-adhesive tapes on an aluminum stub and sputtered with carbon.

2.2.6 Dissolution studies

Spray-dried griseofulvin powders and micronized griseofulvin material were tested for dissolution qualities based on the USP method *<Griseofulvin Capsules>* [24]. Approx. 10 mg spray-dried powder was weight into size 1 gelatin hard capsules. Modified dissolution parameters were applied as follows: dissolution apparatus 1 (basket), 1000 mL dissolution medium (5.4 mg/mL sodium lauryl sulfate in water) of 37 +/- 0.5 °C, 100 rpm stirring speed, 60 min dissolution time, sample withdrawal at 2, 5, 10, 15, 30, 45 and 60 min. Quantification of the dissolved amount of drug was carried out photometrically at 291 nm with an Agilent 8453 spectrophotometer (Agilent, Waldbronn, Germany). All samples were analyzed in triplicate.

2.2.7 Cell culture technique

Caco-2 cells (ATTC, Rockville, Maryland, USA) were maintained at 37 °C in DMEM with 4.5 g/L glucose, 10% FBS, 1% non-essential amino acids (NEAA), 1% sodium pyruvate and HEPES buffer in an atmosphere of 5% CO_2 and 95% relative humidity. The cells were seeded on non-coated inserts (polyester membrane, 0.4 μm pores, 4.7 cm^2 growth area) in Costar Transwell® permeable cell culture plates (Corning, New York, USA) with 6 wells per plate at a density of $3*10^5$ cells / insert. The medium was replaced every 48 hours for the first

6 days and every 24 hours thereafter. After approx. 18 - 21 days in culture, Caco-2 monolayers were utilized.

2.2.8 Transepithelial electrical resistance (TEER) measurement

TEER of transwell inserts was measured using an EndOhm 24SNAP chamber connected to an EVOM system (both World Precision Instruments, Sarasota, Florida, USA) and after taking into account the growth area of the insert (4.7 cm^2) reported as $\Omega * cm^2$. Before seeding Caco-2 cells, electrical resistance of the blank inserts together with buffer medium was measured. To calculate the TEER of the Caco-2 monolayer, the total electrical resistance of the seeded wells was corrected for the TEER value of the blank insert and buffer. TEER measurements were conducted before and after the drug transport study and loss of electrical resistance was calculated by the following equation:

$$\Delta R \ [\%] \ = \ \frac{\left(TEER_{before} - TEER_{after}\right)}{TEER_{before}} * 100$$

2.2.9 Drug transport study

Various spray-dried griseofulvin powders were tested for their drug permeability through Caco-2 cell monolayers (Figure 1). Apical-to-basal permeability of griseofulvin was measured under pH gradient conditions (apical pH = 6.0, basal pH = 7.4) to better mimic intestinal transport in vivo. HBSS buffer was used as medium for drug transport studies (transport medium), after adjusting the pH to 6.0 with MES or to 7.4 with HEPES, respectively. Fresh well plates were used for drug transport studies. After filling the basal compartments with 2.6 mL HBSS buffer of pH 7.4, inserts with an integer cell monolayer (determined by TEER measurements) were placed into the well and 1.0 mL HBSS buffer of pH 6.0 was applied onto the apical side. After 15 min of incubation of both well sides with drug-free transport medium, approx. 1 - 2 mg griseofulvin powder (exactly weighed) was dispersed as powder into the apical compartment and 1.0 mL lucifer yellow buffer were added, resulting in an initial lucifer yellow concentration at the apical side of 50 µM. Thereafter, aliquots of 0.5 mL were taken from the basal side every 10 min for the first hour and every 15 min for the second hour. The volume of the basal solution was maintained constant by adding fresh transport medium.
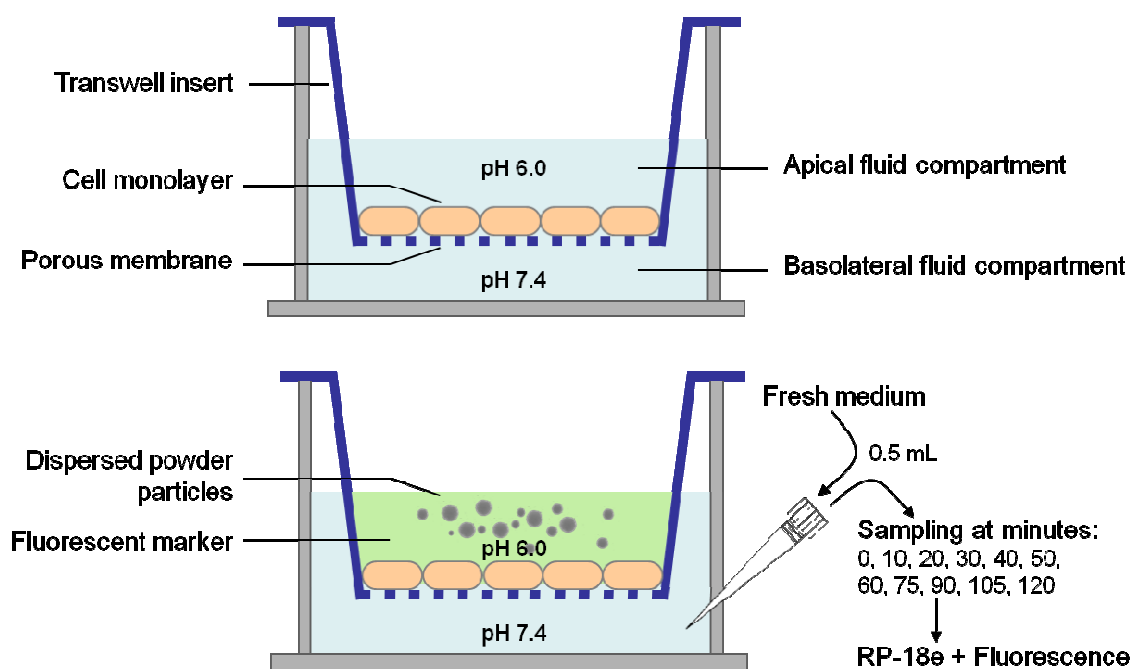
Figure 1 Setup of cell culture plates containing Caco-2 cell monolayers before (top) and during the drug transport study (bottom)

2.2.10 Drug permeability determination

The amount of griseofulvin and lucifer yellow in the aliquots from the basal side was determined chromatographically with fluorescence detection using a Shimadzu LC-600 pump (Shimadzu, Kyoto, Japan) with a Jasco 851 AS auto sampler and a Jasco FP 920 fluorescence detector (Jasco, Easton, Maryland, USA). The injection volume was 10 μL and the flow rate was 0.9 mL/min. Griseofulvin was detected at 300 nm (excitation) and 418 nm (emission) in methanol / 0.5% acetic acid (ratio 61.5 : 38.5) and lucifer yellow at 485 nm (excitation) and 530 nm (emission) in 0.067 M potassium phosphate / acetonitrile / triethanolamine (ratio 75 : 25 : 0.02) as mobile phase on a Chromolith™ Performance RP-18e column (100 - 4.6 mm) (Merck, Darmstadt, Germany). The chromatograms were acquired using the Clarity™ data acquisition software (2.4.4.83; Data Apex, Prague, Czech Republic). Permeability of lucifer yellow was used as indicator for the integrity of Caco-2 cell monolayers and the apparent permeability coefficient P_{eff} (cm/s) was calculated according to the following equation:

$$P_{eff}\ [cm/s] \ = \ \frac{V}{A*c_0}*\frac{dc}{dt} = \frac{2.6\,cm^3}{4.7\,cm^2*50\,\mu M}*\frac{\Delta c\,\mu M}{7200\,s}$$

where *dc/dt* is the flux across the monolayer (µM/s), and is obtained from the plot of lucifer yellow concentration in the basal compartment vs. time, c_0 is the initial lucifer yellow concentration in the apical compartment (µM), *V* is the volume of the basal compartment buffer (cm^3) and *A* is the area of the monolayer in the transwell insert (cm^2). As indication for a good monolayer, P_{eff} should be below $2*10^{-7}$ cm/s.

2.2.11 Statistical analysis

Results were analyzed by one-way analysis of variance (ANOVA) to determine significant differences of permeability. The level of significance was set to $P < 0.05$.

3   Results and Discussion

Development of a robust spray drying process started with the search for suitable solvents and spray drying conditions. Griseofulvin was dissolved in methanol, acetone, dichloromethane, and ethyl acetate, and spray dried with the Nano Spray Dryer B-90 at different inlet temperatures (Table 2; data for dichloromethane and ethyl acetate not shown). Only methanol and acetone, and combinations thereof, were found to give satisfactory spray drying results. Dichloromethane and ethyl acetate were discarded from further investigations as their application resulted in a pronounced product crustification with griseofulvin particles forming a crust on the spray dryer nozzle. Using methanol and acetone, the crust forming tendency was reduced or eliminated and product yields ranging from 30 to 70% were obtained. Some of the formulations were also spray dried with the Mini Spray Dryer B-290. The performance of both bench-top spray dryers was found to be equal in terms of product yields and process safety (Table 2).

3.1   Influence of vibrating mesh aperture size

The vibrating mesh of the Nano Spray Dryer nozzle is available in three different aperture sizes (4.0, 5.5 and 7.0 µm). To investigate the influence of aperture size on particle size, and thereby potentially on the dissolution and permeability of spray-dried powders, a formulation of 0.5% (w/w) griseofulvin in methanol / acetone was spray dried using all three mesh types (Table 2). As shown in Figure 2, the particle size of the spray-dried powders was positively correlated with the aperture size of the vibrating mesh. Application of the 4.0 µm mesh resulted in particles with a medium size of 3.4 µm, the 5.5 µm mesh in a medium size of 4.9 µm, and the 7.0 µm mesh in a medium size of 6.5 µm.
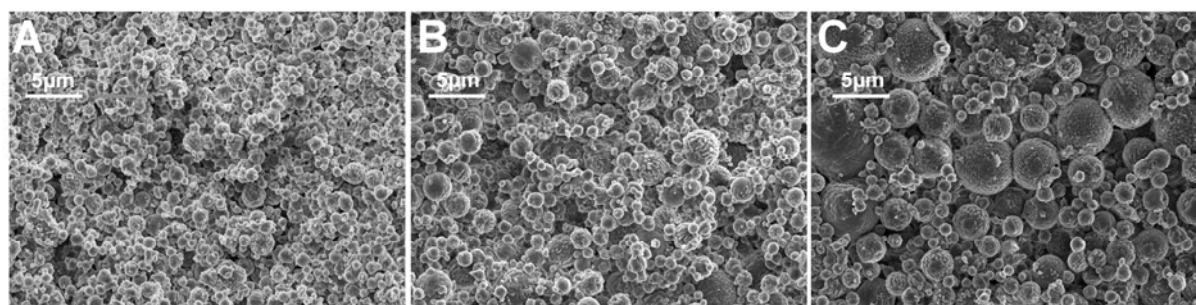
Figure 2 Effect of aperture size on the particle size of spray-dried griseofulvin powders:
    (A) 4.0 µm apertures, **(B)** 5.5 µm apertures, and **(C)** 7.0 µm apertures

In a second step, the spray-dried powders were analyzed for their dissolution rate (Figure 3) and permeability performance (Figure 4). The powder, which was obtained by spray drying with the 4.0 µm mesh, showed a higher dissolution. The effect can be explained by the following correlation: the smaller the apertures of the vibrating mesh, the smaller the spray-dried particles and the larger the specific surface area of the powder accessible for drug dissolution. Based on these results, the permeability of the powders might depend on the aperture size. Hence, the amount of permeated griseofulvin diffusing into the basal compartment of the transwell plates was monitored over time. Griseofulvin, which has been spray dried with the 4.0 µm mesh, showed the highest permeability. The spray drying experiments with the 5.0 and 7.0 µm mesh yielded materials, which both provided lower amounts of permeated griseofulvin. Conclusively, the aperture size of the vibrating mesh was found to be an important process parameter for reducing the particle size and enhancing the dissolution and permeability of a spray-dried drug powder, however, only to a small extent.
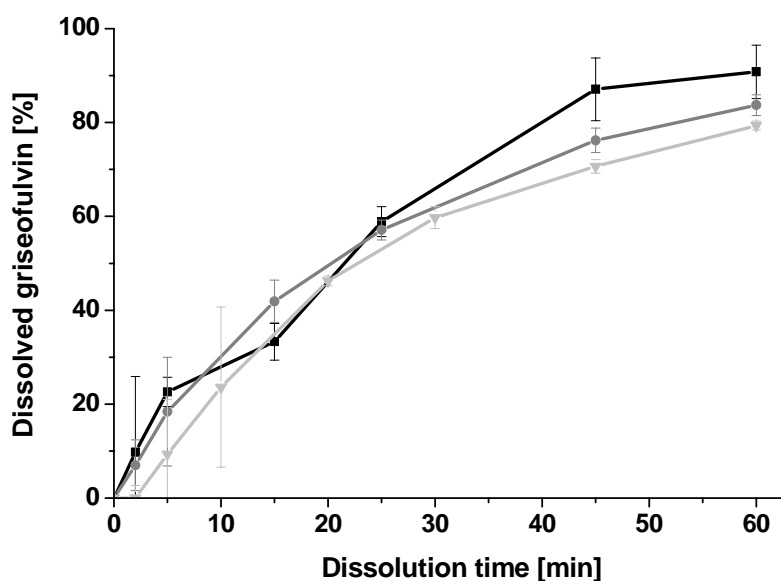
Figure 3 Dissolution profiles of griseofulvin powders spray dried with different vibrating meshes: 4.0 µm (-- ■ --), 5.5 µm (-- ● --), and 7.0 µm (-- ▼ --)
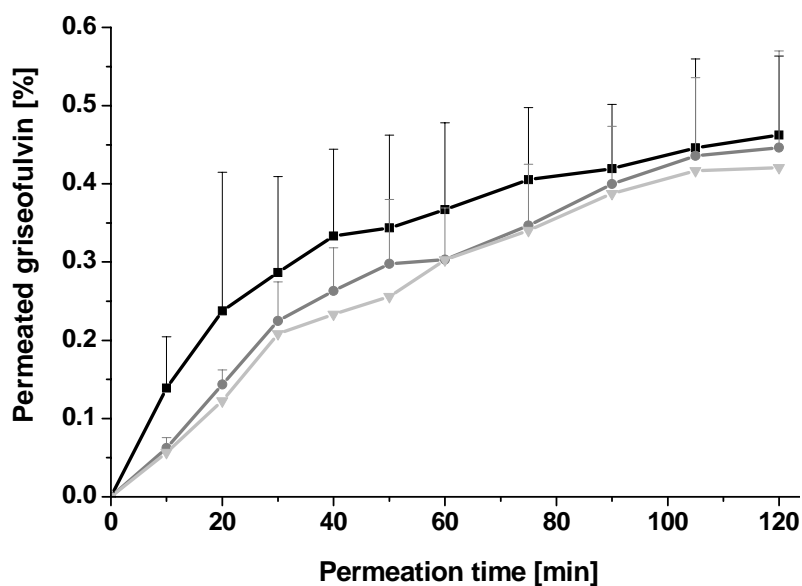
Figure 4 Permeability of griseofulvin powders spray dried with different vibrating meshes: 4.0 µm (-- ■ --), 5.5 µm (-- ● --), and 7.0 µm (-- ▼ --)

3.2   Influence of total solid content

In addition, the influence of total solid content of the spray solution on the griseofulvin particle size, dissolution rate, and permeability was investigated. Literature describes a moderate reduction of particle size associated with a decrease in total solid content, as the latter contributes only in the cube root to the overall particle size [25]. Three different solutions containing 1.5% griseofulvin, 0.44%, and 0.15% were spray dried with the 5.5 µm mesh (Table 2) and the resulting powders compared (Figure 5). Medium particle sizes were determined as 4.9 µm, 4.7 µm and 4.2 µm, respectively, resembling just a weak correlation of total solid content and particle size, particularly compared to the already determined strong influence of the vibrating mesh aperture size on particle size.
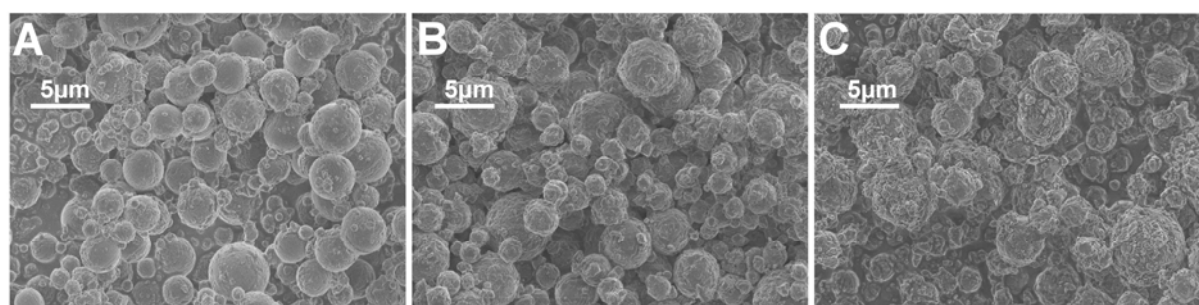
Figure 5 Effect of increasing total solid content on the particle size of spray-dried powders: **(A)** 0.15%, **(B)** 0.44%, and **(C)** 1.5% griseofulvin in the spray solution

Consequently, the influence of the total solid content on the dissolution rate was found to be marginal. If any, the improvement of drug dissolution by reduction of drug concentration in the spray solution was weak (Figure 6). The permeability of the respective powders showed the same tendency. The spray solution with only 0.15% total solid content produced a powder with slightly higher permeability than the spray solutions with 0.44% or 1.5% total solid content (Figure 7).
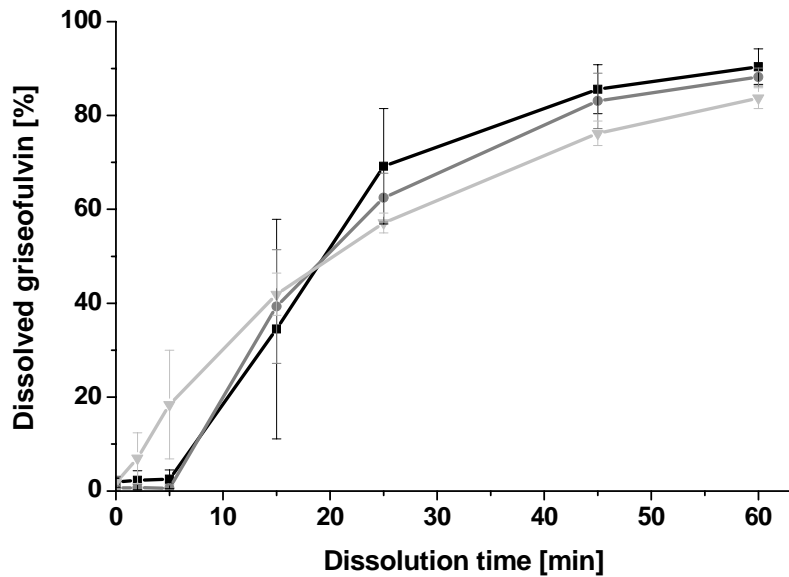
Figure 6 Dissolution profiles of griseofulvin powders from differently concentrated spray solutions: 0.15% (-- ■ --), 0.44% (-- ● --), and 1.5% total solid content (-- ▼ --)
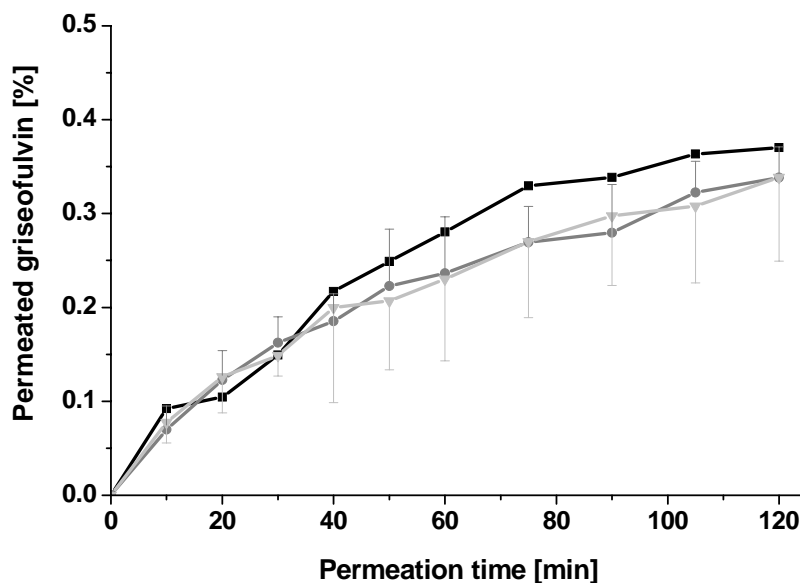
Figure 7 Permeability of griseofulvin powders from differently concentrated spray solutions: 0.15% (-- ■ --), 0.44% (-- ● --), and 1.5% total solid content (-- ▼ --)

3.3   Influence of formulation technique

Furthermore, the influence of different formulation techniques on particle properties was analyzed using micronized and spray-dried griseofulvin powders. Griseofulvin was spray dried with the Nano Spray Dryer B-90 and the Mini Spray Dryer B-290, and both powders were compared to griseofulvin bulk material, which has been produced by micronization. Medium particle sizes and powder appearance were found to be comparable between the different formulation techniques: 4.1 µm for micronized griseofulvin, 3.6 µm for material spray dried with the Nano Spray Dryer B-90, and 3.8 µm for material spray dried with the Mini Spray Dryer B-290 (Figure 8).
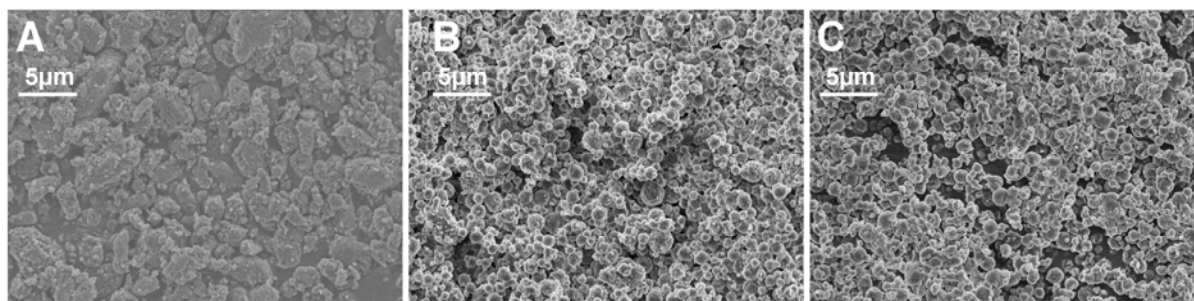
Figure 8 Different formulation techniques: **(A)** micronized griseofulvin, **(B)** Nano Spray Dryer B-90 product, and **(C)** Mini Spray Dryer B-290 product

The micronized bulk material showed excellent dissolution properties (Figure 9). Spray-dried material from the Nano Spray Dryer B-90 also dissolved rapidly, whereas the Mini Spray Dryer B-290 produced powder with a lower dissolution rate. As the particle size of these powders and the particle size distribution were similar, differences in dissolution behavior occurred most probably due to variances in surface structure and porosity of the materials. The micronized material had a very rugged particle structure with manifold curvatures, which are a consequence of the harsh production conditions and pose an ideal contact surface for the dissolution medium. The spray-dried powders, in particular the powder from the Mini Spray Dryer B-290, showed a smoother particle surface, which resulted in a lower drug dissolution rate.
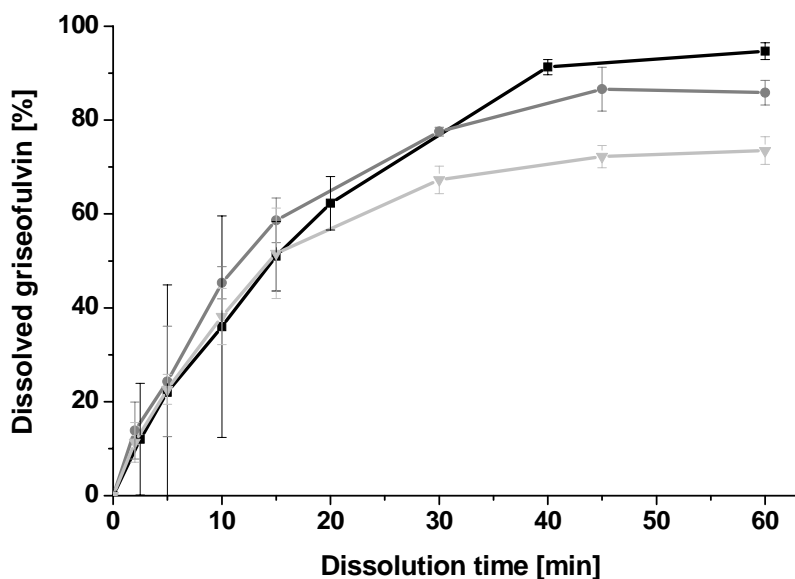
Figure 9 Dissolution rates of differently formulated griseofulvin powders: micronization (-- ■ --), spray drying with the Nano Spray Dryer B-90 (-- ● --), and the Mini Spray Dryer B-290 (-- ▼ --)

The dissolution rates were partially reflected by the permeability study, as the micronized and the Nano Spray Dryer material showed better permeability than the Mini Spray Dryer material. Permeability of griseofulvin spray dried with the Nano Spray Dryer B-90 even appeared superior compared to micronized material, however, given the standard deviation only insignificantly.
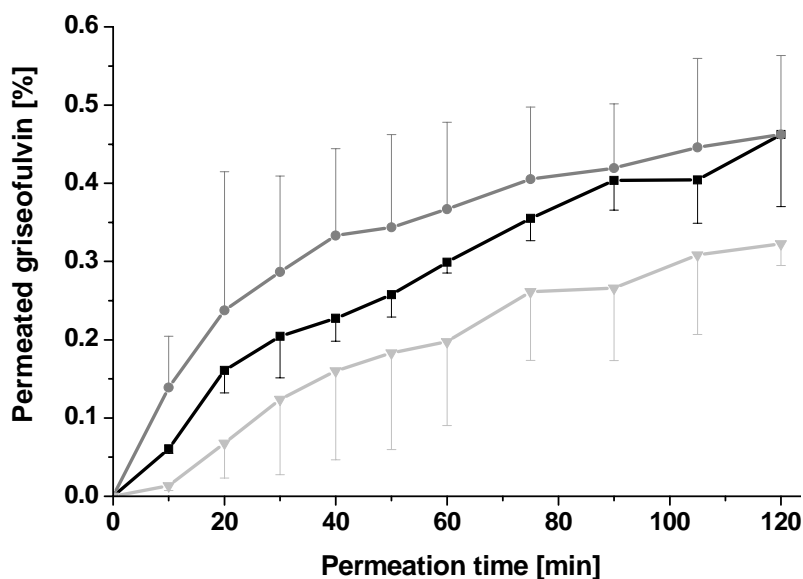
Figure 10 Permeability profiles of micronized griseofulvin (-- ■ --), griseofulvin spray dried with the Nano Spray Dryer B-90 (-- ● --), and with the Mini Spray Dryer B-290 (-- ▼ --)

3.4   Influence of surfactant addition

To improve the dissolution and permeability of griseofulvin, Lutrol F127 was added as solubilizing and wetting excipient to the griseofulvin formulation. Spray solutions of 0.5% griseofulvin containing 0.05% or 0.0025% Lutrol F127, resulting in a griseofulvin / Lutrol F127 ratio of 10 : 1 or 200 : 1, respectively, were spray dried with the Nano Spray Dryer B-90 and the Mini Spray Dryer B-290 (Table 2). Particle size analysis revealed no significant difference between the formulations: griseofulvin / Lutrol F127 (10 : 1) had a particle size of 3.8 µm, independently from the spray dryer used, and griseofulvin / Lutrol F127 (200 : 1) had a particle size of 3.6 µm if spray dried with the Nano Spray Dryer B-90 and 4.1 µm if spray dried with the Mini Spray Dryer B-290. Particle sizes were comparable to formulations without surfactant. As shown in Figure 11, the Nano Spray Dryer B-90 materials (A, B) seem to consist of discrete particles, whereas the Mini Spray Dryer B-290 materials (C, D) appear slightly coalescent.
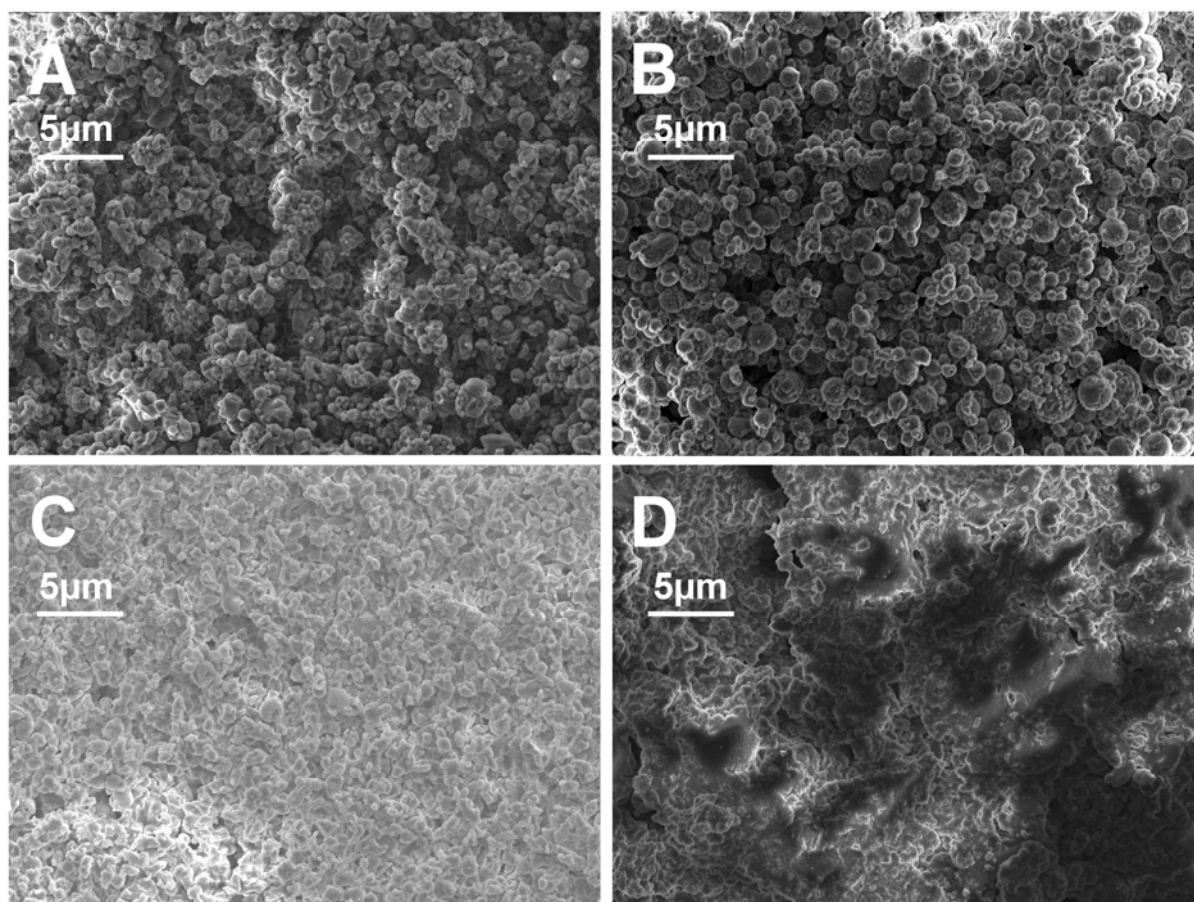
Figure 11 Griseofulvin powders spray dried with the Nano Spray Dryer B-90 **(A, B)** and the Mini Spray Dryer B-290 **(C, D)** containing 0.05% **(A, C)** and 0.0025% Lutrol F127 **(B, D)**

Figure 12 compares the dissolution properties of griseofulvin / Lutrol F127 powders spray dried with the Nano Spray Dryer B-90 to micronized griseofulvin. The addition of Lutrol F127 in the lower ratio (200 : 1) did not increase the dissolution rate. However, when adding a higher amount of Lutrol F127 (10 : 1), the spray-dried powder dissolved more rapidly in the first half hour of the dissolution experiment compared to all other powders, including spray-dried pure griseofulvin and micronized griseofulvin. As the overall amount of dissolved griseofulvin after 60 min was just marginally higher, Lutrol F127 primarily increased the dissolution rate and not the total amount of dissolved drug. Therefore, an increase of powder wettability due to large amounts of surfactant is assumed responsible for these effects.
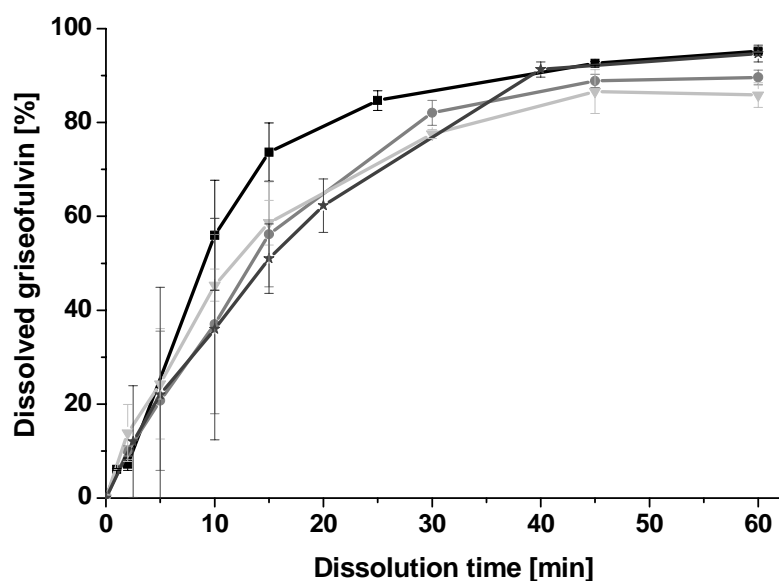
Figure 12 Dissolution profiles of griseofulvin spray dried with the Nano Spray Dryer B-90 containing 0.05% (-- ■ --), 0.0025% (-- ● --), and 0.0% Lutrol F127 (-- ▼ --) compared to micronized material (-- ★ --)

Regarding the corresponding permeability profiles (Figure 13), a similar situation was observed. The addition of high amounts of Lutrol F127 resulted in increased drug permeability, whereas low amounts of Lutrol F127 did not lead to a permeability increase. Conclusively, adding Lutrol F127 as wetting agent increased griseofulvin dissolution and permeability. However, rather high amounts were necessary in order to obtain a significant improvement.
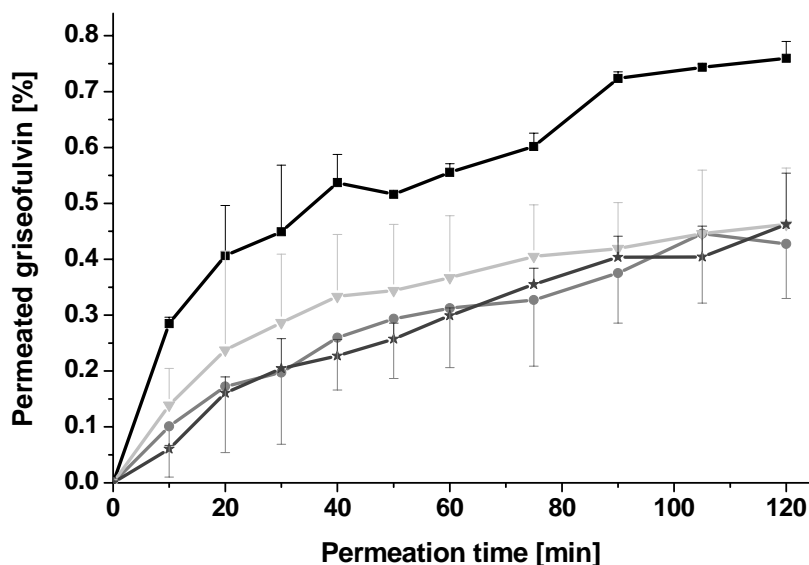
Figure 13 Permeability profiles of griseofulvin spray dried with the Nano Spray Dryer B-90 containing 0.05% (-- ■ --), 0.0025% (-- ● --), and 0.0% Lutrol F127 (-- ▼ --) compared to micronized material (-- ★ --)

Comparable experiments were conducted with the powders obtained using the Mini Spray Dryer B-290 (Figure 14). Only the griseofulvin powder containing high amounts of Lutrol F127 showed a dissolution rate equal to micronized griseofulvin. Pure griseofulvin and griseofulvin / Lutrol F127 200 : 1 were not able to dissolve as rapidly, most probably due to the absence of a wetting agent and the coalescence of powder particles, respectively. The permeability profiles of the respective powders show a superiority of the griseofulvin / Lutrol F127 mixture and the micronized material over the spray-dried pure griseofulvin (Figure 15).
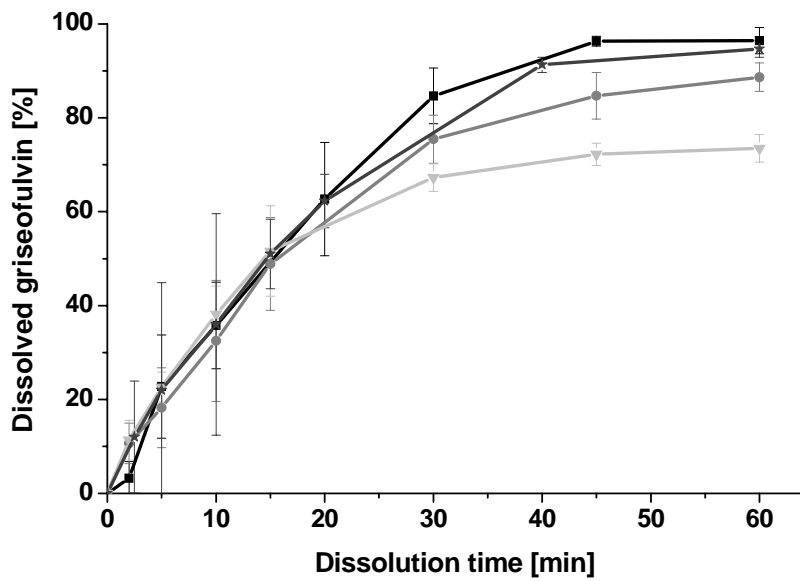
Figure 14 Dissolution profiles of griseofulvin spray dried with the Mini Spray Dryer B-290 containing 0.05% (-- ■ --), 0.0025% (-- ● --), and 0.0% Lutrol F127 (-- ▼ --) compared to micronized material (-- ★ --)
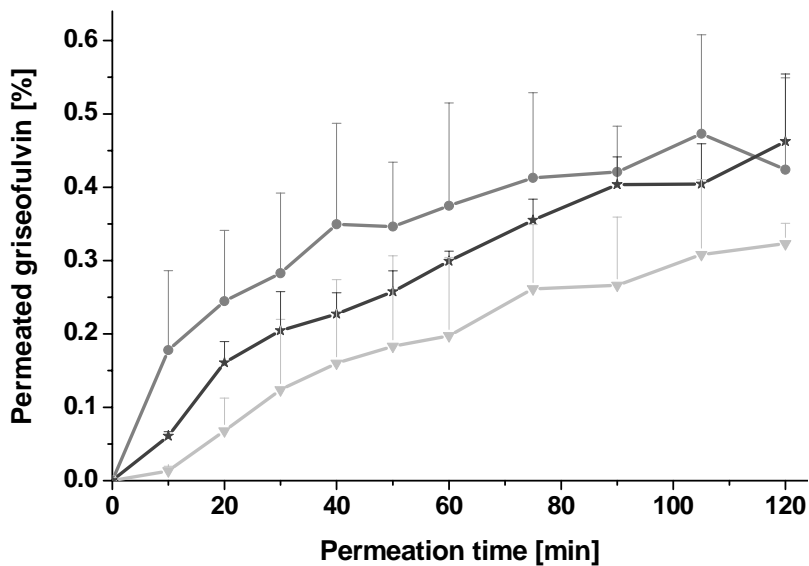

Figure 15 Permeability profiles of griseofulvin spray dried with the Mini Spray Dryer B-290 containing 0.0025% (-- ● --) and 0.0% Lutrol F127 (-- ▼ --) compared to micronized material (-- ★ --)

XRD diffractograms were recorded to evaluate the crystallinity of spray-dried, surfactant containing powders (Figure 16). Micronized griseofulvin and Lutrol F127 were analyzed as references. All samples exhibited a crystalline pattern, independently of surfactant addition or production technique. The amorphous phase of griseofulvin is known to crystallize easily, even at room temperature [26], and the absence of amorphous drug was therefore not surprising, although spray drying often results in the formation of amorphous material. Therefore, the improved dissolution rate of surfactant containing powders was not due to a partially amorphous state, but due to enhanced powder wettability and potentially meso- or nanoporosity resulting from leached Lutrol F127 that had phase separated.
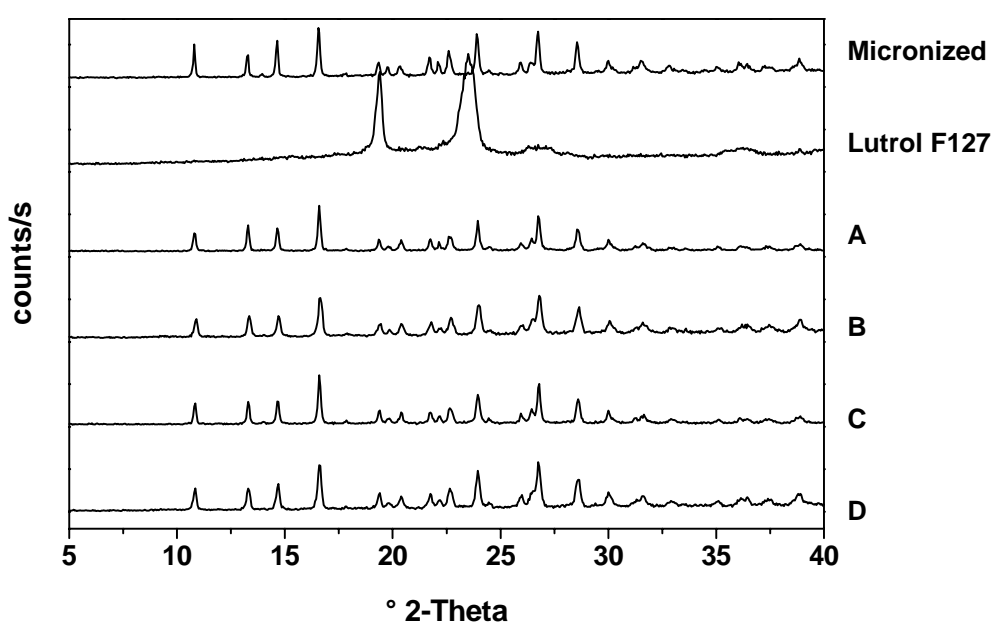
Figure 16 X-ray diffraction patterns of micronized griseofulvin, Lutrol F127, griseofulvin spray dried with the Nano Spray Dryer B-90 **(A)** or the Mini Spray Dryer B-290 **(B)** and griseofulvin / 0.05% Lutrol F127 spray dried with the Nano Spray Dryer B-90 **(C)** or the Mini Spray Dryer B-290 **(D)**

3.5   Integrity of Caco-2 monolayers

Caco-2 cell monolayers were checked for their integrity by measuring TEER values of each transwell before and after the drug transport study and by determining the permeability of the fluorescent dye lucifer yellow. The mean TEER determined before the drug transport study was 440 +/- 100 $\Omega * cm^2$ and varied across experiments within the range of 324 to 832 $\Omega * cm^2$. Both values are in good accordance with literature [27]. The monolayers experienced an average TEER reduction of 28 +/- 12% during the time of the drug transport study (approx. three hours). The electrical resistance of a monolayer is supposed to

resemble the epithelial permeability and the state of the tight junctions of the cell model. Therefore, a TEER decrease reflects an opening of tight junctions in the monolayer, which can occur due to the application of particles as described by Moyes [27]. The influence of Lutrol F127 on cell integrity was studied by separately applying Lutrol F127 to monolayers in triplicate. The average TEER loss caused by Lutrol F127 was determined as 24 +/- 7%. Therefore, a negative effect of the surfactant on cell integrity could be eliminated. No transwell was excluded from analysis because of its TEER loss. Lucifer yellow was used as an internal marker for cell integrity and was applied to the apical compartment of each transwell. An intact cell monolayer is indicated by an apparent permeability coefficient $P_{eff} < 2*10^{-7}$ cm/s, which was met by all investigated transwells.

3.6   Absolute griseofulvin permeability

The total amount of permeated griseofulvin was less than 1% of the applied dose, independently of the powder formulation. Kataoka et al. also found the permeated amount of griseofulvin (percentage of dose) to lie between 0.4 and 0.9% after a permeation time of two hours in a Caco-2 cell model [28]. Although this absolute permeability appears to be rather low, one has to consider the highly lipophilic nature of griseofulvin. After absorption at the apical side of the Caco-2 cell monolayer, the drug is presumably incorporated into lipophilic parts of the Caco-2 cells (e.g. cell membranes). The subsequent drug release at the basal side of the monolayer is therefore rather limited. Furthermore, the analysis time of two hours is shorter compared to the time window available for drug absorption in vivo. Wong et al. observed the griseofulvin plasma concentration in rats over 24 hours and found the time point of maximal drug plasma concentration to lie between three to four hours, depending on the kind of applied griseofulvin powder formulation [29].

4 Summary and Conclusions

For the first time the Nano Spray Dryer B-90 was implemented for inert spray drying of organic solvent solutions. A safe and robust spray drying process for the model drug griseofulvin was established by evaluating various organic solvents for their suitability as spray solution solvents. Acetone and methanol / acetone combinations gave the best spray performance without pronounced crust forming tendency. Griseofulvin powders with medium particle sizes of 3.4 to 6.5 µm were produced and compared to the 'gold standard' micronized griseofulvin concerning particle properties with relevance for drug absorption. Particularly, drug dissolution and cell culture permeability of spray-dried griseofulvin were analyzed and correlated to drug particles size. Spray drying of griseofulvin yielded a comparably fast dissolving and permeable powder compared to micronized milled material. The addition of Lutrol F127 as solubilizing agent improved the wettability of griseofulvin to such an extent that the dissolution rate was even faster than for micronized material. The advantages of spray drying over other micronization techniques were exploited, as for example, spray drying induces less mechanical stress on the drug substance compared to milling procedures, resulting in an enhanced physical and chemical stability of the product. Furthermore, the influence of the hot drying air in the spray dryer is comparable to the thermal stress imposed by melt extrusion processes. However, spray dryers usually have a lower consumption of drugs and excipients than extruders, which is most important at a lab scale development stage. When producing griseofulvin melt granulates, approx. 10 g drug was needed for each formulation [30], whereas the Nano Spray Dryer B-90 can conveniently be evaluated with drug quantities in the mg scale.

5   References

1   Porter CJH, Pouton CW, Cuine JF, Charman WN. Enhancing intestinal drug solubilisation using lipid-based delivery systems. *Adv Drug Deliv Rev* 2008; 60: 673-691.

2   Lobenberg R, Amidon GL. Modern bioavailability, bioequivalence and biopharmaceutics classification system. *Eur J Pharm Biopharm* 2000; 50: 3-12.

3   Rasenack N, Hartenhauer H, Muller BW. Microcrystals for dissolution rate enhancement of poorly water-soluble drugs. *Int J Pharm* 2003; 254: 137-145.

4   Crounse RG. Human pharmacology of griseofulvin: the effect of fat intake on gastrointestinal absorption. *J Invest Dermatol* 1961; 37: 529-533.

5   Charman WN, Rogge MC, Boddy AW, Berger BM. Effect of food and a monoglyceride emulsion formulation on danazol bioavailability. *J Clin Pharmacol* 1993; 33: 381-386.

6   Humberstone AJ, Porter CJH, Charman WN. A Physicochemical Basis for the Effect of Food on the Absolute Oral Bioavailability of Halofantrine. *J Pharm Sci* 1996; 85: 525-529.

7   Welling PG. Effects of food on drug absorption. *Annu Rev Nutr* 1996; 16: 383-415.

8   Khoo SM, Humberstone AJ, Porter CJH, Edwards GA, Charman WN. Formulation design and bioavailability assessment of lipidic self-emulsifying formulations of halofantrine. *Int J Pharm* 1998; 167: 155-164.

9   Kang BK, Lee JS, Lee HB, Cho SH. Development of self-microemulsifying drug delivery systems (SMEDDS) for oral bioavailability enhancement of simvastatin in beagle dogs. *Int J Pharm* 2004; 274: 65-73.

10   Hong JY, Kim JK, Kim CK. A new self-emulsifying formulation of itraconazole with improved dissolution and oral absorption. *J Contr Rel* 2006; 110: 332-338.

11   Mueller EA, Kovarik JM, Grevel J, Kutz K. Improved dose linearity of cyclosporine pharmacokinetics from a microemulsion formulation. *Pharm Res* 1994; 11: 301-304.

12   Sekiguchi K, Obi N, Ueda Y. Studies on absorption of eutectic mixture: II. Absorption of fused conglomerates of chloramphenicol and urea in rabbits. *Chem Pharm Bull* 1964; 12: 134-144.

13   Forster A, Rades T, Hempenstall J. Selection of suitable drug and excipient candidates to prepare glass solutions by melt extrusion for immediate release oral formulations. *Pharm Tech Eur* 2002; 14: 27-31.

14   Qian F, Huang J, Hussain MA. Drug-polymer solubility and miscibility: Stability consideration and practical challenges in amorphous solid dispersion development. *J Pharm Sci* 2010; 99: 2941-2947.

15   Timpe C. Oral drug solubilization strategies: applying nanoparticulate formulation and solid dispersion approaches in drug development. *APV Drug Delivery Focus Group Newsletter* 2010; 1.

16   Patterson JE, James MB, Rades T. Preparation of glass solutions of three poorly water soluble drugs by spray drying, melt extrusion and ball milling. *Int J Pharm* 2007; 336: 22-34.

17   Muller RH, Jacobs C, Kayser O. Nanosuspensions as particulate drug formulations in therapy. Rationale for development and what we can expect for the future. *Adv Drug Deliv Rev* 2001; 47: 3-19.

18   Van Eerdenbrugh B, Froyen L, Van den MG. Drying of crystalline drug nanosuspensions - The importance of surface hydrophobicity on dissolution behavior upon redispersion. *Eur J Pharm Sci* 2008; 35: 127-135.

19   Yasuji T, Takeuchi H, Kawashima Y. Particle design of poorly water-soluble drug substances using supercritical fluid technologies. *Adv Drug Deliv Rev* 2008; 60: 388-398.

20   Sharma A, Jain CP. Techniques to enhance solubility of poorly soluble drugs: a review. *J Global Pharm Tech* 2010; 2: 18-28.

21   Nuernberg E, Buhl-Wiederholt A, Schenk D. Pharmaceutically relevant properties of griseofulvin with special reference to spray embedding. *Pharmazeutische Industrie* 1976; 38: 907-912.

22   Atkinson RM, Bedford C, Child KJ, Tomich EG. Effect of particle size on blood griseofulvin-levels in man. *Nature* 1962; 193: 588-589.

23   Veiga MD, Diaz PJ, Ahsan F. Interactions of griseofulvin with cyclodextrins in solid binary systems. *J Pharm Sci* 1998; 87: 891-900.

24   United States Pharmacopeia USP32-NF27. Griseofulvin Capsules. 2531

25   Masters K. Spray Drying1976: 684.

26   Ahmed H, Buckton G, Rawlins DA. Crystallization of partially amorphous griseofulvin in water vapor: determination of kinetic parameters using isothermal heat conduction microcalorimetry. *Int J Pharm* 1998; 167: 139-145.

27   Moyes SM, Morris JF, Carr KE. Culture conditions and treatments affect Caco-2 characteristics and particle uptake. *Int J Pharm* 2009; 387: 7-18.

28   Kataoka M, Masaoka Y, Yamashita S. In vitro system to evaluate oral absorption of poorly water-soluble drugs: simultaneous analysis on dissolution and permeation of drugs. *Pharm Res* 2003; 20: 1674-1680.

29   Wong SM, Kellaway IW, Murdan S. Enhancement of the dissolution rate and oral absorption of a poorly water soluble drug by formation of surfactant-containing microparticles. *Int J Pharm* 2006; 317: 61-68.

30   Yang D, Kulkarni R, Kotiyan PN. Effect of the melt granulation technique on the dissolution characteristics of griseofulvin. *Int J Pharm* 2007; 329: 72-80.

Chapter 4

Protein spray drying with the Nano Spray Dryer B-90 – evaluation of the stress factors and the methods of stabilization

Abstract

This study evaluated the process related stress factors, which could influence protein stability during spray drying with the Nano Spray Dryer B-90. As the nozzle design of this novel spray dryer is essentially different, special attention was given to the effect of spray solution atomization on protein stability. As possible stresses the influence of temperature (inlet / outlet, spray head, spray mesh), spray intensity, air–liquid interfaces, prolonged spray drying times, and cavitation were identified. Spray drying was performed at various experimental setups using a monoclonal IgG_1 antibody and L-Lactic dehydrogenase (LDH), and protein stability of spray solutions and reconstituted powders was assessed by an enzymatic activity assay, HP-SEC, turbidity, and light obscuration. In general, the Nano Spray Dryer B-90 enabled to gain protein powder at high yields from small sample quantities. The IgG_1 antibody very well preserved its stability throughout the spray drying process. Instead, the more delicate LDH suffered from pronounced aggregate formation and thermal inactivation due to contact with the vibrating spray mesh. The mesh heats up to elevated temperatures during the spray drying process depending on the applied drying temperature, which therefore must be regarded as critical when spray drying sensitive proteins with the Nano Spray Dryer B-90.

1 Introduction

1.1 Stress factors during spray drying

While freeze drying is by far the most popular drying method for protein solutions in the pharmaceutical industry, spray drying has been successfully employed as alternative to ameliorate protein storage stability [1]. The choice of drying method is mainly determined by the intended route of administration of protein formulations. Pulmonary application is commonly the decisive factor to opt for spray drying, as this process yields fine and flowable powders while providing setup parameters for targeted adjustment of particle size [2]. The challenge of protein spray drying is to avert a negative impact of the multiple process related stress factors on protein stability by finding suitable formulation compositions and process conditions. Amongst the main causes for chemical and physical protein instabilities, the influence of the following process parameters must be emphasized:

- Temperature
- Air–liquid interfaces
- Dehydration

Temperature

Most proteins undergo reversible or irreversible thermal denaturation when exposed to high temperatures and lose biological activity or solubility. However, negative influences of high inlet air temperatures during spray drying are attenuated by the self-cooling effect of droplets due to solvent evaporation, which prevents a temperature increase of the droplet surface above the wet bulb temperature. Furthermore, the development of high solid concentrations inside the drying droplet increases viscosity and decelerates protein unfolding, and the protein denaturation temperature (T_m) increases with decreasing water content. Finally, thermal protein denaturation during spray drying not only depends on the temperature level, but also on the time of exposure of the proteins to the hot drying air [1]. As the exposure time of drying droplets to the elevated temperature ranges in the millisecond scale, thermal denaturation during spray drying is often regarded as negligible.

Air–liquid interfaces

The atomization of the protein solution during spray drying negatively affects the stability of most proteins due to the tremendous expansion of the air–liquid interface. As amphiphilic and surface-active polyelectrolytes, proteins can adsorb to surfaces and interfaces, which leads to the orientation of hydrophobic amino acid residues towards the nonaqueous environment and in the end to protein unfolding. Unfolded proteins are prone to aggregation triggered by hydrophobic interaction. The extend of protein surface adsorption depends on the number and the distribution of hydrophobic amino acids on the protein surface and the rigidity or flexibility of the protein in solution. In order to prevent protein adsorption and aggregation at the air–liquid interface, surfactants are commonly added to the spray solution [3]. Their preventive action is mainly ascribed to the displacement of protein molecules from the air–liquid interface [4]. In addition, their binding to the hydrophobic sites of protein molecules avoids intermolecular protein interactions and aggregation [1].

Dehydration

In course of the drying process, the protein molecules are deprived of the surrounding, protective water and are thermodynamically destabilized by losing their hydrogen bonding to water molecules. Therefore, small molecule stabilizers like sugars or polyols are commonly incorporated as 'water substitutes' in protein spray drying formulations, as they are capable of replacing the hydrogen bonding existing in an aqueous environment. Thus, protein stabilization is achieved by maintaining the free energy of unfolding high and the protein molecules remain in their native conformation. Apart from this water substitution action, saccharide or poylol protectants can form glassy solid matrices during the drying process, which mechanically immobilize the protein molecules and provide enough kinetic stabilization against protein unfolding [5]. Thereby, conformational stabilization is accomplished independently of the free energy of unfolding. Regardless of the mechanism leading to protein stabilization, a key requirement for all protective excipients is to remain in the same amorphous phase together with the protein during dehydration, thus avoiding phase separation and crystallization.

1.2 Protein spray drying with the Nano Spray Dryer B-90

Although the elevated temperatures applied in a spray dryer are usually seen as minor stress factor, proteins might suffer from thermal denaturation if they are rather thermosensitive. Adler et al. found a reduced process stability for LDH, when spray drying with a Büchi Mini Spray Dryer B-190 was performed at T_{in} / T_{out} settings of 150 / 95 °C instead of 90 / 60 °C, and ascribed the protein inactivation to thermal stress [6]. The Nano Spray Dryer B-90 (Büchi Labortechnik AG, Flawil, Switzerland) could represent a valuable option for spray drying proteins like LDH, which are prone to temperature induced inactivation. Due to its ability to generate small droplets, drying temperatures in the lower range are sufficient to gain a dry powder [7]. Furthermore, the drying air or gas that is fed into the drying chamber is characterized by a very low residual humidity of less than 8%, which ensures a high drying efficiency even at low T_{in} settings. The evaluation of the Nano Spray Dryer B-90 for spray drying pharmaceutical proteins was performed using IgG_1 and LDH. The former represents a rather robust class of proteins, which shows good process stability during spray drying [8, 9], whereas the latter poses a greater challenge for the formulation scientist due to its sensitivity towards elevated temperatures and interfaces [10].

Properties of the Nano Spray Dryer B-90 critical to protein stability

Challenges to protein stability, like temperature, interfaces, and dehydration are inherent in spray drying processes and are therefore expected to also become relevant when spray drying with the Nano Spray Dryer B-90. However, further influences potentially compromising protein stability must be considered, which arise from the design and functional principle of the Nano Spray Dryer B-90. In particular, the configuration of the spray dryer nozzle (Figure 1) could possibly be an origin of protein stress.
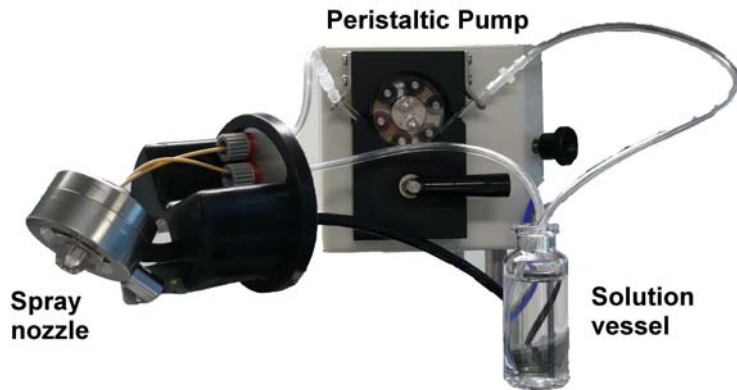
Figure 1 Setup of the Nano Spray Dryer B-90 nozzle with bulk solution vessel and peristaltic pump

In contrast to the pressurized air nozzles typically implemented in conventional spray dryers, the Nano Spray Dryer B-90 nozzle atomizes spray solutions based on the vibrating mesh spray technology. From the bulk vessel, the spray solution is delivered to the nozzle via a peristaltic pump. The solution volume, which can be atomized, depends on the aperture size of the applied vibrating mesh. Even for the largest apertures of 7.0 µm, the spraying rate is much lower than the pumping rate. Consequently, spray solution returns into the bulk solution vessel. This circulation of spray solution is also mandatory for an efficient and continuous atomization, as otherwise the push–pull action of the mesh would lead to the accumulation of an air or drying gas bubble on top of the spray mesh, impeding close contact of solution and mesh and ultimately ceasing the spray (Figure 2).
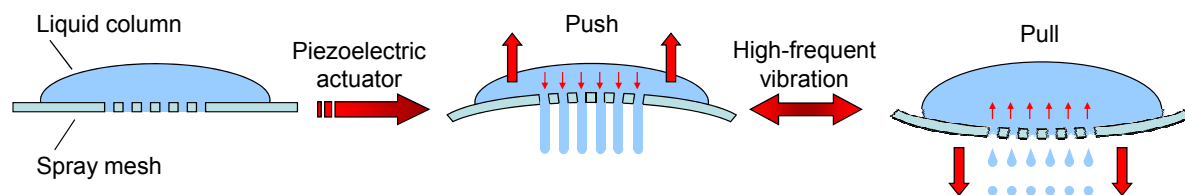
Figure 2 Push–pull operating mode of the vibrating mesh (adopted from Büchi Labortechnik AG)

This nozzle setup implicates several factors that have the potential to provoke protein denaturation:

- **Surfaces (silicon / PEEK tubes)**

  Protein adsorption to surfaces is a ubiquitous phenomenon and depends on multiple protein and surface related characteristics. Usually, the formulation of the protein solution is adopted in terms of surfactant addition, pH, and ionic strength, in order to prevent extensive protein adsorption. In this study, LDH was employed as a model protein with high affinity to surfaces, and its adsorption to the spray nozzle tubes was studied in absence and presence of surfactant.

- **Additional air–liquid interface**

  Entrainment of air or drying medium into the bulk spray solution occurs due to the push–pull action of the mesh. This generates an additional air–liquid interface even before the atomization of the spray solution occurs. In order to moderate negative effects on protein stability, surfactant was added to the spray solution.

- **High frequency vibration of the spray mesh**

  The spray mesh vibrates at resonance frequency in the ultrasonic range, which cannot be influenced by the spray dryer operator. The 'spray intensity' corresponds to the time, in which the vibration of the spray mesh is activated, and can be set by the operator in a range from 0 – 100%. Lower spray intensities result on the one hand in a reduced throughput of spray solution per time, but on the other hand in a slower and less heating of the vibrating mesh. The first effect might aggravate protein instabilities due to elongated process times, whereas the latter might be beneficial regarding thermosensitive proteins.

- **Elevated temperature of the spray mesh**

  Due to its position inside the drying tower, the spray nozzle heats up leading to a steady temperature increase of the spray solution. Furthermore, the activity of the piezoelectric actuator causes continuous heating of the spray mesh, which is limited to a maximum value of 6 °C above T_{in}. However, the spray solution gets into contact with the hot metallic mesh and has to pass through it during atomization. Cooling of the solution vessel was applied as default measure against extensive spray solution heating, and low inlet temperatures were used in order to reduce the overall heating. The thermosensitivity of LDH was determined by T_m measurements and the temperature of the vibrating mesh was measured by an external temperature probe.

- **Elongated atomization process times**

  Due to the low throughput of spray solution, e.g. 10 mL per hour for the small vibrating mesh with 4.0 µm apertures at 100% spray intensity, the overall time to achieve a dry protein powder increases compared to a standard spray drying process. This process time can be further extended if a reduced spray intensity is chosen. Consequently, the liquid protein formulation must be sufficiently stable throughout the complete spray drying process. Therefore, LDH stability in spray solutions was determined in short term storage experiments.

- **Cavitation**

  The cavitation phenomenon was also considered as possible cause for protein instability upon atomization with the Nano Spray Dryer B-90. Transient (or inertial) cavitation describes the creation, subsequent expansion and implosive collapse of gas bubbles in fluids [11]. One reason for the formation of cavities is the impact of high kinetic energy on fluids due to hydrodynamic or acoustic agitation, because this energy impact generates regions with a local pressure below the vapour pressure of the liquid. As the spray mesh of the Nano Spray Dryer B-90 vibrates with ultrasonic frequency (~ 60 kHz), the spray solution might encounter cavitation stress. During the collapse of cavities, reaction zones of high temperature and pressure ('hot spots') are formed [11] and the generation of free radicals due to the thermal decomposition of water molecules is postulated [12]. Free radicals (e.g. hydroxyl radicals, hydrogen atoms) could react with protein molecules and compromise protein stability to a considerable extent [13]. To quantify the extend of radical formation in spray solutions, chemical dosimetry with potassium iodide was conducted as standard analysis method [14].

2   Materials and Methods

2.1   Materials

2.1.1   Excipients

Sodium phosphate monobasic anhydrous, sodium pyruvate, β-nicotinamide adenine dinucleotide (β-NADH), potassium iodide and bovine serum albumin (BSA) were obtained from Sigma (Munich, Germany), trehalose from Ferro Pfanstiehl (Cleveland, Ohio, USA), polysorbate 20 and 80 from Merck (Darmstadt, Germany). MilliQ water was used for dialysis and preparation of excipient solutions.

2.1.2   Proteins

- Monoclonal IgG_1 antibody (IgG_1)

  A humanized monoclonal antibody of the IgG_1 class was provided at approx. 50 mg/mL in an aqueous buffer containing glycine and histidine. The IgG_1 stock solution was filtered through a 0.2 μm polyethersulfone sterile syringe filter (VWR, Darmstadt, Germany) before use.

- L-Lactic dehydrogenase (LDH)

  L-Lactic dehydrogenase Type II from rabbit muscle was purchased as aqueous crystalline suspension in 3.2 M ammonium sulfate at pH 6.0 containing 10.9 mg/mL or 1150 units/mg protein (Sigma, Munich, Germany). This suspension was dialyzed against 100 mM phosphate buffer to pH 7.5 immediately before use. Dialysis was performed for 3 hours at 4 °C using a cellulose membrane with 14 kDa MWCO (Roth, Karlsruhe, Germany).

2.2   Methods

2.2.1   Preparation of spray solutions

Spray solutions were prepared from protein and excipient stock solutions and filtered before spray drying using 0.22 µm PTFE sterile syringe filters (VWR, Darmstadt, Germany). IgG_1 spray solutions contained 2.5% (w/w) IgG_1 / trehalose (ratio 70 : 30) either with or without 0.02% polysorbate 20. LDH spray solutions contained 5% (w/w) LDH / trehalose (0.2 : 99.8) either with or without 0.1% polysorbate 80.

2.2.2   Spray drying experiments

The Nano Spray Dryer B-90 (Büchi Labortechnik AG, Flawil, Switzerland) was used in tall configuration and open cycle mode with compressed air from in-house supply (≤ 8% r.h.). The drying air flow rate was set to 115 L/min, the inlet temperature to 20 - 120 °C, and the spray intensity to 25% or 100%. Vibrating meshes with 4.0 µm and 7.0 µm apertures were applied for spray drying approx. 10 mL of each spray solution. After finishing the spray drying process, collection of the spray-dried powders was carried out in controlled humidity and samples were stored in a desiccator (< 20% r.h.) at room temperature until further analysis.

2.2.3   Circulation experiments

The influence of the circulation of the spray solution on protein stability was evaluated by pumping spray solution for 60 min through the spray nozzle. Heating and spraying were not activated. After 30 and 60 min, samples were taken and analyzed.

2.2.4   Temperature measurements

The actual temperature of the vibrating mesh was measured by placing a temperature probe directly on the surface of the mesh (Figure 3). Spray processes with water at various temperature and spray intensity settings were conducted and the temperatures determined immediately after dismounting the spray dryer nozzle from the drying chamber.

Figure 3 Dismounted spray dryer nozzle: **(A)** view of PEEK tubes and spray head, **(B)** detail of piezo crystals and thermocouples, and **(C)** external temperature probe placed on the spray mesh

2.2.5 Quantification of protein content

Spray-dried powders were reconstituted to the concentration of the initial protein spray solution with water in glass vials under gentle agitation. IgG_1 concentration of bulk solution, spray solutions, and reconstitutes was determined photometrically at 280 nm using an Agilent 8453 UV-Vis spectrophotometer (Agilent, Waldbronn, Germany).

The LDH concentration of dialysates, spray solutions, and reconstitutes was determined by a Micro BCA™ protein assay (Thermo Scientific, Rockford, Illinois, USA). In a micro well plate 150 µL protein sample, adequately diluted with buffer, and 150 µL assay reagent were mixed and incubated for 2 hours at 37 °C. The absorbance at 562 nm was measured on a plate reader (FluoStar Omega, BMG Labtech, Offenburg, Germany).

2.2.6 LDH activity assay

The enzymatic activity of LDH was determined using the assay provided by Sigma (Munich, Germany). This activity assay utilizes the reaction of pyruvate and β-NADH to L-lactate and β-NAD. The reduction of β-NADH is monitored by the decrease of absorption at 340 nm. A mixture of 0.1 mL sodium pyruvate (69 mM) and 2.8 mL β-NADH (0.13 mM) was equilibrated for at least 30 min to 37 °C in disposable plastic cuvettes using a water bath. Evaporation of solution was prevented by parafilm coverage of the cuvettes. Protein samples were diluted to a final LDH concentration of approx. 0.25 - 0.75 units/mL with a 1.0% (w/v) BSA solution. 0.1 mL LDH sample was added to the sodium pyruvate / β-NADH mixture and the decrease of absorption at 340 nm was recorded over 4 min using an Agilent 8453 UV-Vis spectrophotometer (Agilent, Waldbronn, Germany). The linear slope *a* was determined by regression and the activity was calculated using the following equation:

$$a\left[units/ml_{enzyme}\right]=\frac{\left(\Delta A_{340}/\min{}_{Sample}-\Delta A_{340}/\min{}_{Blank}\right)*V_{T}*df}{6.22*V_{E}}$$

where V_T and V_E are the total volume of the assay and the volume of enzyme used, *6.22* the millimolar extinction coefficient of β-NADH at 340 nm and *df* the dilution factor.

2.2.7 Subvisible particle analysis by light obscuration

Concentration and size distribution of subvisible particles in spray solutions and reconstitutes were determined by light obscuration using a SVSS C32 apparatus (Pamas, Rutesheim, Germany). The system was flushed with particle free water until there were less than 100 particles larger than 1 µm per 1 mL. Test measurements with particle free water were performed at the beginning and at the end of analysis. After each measurement, the system was flushed with 5 mL of particle free water to exclude cross contamination.

2.2.8 Turbidity

Optical density measurements were performed at 350 nm with an Agilent 8453 UV-Vis spectrophotometer (Agilent, Waldbronn, Germany).

2.2.9 Microcalorimetry

The differential scanning calorimetry (DSC) thermograms of LDH dialysate and LDH spray solutions were acquired using a VP-DSC differential scanning calorimeter (MicroCal, Northampton, USA) and the midpoint of the unfolding transition peak T_m was calculated. The thermograms were obtained in triplicate after subtraction of the corresponding buffer scan by heating 1 mg/mL LDH solutions from 20 to 90 °C at a scan rate of 10 °C/h.

2.2.10 High performance size exclusion chromatography (HP-SEC)

IgG$_1$ samples were analyzed for soluble aggregates by HP-SEC using a HP 1100 instrument (Agilent, Waldbronn, Germany) equipped with a TSKgel® G3000 SW$_{XL}$ column (300-7.8 mm) and guard column (Tosoh Bioscience, Tokyo, Japan). The running buffer was composed of 100 mM disodium hydrogen phosphate dihydrate and 100 mM sodium sulfate

and was adjusted with ortho-phosphoric acid 85% to pH 6.8 . The flow rate was set to 0.5 mL/min and the injection volume to 25 µL. Samples were centrifuged prior to analysis in order to remove insoluble aggregates. Protein aggregates, monomer and fragments were detected photometrically at 280 nm. The chromatograms were integrated manually using the HP ChemStation software 9.0 (Agilent, Waldbronn, Germany). Percentage of aggregates was calculated by comparing the area under the curve (AUC) of the aggregate peak to the total AUC. Of each sample, three chromatographic samples were prepared and analyzed.

2.2.11 Scanning electron microscopy (SEM)

The particle morphology of the spray-dried powders was determined with a JSM-6500F JEOL scanning electron microscope (JEOL, Eching, Germany). For analysis, the samples were fixed on self-adhesive tapes on an aluminum stub and sputtered with carbon.

2.2.12 Chemical dosimetry

Chemical dosimetry with potassium iodide was used to quantify the formation of free radicals due to cavitation. Free radicals oxidize iodide to iodine and due to the equilibrium of $I_2 + I^- \leftrightarrow I_3^-$, their presence can be quantified by an increase of I_3^-. The concentration of I_3^- was measured photometrically at 355 nm in microwell plates using a FluoStar Omega plate reader (BMG Labtech, Offenburg, Germany) at several time points (0, 4, 30, 60 and 90 min). 15 mL of a 0.1 mol/L aqueous potassium iodide solution were subjected to either

- Storage at 2 – 8 °C to quantify unspecific oxidation,

- Circulation in the spray nozzle without activation of spraying or heating,

- Spray drying with the Nano Spray Dryer B-90 (T_{in} 120 °C, vibrating mesh aperture size 4.0 µm, 100% spray intensity) or

- Sonication using a SONOPULS UW2200 ultrasonic homogenizer with a MS73 probe (both Bandelin, Berlin, Germany) at 40% power and 60% cycle intensity. The tip of the probe was immersed into the potassium iodide solution, which was cooled in an ice-water bath to account for the thermal heating upon sonication.

3 Results and Discussion

The Nano Spray Dryer B-90 was found feasible of spray drying protein solutions without any crust formation tendencies. This phenomenon has been found previously for some saccharide based spray solutions without protein [7]. Its nozzle stayed clear of any powder depositions independently of the kind of protein and surfactant addition, respectively. This excellent spray dryer performance is reflected in the consistently high yields of protein spray drying processes (Table 1).

3.1 Stability of IgG_1 during spray drying

An IgG_1 antibody spray solution, consisting of 2.5% (w/w) IgG_1 / trehalose (70 : 30), was further varied by addition of 0.02% polysorbate 20. Trehalose was added to the formulation as common stabilizer in protein spray drying. The improvement of protein stability in the presence of trehalose can be ascribed on the one hand, to the 'vitrification' of protein molecules in the amorphous state [15] and on the other hand, to the 'water substitution' effect replacing hydrogen bonds between protein and water molecules [16]. Furthermore, the high glass transition temperature (T_g) of amorphous trehalose is particularly favorable with regard to the storage stability of protein formulations [6]. Spray drying antibodies with traditional spray dryers had proven good protein stability for drying temperatures of 130 / 75 °C (T_{in} / T_{out}), even without surfactant addition [8]. Therefore, the evaluation of the Nano Spray Dryer B-90 was started by applying drying temperatures close to the established settings. Table 1 summarizes the spray drying parameters and the analytical results for the spray-dried protein powders after reconstitution. In HP-SEC analysis, only IgG_1 dimers were detected at unchanged AUC.

Table 1 Overview of process parameters and results of IgG_1 spray drying experiments
        Ab_#:   antibody solution without surfactant
        AbPS_#:   antibody solution containing 0.02% polysorbate 20

#	Mesh size [μm]	Intensity [%]	T_{in} / T_{out} [°C]	$T_{spray head}$ [°C]	Yield [%]	Aggregates [%]	OD_{350nm} [AU]
Ab_1	4.0	100	120 / 50	126	69	0.85	0.262
Ab_2	4.0	100	90 / 33	97	82	1.15	0.115
AbPS_1	4.0	100	120 / 50	100	83	1.16	0.217
AbPS_2	4.0	100	90 / 36	97	77	0.49	0.075
AbPS_3	5.5	100	90 / 33	97	86	0.39	0.071
AbPS_4	7.0	25	90 / 30	76	73	0.39	0.053

Spray drying the antibody standard formulation Ab_1 at T_{in} / T_{out} of 120 / 50 °C resulted in numerous soluble and insoluble aggregates compared to the unprocessed spray solution (initial values: 0.39% and 0.036 AU). The lower temperature setting of 90 / 33 °C also induced aggregate formation, but the increase in insoluble aggregates was less pronounced at this lower T_{in} / T_{out} setting (Ab_2). The formulation, which contained polysorbate 20, showed comparable results at 120 / 50 °C (AbPS_1). However, when spray drying was performed at 90 / 36 °C (AbPS_2), protein stability was better preserved compared to the surfactant free formulation. To evaluate the influence of the vibrating mesh aperture size on process performance and protein stability, the surfactant containing solution was also spray dried with the 5.5 and 7.0 µm mesh (AbPS_3 and AbPS_4). Both processes showed high yields without crustification and yielded material with good protein stability. The best results were obtained with the 7.0 µm mesh. When applying this mesh, the spray solution throughput increased to such an extent, that the spray intensity had to be reduced to prevent solution deposition on the drying chamber walls. The lower spray intensity slowed down the heating of the spray head, which reached only 76 °C instead of 97 °C at the end of the spray drying procedure. The spray head temperature is determined by the inlet temperature, the spray intensity, and the process duration and can be regarded as indicator for the actual temperature of the vibrating mesh. Therefore, it is hypothesized that the application of the lower drying temperatures (90 / 30 °C) and / or the lower spray intensity (25%) might have been beneficial with regard to protein stability, as the heating of the spray mesh and the thermal stress exerted on the IgG_1 were reduced. The spray-dried particles had a perfectly spherical appearance with a smooth surface and the particle size showed a strong correlation to the aperture size of the vibrating mesh (Figure 4).
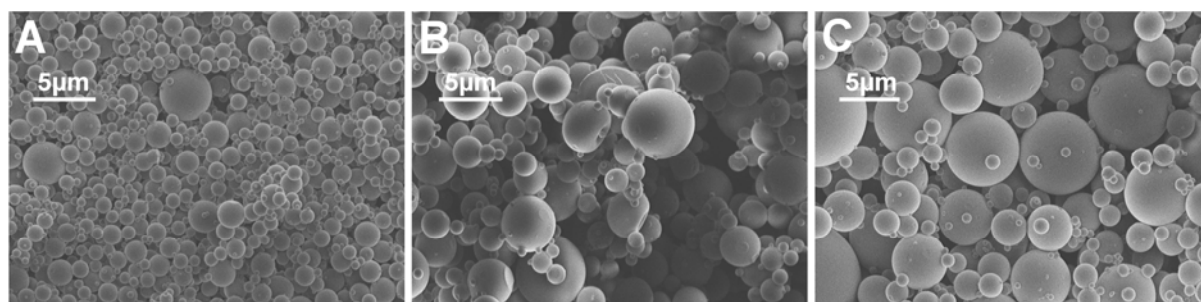
**Figure 4** SEM of spray-dried IgG_1 / trehalose / 0.02% polysorbate 20 particles by different mesh sizes: **(A)** 4.0 µm (AbPS_2), **(B)** 5.5 µm (AbPS_3), and **(C)** 7.0 µm (AbPS_4)

Thus, the IgG_1 antibody could be successfully spray dried with the Nano Spray Dryer B-90 at high yields. The spray drying induced only marginal aggregate formation, which appears to be related to the vibrating mesh temperature.

3.2 Stability of LDH in spray solutions

In order to further evaluate the influence of temperature on protein stability during spray drying with the new spray dryer, LDH was chosen as a very temperature sensitive model protein. Elkordy et al. described the thermal sensitivity of LDH and showed that high temperatures of 125 / 66 °C (T_{in} / T_{out}) perturbed secondary and tertiary protein structures, which resulted in a loss of enzyme activity [17]. Comparing the Nano Spray Dryer B-90 to conventional spray dryers, a lower throughput of spray solution per time becomes evident and proteins in the spray solution might be exposed to destabilizing factors for a longer period of time. Therefore, LDH spray solutions with trehalose and polysorbate 80 were prepared and stored for 90 min at 4 °C. The enzyme activity and particle content were determined at 30 min intervals. Trehalose was added as carrier material to the LDH spray solution, because as described above, its stabilizing effects are well known and widely utilized in protein drying techniques. In the present study, LDH substantially preserved its activity over 90 min in the presence of trehalose (Figure 5), providing a broad time window for lengthy spray drying processes. Formation of protein aggregates was not observed during this time, as the number of particles remained in the range of water considered as particle free (Figure 6). Turbidity was below 0.005 AU for all formulations indicating essentially the absence of nm-size aggregates.
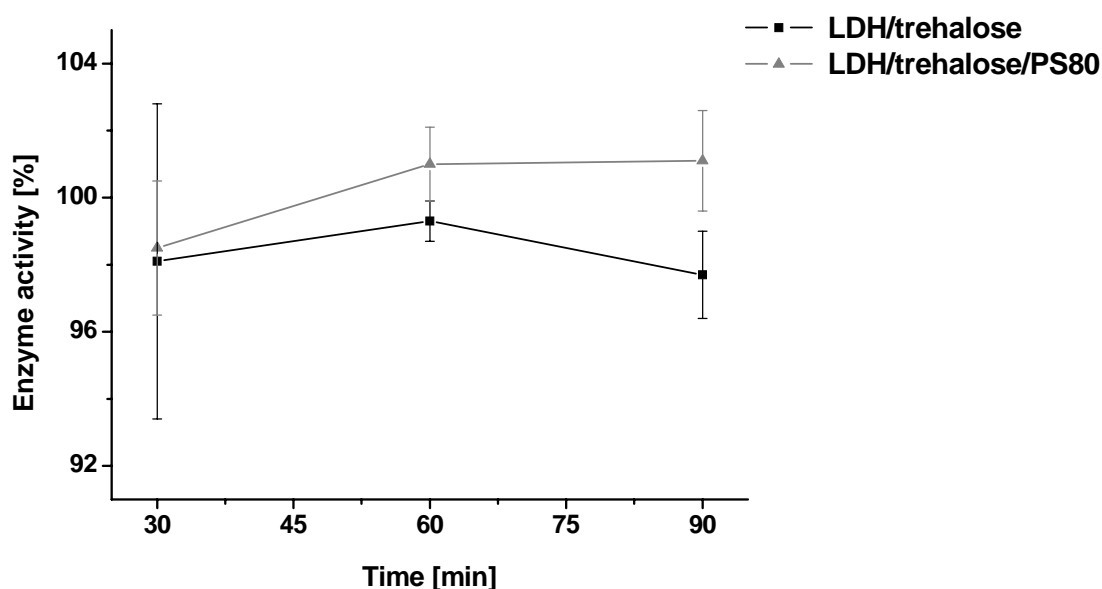

Figure 5 Enzyme activity of LDH in solution during storage at 4 °C

In a next step, LDH stability was tested in a trehalose solution containing polysorbate 80. The rationale for adding surfactant to the spray solution was to avoid protein adsorption at air–liquid interfaces during spray drying. As aforementioned, its protective mechanism is based on the competition for interfaces between surfactant and protein molecules [6]. Under the combined influence of trehalose and polysorbate 80, LDH activity also remained on a high level during the 90 min storage time (Figure 5). No formation of subvisible particles or large aggregates was observed (Figure 6).
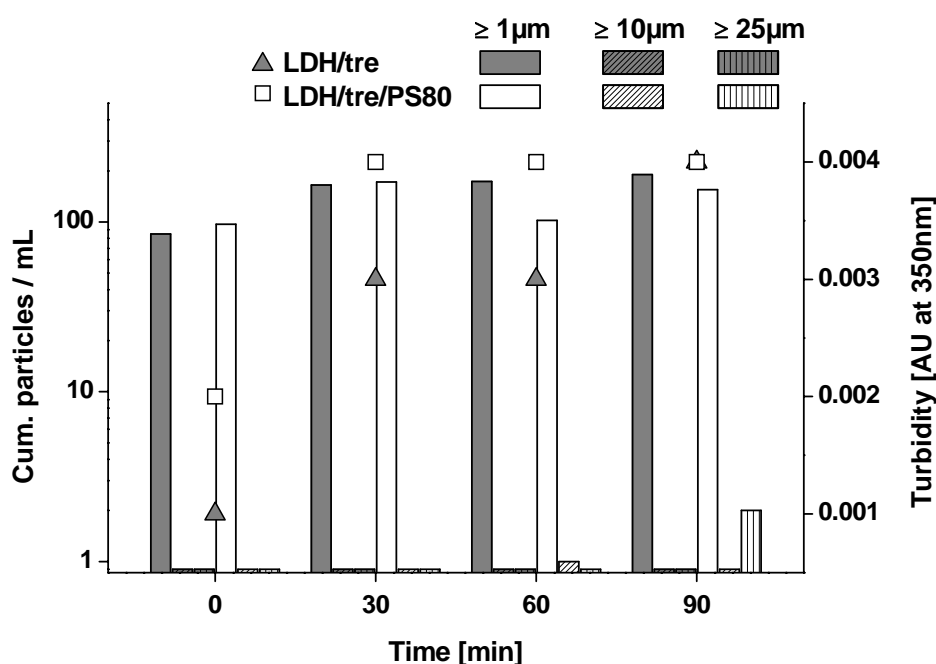
Figure 6 Subvisible particles (columns) and turbidity (symbols) of LDH / trehalose solution with and without polysorbate 80 during storage at 4 °C

In addition to the analysis of the enzyme activity and the particle content, the melting temperature (T_m) of LDH in both formulations was assessed (Figure 7). The DSC thermograms of LDH showed a single endothermic peak with a maximum at approx. 56 °C. Visual inspection of the samples after analysis showed that precipitates had formed due to protein aggregation. T_m of the enzyme was determined with 56.2 +/- 0.3 °C in the dialysis buffer, 56.0 +/- 0.4 °C in the LDH / trehalose formulation and 56.4 +/- 0.6 °C in the LDH / trehalose / PS80 formulation. Thus, no significant effect of trehalose or polysorbate 80 on T_m was detected. LDH unfolding started at about 49 °C in the dialysis buffer and in the LDH / trehalose / PS80 formulation and at about 53 °C in the LDH / trehalose formulation, indicating the thermal sensitivity of the enzyme. Conclusively, LDH showed sufficient storage stability at 4 °C for 90 min and was regarded appropriate for evaluating the Nano Spray Dryer B-90 due to its pronounced temperature sensitivity.
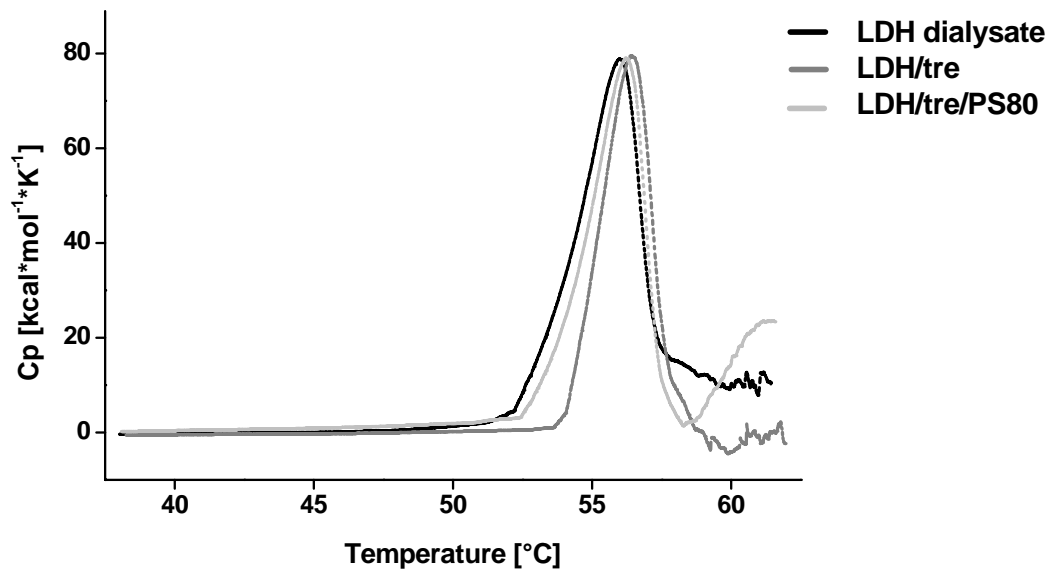
Figure 7 Representative DSC thermograms of LDH dialysate, LDH / trehalose and
LDH / trehalose / PS80 spray solutions

3.3   Stability of LDH during circulation of spray solutions

Circulation of the spray solution is mandatory when spray drying with the Nano Spray Dryer B-90, as it ensures the constant and steady spray of the vibrating mesh nozzle. It might have a negative influence on protein stability, as for example, the PEEK and silicon tubes of the nozzle present surfaces, which could provoke protein adsorption. In addition, the agitation of the spray solution by the peristaltic pump might impose stress on proteins. Furthermore, when the spray solution passes the vibrating mesh, it is partially enriched with drying medium (in this case compressed air, although a nitrogen / carbon dioxide mix is also possible), which flows through the apertures of the vibrating mesh due to the overpressure in the drying chamber. Consequently, air or gas bubbles are formed in the bulk spray solution, which are pumped back into the storage vessel together with the spray solution. To minimize the influence of these air bubbles, it is recommended to position the outlet tube into the storage vessel in a way that its orifice is not submerged. Particularly, when surfactant containing solutions were spray dried this simple expedient avoided an excessive foam formation in the storage vessel, which occurred in case the end of the tube was submerged.

The influence of circulation on protein stability was analyzed by pumping the spray solution for 60 min through the spray nozzle system. The spraying mechanism of the nozzle was not activated. After 30 and 60 min, samples were taken and analyzed for enzymatic activity and particle content. The LDH / trehalose formulation showed an immense reduction

to 53.8% of the initial enzyme activity after 60 min, whereas the LDH / trehalose / PS80 formulation retained its initial activity (98.5% after 60 min) (Figure 8). The loss of enzyme activity in the surfactant free formulation was accompanied by the formation of aggregates. Light obscuration data showed an increase in subvisible particles for both formulations (Figure 9). However, in the surfactant free formulation this increase was much more pronounced. The turbidity measurements emphasized the protective action of surfactant, as the LDH / trehalose formulation reached 0.384 AU after 60 min circulation time, in contrary to 0.059 AU for the LDH / trehalose / PS80 formulation, both starting from 0.010 AU and 0.004 AU, respectively. Obviously, LDH is not sufficiently stabilized by addition of trehalose alone against the stresses occurring during circulation of the spray solution. Therefore, the conclusion was drawn that the surfaces in the spray dryer nozzle and the interactions of proteins with these surfaces must be regarded as critical for protein stability.
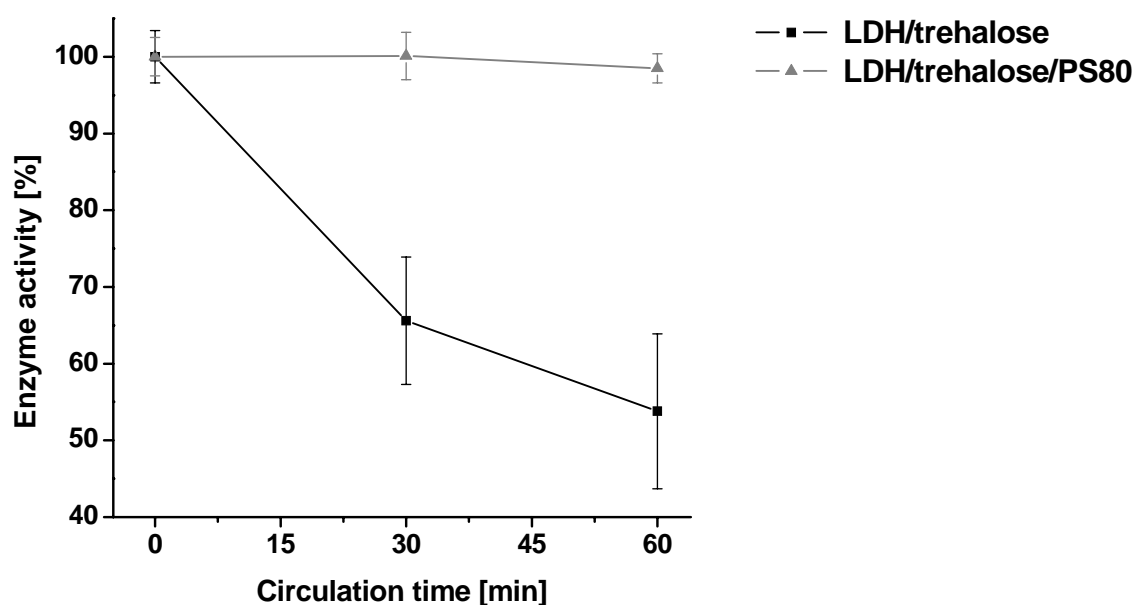

Figure 8 Reduction of enzyme activity during circulation of LDH / trehalose with and without polysorbate 80
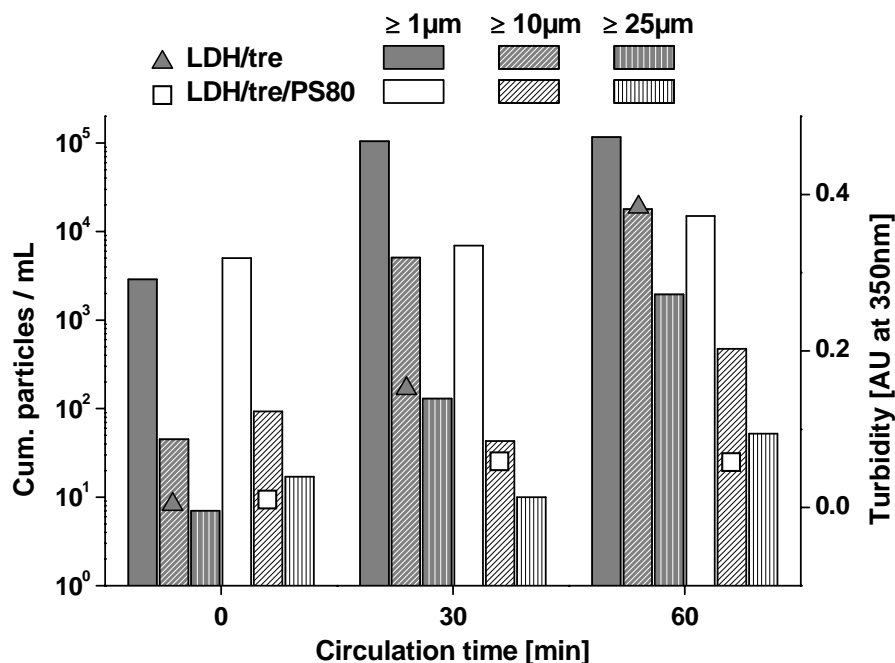
Figure 9 Subvisible particles (columns) and turbidity (symbols) of LDH / trehalose
solution with and without polysorbate 80 during circulation

3.4   Temperature measurements on the spray mesh

The design of the Nano Spray Dryer B-90 implicates that the spray nozzle is positioned inside the drying chamber and is therefore inevitably exposed to the warm drying air. Nozzle cooling by a cooling liquid or peltier element is not yet available. Furthermore, the piezoelectric actuator causing ultrasonic vibrations of the aperture plate leads to a continuous heating of the spray mesh. A temperature sensor inside the spray nozzle records the local temperature in close proximity to the actuator, the so called spray head temperature (Figure 3). In order to protect the piezocrystals from heat induced damage, the sensor limits the actuator heating to approx. 6 °C above the applied inlet temperature of the drying air. The inlet temperature is measured below the heater block at the top of the drying chamber and can be set to a maximum of 120 °C, which allows heating of the actuator up to 126 °C. Of course, the actual temperature of the spray solution is far lower, as the solution is shielded by PEEK tubes and the surrounding air cushion. A critical step during the spray drying process is the contact of the spray solution with the vibrating mesh, which has taken up heat from the drying air and the spray nozzle. The recordings of the spray head temperature sensor can at most be indicative of the temperature, which the spray solution encounters upon contact with the spray mesh. Therefore, the actual temperature of the vibrating mesh was measured separately by placing a temperature probe directly on the surface of the

vibrating mesh. For these measurements, water was used as spray solution and the spray drying process was interrupted for a short period to dismount the spray nozzle from the drying chamber.

Drying air inlet temperatures of 20 °C resulted in the maximal tolerated spray head temperature of 26 °C, independently of the applied spray intensity (Table 2).The temperature of the spray mesh also reached 26 °C. The same phenomenon was observed for a T_{in} of 30 °C, where spray head and spray mesh reached 36 °C, independently of the applied spray intensity. At a higher T_{in} of 60 °C, the spray intensity had a substantial influence on the heating of spray head and spray mesh. A reduction of spray intensity from 100% to 25% led to a drop by 17 °C in spray head temperature and by 13 °C in spray mesh temperature. This effect was even more pronounced with the higher inlet temperatures of 90 and 120 °C. A reduction of spray intensity can be considered as valuable step to prevent the heating of the vibrating mesh and the spray head at higher drying temperatures. Furthermore, these temperature measurements revealed the necessity to monitor the spray mesh temperature, as it can reach temperatures, which are highly critical for thermosensitive proteins. Temperatures as high as 80 °C might be tolerated by some protein species for a short period, however, as the spray solution is circulated in the spray nozzle, protein molecules may encounter these high temperatures multiple times. A drying air inlet temperature of 60 °C was also used for a spray drying experiment applying the 7.0 µm spray mesh. However, the corresponding spray head and mesh temperatures gave no clear indication for an influence of the mesh size on resulting temperature conditions in the spray nozzle.

Table 2 Applied inlet temperatures and spray intensities and measured spray head
and spray mesh temperatures (*application of the 7.0 µm mesh)

Inlet temperature [°C]	Spray intensity [%]	Spray head temperature [°C]	Spray mesh temperature [°C]
20	25	26	25
20	100	26	26
30	25	36	31
30	100	36	30
60	25	49	40
60	100	66	53
90	25	60	50
90	100	96	69
120	25	75	59
120	100	126	80
60*	25	48	37

3.5 Spray drying LDH with the Nano Spray Dryer B-90

The evaluation of the Nano Spray Dryer B-90 for spray drying the temperature sensitive protein LDH was started using the following parameters:

- Inlet temperature: 60 °C
- Spray intensity: 100%
- Mesh size: 4.0 µm apertures
- Formulation: LDH / trehalose (0.2 : 99.8) + 0.1% polysorbate 80

By experience with the Nano Spray Dryer B-90, an inlet temperature of 60 °C was expected to result in a spray drying process with sufficient thermal efficiency to gain a dry product. Yet, 60 °C were also considered as the maximal feasible inlet temperature given the thermal sensitivity of LDH, and were expected to pose a challenge for protein stability. Conditions should also allow for a reducing of spray head and mesh temperature by decreasing the spray intensity at the expense of longer process times. The spray mesh with the smallest apertures was chosen to minimize the protein particle size. The spray solution vessel was cooled in an ice water bath, and the temperature of bulk spray solutions was determined as 16 +/- 1 °C at the end of experiment. Immediately after spray drying, the enzyme activity and the particle content were determined in the residual bulk spray solution and in the spray-dried powder after reconstitution.

Table 3 Spray drying experiments with LDH / trehalose / PS80

#	T_{in} / T_{out} [°C]	$T_{spray\ head}$ [°C]	Spray intensity [%]	Mesh [µm]	Yield [%]	Spray solution		Reconst. powder	
						Activity [%]	Turbidity [AU]	Activity [%]	Turbidity [AU]
1	60 / 34	66	100	4.0	76	66.1	0.021	27.3	0.008
2	60 / 35	50	25	4.0	61	92.2	0.019	27.9	0.013
3	60 / 32	52	25	7.0	64	88.0	0.026	28.3	0.010
4	30 / 25	36	25	4.0	65	98.9	0.016	73.5	0.008
5	30 / 26	36	100	4.0	69	101.5	0.016	80.3	0.009
6	20 / 19	26	25	4.0	66	100.2	0.007	83.4	0.005

The default spray drying parameters resulted in a rigorous reduction of enzyme activity in the spray solution to 66.1% (Table 3 / #1). The activity assay of the reconstituted spray-dried powder confirmed the loss, as only 27.3% of the initial enzyme activity could be found. As anticipated, the selected process parameters were too harsh on protein stability.

From the conducted temperature measurements on the vibrating mesh (Table 2), heating of the vibrating mesh to approx. 53 °C can be assumed. LDH most probably suffered from thermal denaturation upon contact with the hot vibrating mesh. As the spray mesh temperature definitely was in the range of the T_m of LDH, the formation of denatured and inactive protein must have occurred. The enzymatic activity of the reconstituted spray-dried powder was far below the residual spray solution activity. This can be explained by increased thermal stress for the protein upon actually passing through the apertures of the hot vibrating mesh and during the drying of warmed droplets in the 60 °C T_{in} air stream. Light obscuration measurements indicated an increase of subvisible particles by one order of magnitude in the residual spray solution and in the spray-dried powder compared to the starting solution (Figure 11; for start see Figure 9), whereas turbidity measurements revealed just a marginal formation of large aggregates.

In order to reduce temperature stress, LDH was spray dried at a reduced spray intensity of 25% (Table 3 / #2). The recorded spray head temperature reached 50 °C instead of 66 °C, which presumably reduced the spray mesh temperature to approx. 40 °C. The lower spray head and mesh temperatures had no beneficial effect on the formation of subvisible particles, but resulted in a better preservation of enzyme activity of 92.2% in the bulk spray solution. However, the enzyme activity of the reconstituted powder was maintained only to 27.9%, which virtually represents no improvement compared to the 100% spray intensity process. The reduction of spray intensity was obviously insufficient to prevent the thermal stress for the enzyme. However, the higher residual activity in the spray solution indicates that at least the reduction in head and mesh temperature helped to keep the non-sprayed bulk material better intact. Nevertheless, the generated aerosol droplets still experienced the high temperature upon passing the hot vibrating mesh. They reached the drying chamber with higher droplet temperatures and droplet drying occurred under increased temperature with detrimental effects for protein stability. Literature positively correlates an increased drying air inlet temperature with a higher droplet drying rate and droplet surface temperature [18]. Typically, spray drying in the standard Mini Spray Dryer B-290 is performed with a cooled nozzle [19]. Spray drying processes in the novel Nano Spray Dryer B-90 cannot yet revert to this option. The influence of an initially increased spray solution temperature on the droplet drying rate and surface temperature under constant inlet air conditions has not been described in literature.

The experimental setting was further modified by implementing the 7.0 µm mesh (Table 3 / #3), which showed no influence on temperature conditions in the spray nozzle. Although, the 7.0 µm mesh produced larger aerosol droplets and consequently larger particles (Figure 10 A and B), the enzyme activity of the spray-dried powder (28.3%) remained unchanged. A beneficial influence of the reduced air–liquid interface due to the generation of larger droplets was obliterated by the presence of 0.1% polysorbate 80 in the spray solution.

The Nano Spray Dryer B-90 provides the opportunity to apply rather low spray drying temperatures, as small droplets with a narrow size distribution can be generated and efficiently dried. Therefore, an inlet temperature of 30 °C was chosen in a next evaluation step (Table 3 / #4 and #5), resulting in an outlet temperature of 25 °C. Despite this low outlet temperature, the yields of the spray drying processes were 65 to 69% and comparable to the 60 / 35 °C T_{in} / T_{out} experiments. The vibrating mesh with the 4.0 µm apertures was tested at 25% and 100% spray intensity. Although, lower spray intensities usually reduce the heating of the spray nozzle, both experiments showed spray head temperatures of 36 °C. This temperature was probably necessary for an effective vibration of the spray mesh at 25% spray intensity. It can be assumed that the vibrating mesh reached a temperature of 30 °C during the spray drying process, which allowed for a reduced formation of subvisible particles and a better preservation of enzyme activity. The activity of LDH in the residual bulk spray solution was entirely preserved (98.8% and 101.5%, respectively), and the reconstituted powders showed a higher enzymatic activity: 73.5% of the initial activity at 25% spray intensity and 80.3% at 100% spray intensity. A further reduction of inlet temperature to 20°C with a corresponding spray head temperature of only 26°C was even more beneficial and preserved the enzyme activity in the spray-dried powder to 83.4% (Table 3 / #6). Even at these low inlet air temperatures, the aerosol was dried sufficiently to form spherical particles with a smooth surface (Figure 10 C), and the powder could be collected with 66% yield.
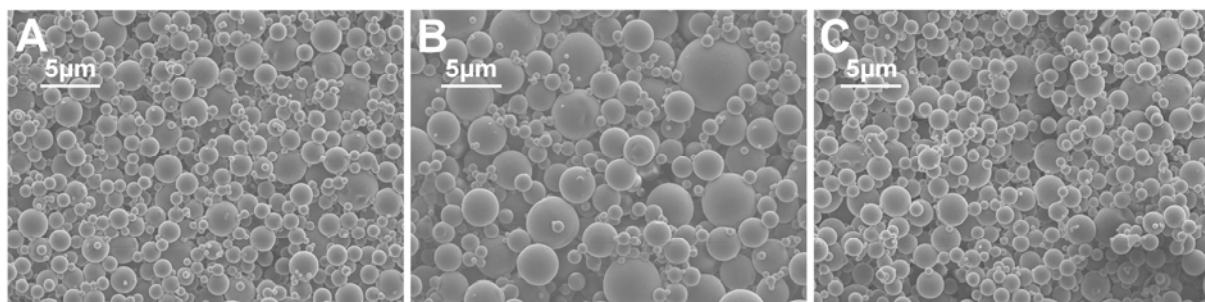

Figure 10 SEM of spray-dried LDH / trehalose / PS80 particles with T_{in} / mesh size settings of **(A)** 60 °C / 4.0 µm, **(B)** 60 °C / 7.0 µm, and **(C)** 20 °C / 4.0 µm
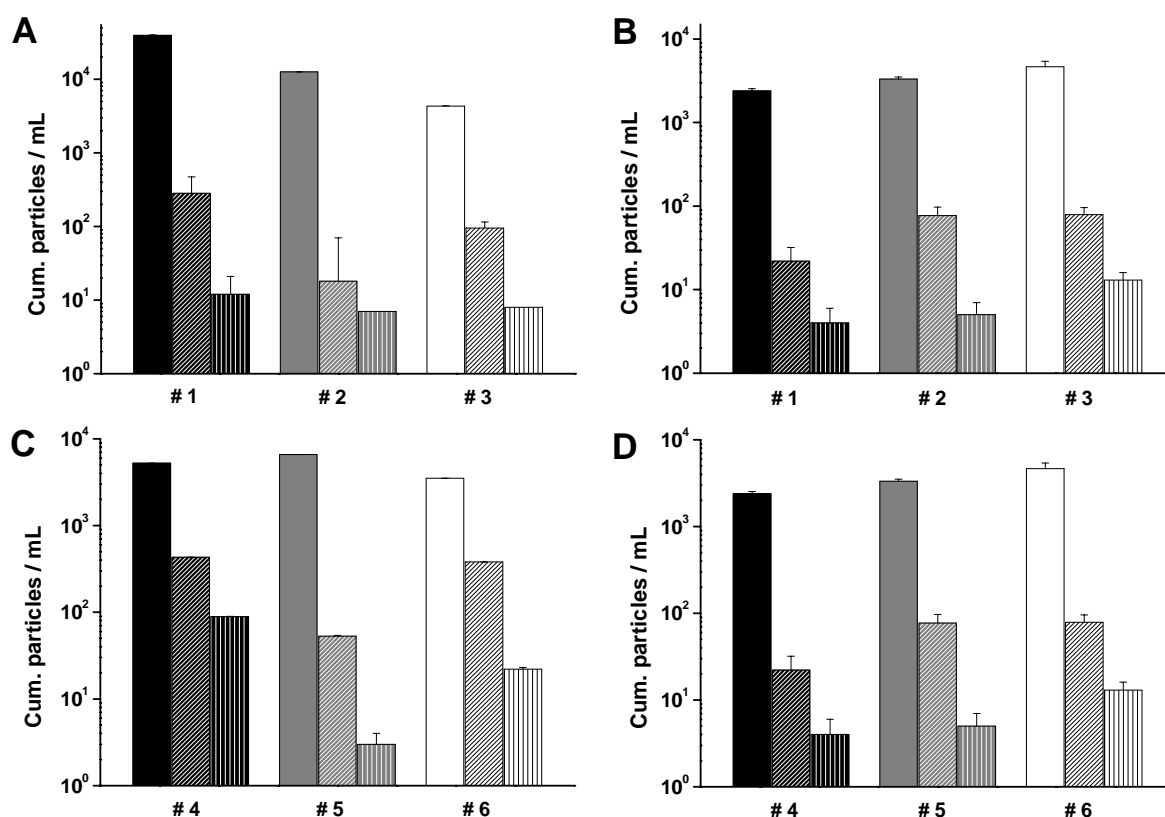
Figure 11 Number of subvisible particles per mL (filled > 1µm; diagonal > 10µm; longitudinal > 25µm):
       (A) Bulk spray solutions of experiments #1 – 3
       (B) Reconstituted powders of experiments #1 – 3
       (C) Bulk spray solutions of experiments #4 – 6
       (D) Reconstituted powders of experiment #4 – 6

3.6 Cavitation – critical for protein spray drying with the Nano Spray Dryer B-90?

In order to complete the study of influences on protein stability during spray drying with the Nano Spray Dryer B-90, the occurrence of cavitation was investigated. The spray mesh of the Nano Spray Dryer B-90 vibrates with ultrasonic frequency, which could lead to cavitation. Specifically, the development of free radicals due to thermal decomposition of water in the spray solution was analyzed by chemical dosimetry using potassium iodide. As shown in Figure 12, formation of free radicals in the potassium iodide solution could not be observed upon simple circulation through the system including the spray nozzle. The absorbance over time was comparable to the potassium iodide solution, which was subjected to storage and served as blank. Furthermore, no relevant free radicals were detected in the bulk solution upon spray drying of the potassium iodide solution. In contrast, the sonication with the ultrasonic homogenizer as positive control led to a continuous rise in absorbance by approx. 0.005 AU/min, which indicates oxidative processes and is in good accordance with literature [20].
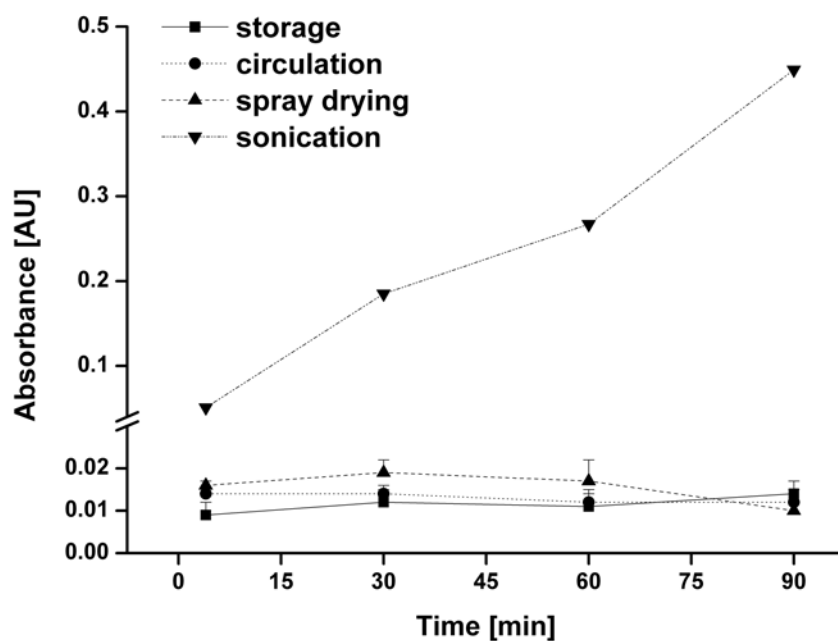
Figure 12 Concentration of I_3^- in the potassium iodide solution upon various process steps

Conclusively, the atomization process in the Nano Spray Dryer B-90 nozzle did not provoke the formation of free radicals, which is beneficial with regard to the chemical stability of proteins in the spray solution.

4   Summary and Conclusions

The Nano Spray Dryer B-90 was evaluated for protein spray drying using an IgG_1 antibody and the enzyme LDH. The focus of the study lay on the influence of process parameters and spray dryer features on protein stability. Instead of conducting traditional formulation development by testing various stabilizers at different concentrations, standard formulations were applied with proven ability to yield stable powders upon spray drying with conventional spray dryers. In addition to the stress factors already known from traditional spray drying processes, the influence of the nozzle design on protein stability was investigated. Special attention was paid to the heating of the spray solution due to contact with the vibrating mesh.

In general, the Nano Spray Dryer B-90 was feasible of spray drying all protein solutions at comparatively high yields as no crust formation on the spray dryer nozzle occurred. The rather robust IgG_1 showed good process stability, however, addition of surfactant was necessary in order to prevent the formation of protein aggregates. The more sensitive LDH was also stabilized with surfactant addition against adsorption to air–liquid interfaces and surfaces. However, it lost enzymatic activity even upon spray drying at T_{in} as low as 60 °C. The temperature increase of the vibrating mesh was monitored and identified as most critical factor, because the spray solution is exposed to the spray mesh multiple times and has to pass its apertures for atomization.

In comparison to spray drying LDH with a conventional spray dryer, the observed loss of enzyme activity in the Nano Spray Dryer B-90 was more pronounced. Adler et al. spray dried 0.3% LDH as trehalose / 0.1% polysorbate 80 formulation at T_{in} / T_{out} of 150 / 95 °C. The activity recovery of the reconstituted powder immediately after spray drying was determined with approx. 92% [6]. The nozzle design of a conventional spray dryer seems to be more appropriate if delicate proteins are processed, as it ensures a fast atomization at moderate temperatures. The spray mesh of the Nano Spray Dryer B-90 vibrates with ultrasonic frequency, which could lead to cavitation. The formation of free radicals was not observed and cavitation as stress factor for protein stability seems to be negligible.

5 References

1 Abdul-Fattah AM, Lechuga-Ballesteros D, Kalonia DS, Pikal MJ. The impact of drying method and formulation on the physical properties and stability of methionyl human growth hormone in the amorphous solid state. *J Pharm Sci* 2007; 97: 163-184.

2 Sollohub K, Cal K. Spray drying technique: II. Current applications in pharmaceutical technology. *J Pharm Sci* 2009; 99: 1-11.

3 Millqvist-Fureby A, Malmsten M, Bergenstahl B. Spray-drying of trypsin - surface characterisation and activity preservation. *Int J Pharm* 1999; 188: 243-253.

4 Adler M, Unger M, Lee G. Surface composition of spray-dried particles of bovine serum albumin/trehalose/surfactant. *Pharm Res* 2000; 17: 863-870.

5 Abdul-Fattah AM, Kalonia DS, Pikal MJ. The challenge of drying method selection for protein pharmaceuticals: product quality implications. *J Pharm Sci* 2007; 96: 1886-1916.

6 Adler M, Lee G. Stability and surface activity of lactate dehydrogenase in spray-dried trehalose. *J Pharm Sci* 1999; 88: 199-208.

7 Schmid K, Arpagaus C, Friess W. Evaluation of the Nano Spray Dryer B-90 for pharmaceutical applications. *Pharm Dev Technol* 2010: 1-8.

8 Schuele S, Schulz-Fademrecht T, Garidel P, Bechtold-Peters K, Friess W. Stabilization of IgG$_1$ in spray-dried powders for inhalation. *Eur J Pharm Biopharm* 2008; 69: 793-807.

9 Bechtold-Peters K, Bassarab S, Fuhrherr R, Garidel P, Friess W, Schultz-Fademrecht T. 1,4 O-Linked saccharose derivatives for stabilizing antibodies of antibody derivatives. 2005 (Patent: 2565019).

10 Miller DP, Anderson RE, De Pablo JJ. Stabilization of lactate dehydrogenase following freeze-thawing and vacuum-drying in the presence of trehalose and borate. *Pharm Res* 1998; 15: 1215-1221.

11 Gogate PR, Kabadi AM. A review of applications of cavitation in biochemical engineering/biotechnology. *Biochem Eng J* 2009; 44: 60-72.

12 Riesz P, Kondo T. Free radical formation induced by ultrasound and its biological implications. *Free Radical Bio Med* 1992; 13: 247-270.

13 Coakley WT, Brown RC, James CJ, Gould RK. The inactivation of enzymes by ultrasonic cavitation at 20 kHz. *Arch Biochem Biophys* 1973; 159: 722-729.

14 Koda S, Kimura T, Kondo T, Mitome H. A standard method to calibrate sonochemical efficiency of an individual reaction system. *Ultrasonics Sonochem* 2003; 10: 149-156.

15 Moran A, Buckton G. Adjusting and understanding the properties and crystallisation behaviour of amorphous trehalose as a function of spray drying feed concentration. *Int J Pharm* 2007; 343: 12-17.

16   Arakawa T, Prestrelski SJ, Kenney WC, Carpenter JF. Factors affecting short-term and long-term stabilities of proteins. *Adv Drug Deliv Rev* 2001; 46: 307-326.

17   Elkordy AA, Forbes RT, Barry BW. Study of protein conformational stability and integrity using calorimetry and FT-Raman spectroscopy correlated with enzymatic activity. *Eur J Pharm Sci* 2008; 33: 177-190.

18   Masters K. Spray Drying1976: 684.

19   Maa YF, Nguyen PA, Andya JD, Dasovich N, Sweeney TD, Shire SJ, Hsu CC. Effect of spray drying and subsequent processing conditions on residual moisture content and physical/biochemical stability of protein inhalation powders. *Pharm Res* 1998; 15: 768-775.

20   Vonhoff S. The influence of atomization conditions on protein secondary and tertiary structure during microparticle formation by spray-freeze-drying (*Thesis*) 2010.

Chapter 5

Summary of the thesis

The objective of the present thesis was to tread new paths in pharmaceutical spray drying. Compared to other drying techniques in formulation development, spray drying offers the advantage of a comprehensive particle design depending on the intended application of the powder. Moreover, spray drying is characterized by short process times and moderate acquisition costs for lab scale equipment. In Chapter 1, the application of spray drying for the production of stable protein powders was evaluated. As a matter of principle, spray drying challenges protein stability. The atomization of the spray solution leads to a tremendous increase of the air–liquid interface, at which proteins with inherent surface affinity tend to adsorb. Adsorption is often followed by protein unfolding and subsequently aggregation, which are seen as critical with respect to safety and efficacy. The default measure to prevent protein adsorption in the first place constitutes the addition of a surfactant to the spray solution. Surfactant molecules are known to compete with protein molecules for the interfacial space. However, the use of surfactants, especially polysorbates, may be associated with a reduced long-term protein stability due to enhanced protein oxidation by residual peroxides. Instead of adding surfactant to the spray solution, the concept of protein precipitation before spray drying was investigated as alternative approach to stabilize proteins against interface related stress. Protein precipitation by 'salting-out' was conducted for a monoclonal IgG_1 antibody and recombinant human interleukin-11 (rhIL-11) using volatile ammonium salts. The volatility of the precipitating salts was considered to be of high importance, as their elimination from the final protein formulation was to be accomplished at the increased temperature during spray drying. Specifically, ammonium carbamate showed appropriate qualities as precipitating agent: by applying elevated spray drying temperatures, the salt was completely removed from the spray-dried powders. Furthermore, excellent precipitation efficiency was realized for both proteins tested. Regarding the IgG_1, a beneficial effect on protein stability by ammonium carbamate precipitation was not achieved, as this protein shows a low surface affinity and can be spray dried as surfactant-free formulation. However, the stability of spray-dried rhIL-11 was substantially improved by ammonium carbamate precipitation in comparison to a surfactant-free formulation. Precipitation as controlled protein association prevented the adsorption of rhIL-11 at the droplet surface.

These studies proved that proteins with high surface affinity can benefit from the concept of precipitation by volatile salts before spray drying as valuable alternative to the addition of a surfactant.

The focus in Chapter 2 lay on the evaluation of the novel Nano Spray Dryer B-90 for pharmaceutical purposes. Büchi Labortechnik AG provided a prototype of the spray dryer for alpha- and beta-testing and our experiences and results were incorporated into the design and development of the spray dryer ready for market. Compared to a conventional spray dryer, the Nano Spray Dryer B-90 comprises two technological novelties: firstly, the spray solution is atomized by the piezoelectric driven vibrations of a spray mesh containing hundreds of micron sized apertures. Secondly, the spray-dried powder is separated from the drying air current via an electrostatic particle collector. Both features are crucial with regard to sophisticated particle design and powder formulation. The small apertures of the vibrating mesh enabled the production of small aerosol droplets with narrow size distribution, resulting in particles with a mean size of less than 1 µm. The electrostatic particle collector allowed the quantitative yield of these submicron particles. This study also showed that the droplet size is defined by the aperture size of the applied vibrating mesh, whereas the total solid content, the viscosity and the surface tension of the spray solution exert no significant influence on the droplet size. In addition, the occurrence of powder depositions on the spray nozzle was investigated, because this crustification phenomenon led to yield reductions and product loss. No correlation of the crustification to the spray solution parameters viscosity, surface tension or conductivity could be established. Powder depositions were avoided by varying the solute concentration or the solvent. Conclusively, the Nano Spray Dryer was assessed as valuable tool for producing micron to submicron sized particles starting from small sample quantities.

The spray drying experiments described in Chapter 3 aimed at the improvement of the oral bioavailability of griseofulvin as a model BCS class II drug. Common approaches to increase drug bioavailability include drug dispersion, micronization and solubilization. Spray drying with the Nano Spray Dryer B-90 was conducted to produce micronized powder particles and also to incorporate a wetting agent for better solubilization. Furthermore, the inert spray drying of organic solvent solutions was tested. A safe and robust spray drying process for griseofulvin was established by evaluating various organic solvents. Acetone and methanol / acetone combinations gave the best spray performance without pronounced crustification. Griseofulvin powders with medium particle sizes of 3.4 to 6.5 µm were produced and compared to the 'gold standard' micronized griseofulvin concerning particle properties with relevance for drug absorption. Particularly, drug dissolution and cell culture

permeability of spray-dried griseofulvin were analyzed and correlated to drug particles size. Spray drying of griseofulvin yielded powder comparable to micronized milled material with respect to dissolution and permeability. The addition of Lutrol F127 as wetting agent improved the solubilization of griseofulvin to such an extent that the dissolution rate was even faster than for micronized material.

In Chapter 4, the Nano Spray Dryer B-90 was applied for spray drying a monoclonal IgG$_1$ antibody and L-lactic dehydrogenase (LDH) as two relevant model proteins. The possibility to process minute sample quantities makes the Nano Spray Dryer B-90 highly attractive for the drying of expensive compounds like pharmaceutical proteins. A simple transfer of the correlations between conventional spray drying process parameters and protein stability was not justified as the design of the Nano Spray Dryer B-90 comprises several novel features. Therefore, special attention was paid to the influence of the spray dryer nozzle on protein stability. In general, the Nano Spray Dryer B-90 enabled to spray dry both proteins at high yields without crustification tendencies. The rather robust IgG$_1$ showed good process stability and formation of protein aggregates was avoided by addition of surfactant. The rather sensitive LDH could also be stabilized by surfactants against adsorption to air–liquid interfaces and surfaces in the spray dryer nozzle. However, its enzymatic activity significantly decreased upon spray drying with the Nano Spray Dryer B-90 and the formation of protein aggregates was observed. The vibrating mesh was identified as considerable stress factor for protein stability. As the spray nozzle is exposed to the elevated drying temperatures and the vibration activity of the mesh also produces heat, the spray mesh heats up continuously during a spray drying process and can reach critical temperatures with regard to protein stability. In the course of a spray drying process, the spray solution contacts the mesh multiple times and has to pass through the apertures upon atomization. These effects are detrimental for exceptionally temperature sensitive proteins like LDH. In this study, spray drying at lower T_{in} was identified as measure to minimize the spray mesh heating. A reduction in spray intensity also enabled to limit the spray mesh heating, however was accompanied by prolonged process times. Drying temperatures of 30 / 25 °C (T_{in} / T_{out}) were sufficient to yield dry and stable protein material at satisfying yields (approx. 70%) and preserved 80% of the initial LDH activity. In conclusion, the evaluation of the Nano Spray Dryer B-90 for protein spray drying revealed the crucial differences of this new device compared to conventional spray dryers and identified the challenges in developing a stable protein powder.

List of Abbreviations

ACA	ammonium carbamate
AS	ammonium sulfate
AU	absorbance unit
AUC	area under the curve
avd	after vacuum drying
BCS	biopharmaceutical classification system
β-NADH	β-nicotine amide adenine dinucleotide
BSA	bovine serum albumin
CHN	elementary analysis for carbon, hydrogen and nitrogen
CMC	critical micelle concentration
Decomp.	decomposition
DMEM	Dulbecco's modified eagle's medium
DMSO	dimethyl sulfoxide
DSC	differential scanning calorimetry
EDTA	ethylendiaminetetraacetic acid
FBS	fetal bovine serum
FNU	formazine nephelometric units
FTIR	Fourier transformed infrared spectroscopy
GCSF	granulocyte colony stimulating factor
HBSS	Hank's balanced salt solution
HEPES	4-(2-hydroxyethyl)-1-piperazineethanesulfonic acid
HPC	hydroxypropyl cellulose
HPMC	hydroxypropyl methyl cellulose
HP-SEC	high performance size exclusion chromatography
HPβCD	hydroxypropyl-beta-cyclodextrin
HSA	human serum albumin
IEP	isoelectric point
IgG_1	immunoglobulin G_1
LD_{50}	lethal dose 50%
LDH	L-lactic dehydrogenase
Mab	monoclonal antibody
MEM	minimum essential medium
MES	2-(N-morpholino)ethanesulfonic acid
M_r	molecular weight
MWCO	molecular weight cut off

n.a.	not available
NEAA	non-essential amino acid
OD	optical density
PEEK	polyether ether ketone
PEG	polyethylene glycol
PLGA	poly(lactic-*co*-glycolic acid)
PS	polysorbate
PTFE	polytetrafluoroethylene
PVA	polyvinyl alcohol
PVP	polyvinyl pyrrolidone
r.h.	residual humidity
rhGCSF	recombinant human granulocyte colony stimulating factor
rhIL-11	recombinant human interleukin-11
rM	residual moisture
SCF	supercritical fluid
SDS	sodium dodecyl sulfate
SEDDS	self-emulsifying drug delivery system
SEM	scanning electron microscopy
SMEDDS	self-micro-emulsifying drug delivery system
TEER	transepithelial electrical resistance
T_g	glass transition temperature
T_{in} / T_{out}	spray drying inlet / outlet temperature
T_m	melting temperature
USP	United States Pharmacopoeia
XRD	X-ray powder diffraction

Posters and Publications associated with this work

Posters

K. Schmid, C. Arpagaus, W. Frieß. Evaluation of the Nano Spray Dryer B-90 for protein formulation. 7th World Meeting on Pharmaceutics, Biopharmaceutics and Pharmaceutical Technology, Valetta, Malta (2010).

K. Schmid, W. Frieß. Innovative spray drying technology for the formulation of a BCS class II drug. AAPS Annual Meeting and Exposition, Los Angeles, USA (2009).

K. Schmid, C. Arpagaus, W. Frieß. Evaluation of a vibrating mesh spray dryer. PharmSciFair, Nice, France (2009).

K. Schmid, C. Arpagaus, W. Frieß. Evaluation of a vibrating mesh spray dryer for preparation of submicron particles. Respiratory Drug Delivery Europe, Lisbon, Portugal (2009).

K. Schmid, W. Frieß. Protein precipitation and spray drying as new approach to high concentration formulations. 6th World Meeting on Pharmaceutics, Biopharmaceutics and Pharmaceutical Technology, Barcelona, Spain (2008).

Publications

K. Schmid, C. Arpagaus, W. Frieß. Evaluation of the Nano Spray Dryer B-90 for pharmaceutical applications. *Pharm Dev Technol* 2010: 1-8.

K. Schmid, C. Arpagaus, W. Frieß. Nano spray drying in laboratory scale – Fine particles from small sample quantities. *GIT Application notes* 2009: 11-12.

Curriculum Vitae

Katja Christine Schmid

Personal Data
_____

Date of Birth   September 12, 1981

Place of Birth   Munich, Germany

Nationality   German

Professional Experience
_____

Since 10/10   Pharma Project Manager
                Swiss Caps AG, Kirchberg, Switzerland

Education
_____

02/07 – 09/10   PhD thesis
                 Department of Pharmacy, Pharmaceutical Technology and
                 Biopharmaceutics, Ludwig-Maximilians-University, Munich

        03/07   Pharmacist license

05/06 – 10/06   Internship in pharmaceutics
                 University of Alberta, Edmonton, Canada

11/05 – 04/06   Internship in public pharmacy
                 Rosen Apotheke, Munich

10/01 – 07/05   Study of pharmacy
                 Ludwig-Maximilians-University, Munich